UNITED STATES DEPARTMENT OF COMMERCE
HARRY L. HOPKINS, Secretary
NATIONAL BUREAU OF STANDARDS
Lyman J. Briggs, Director

✦

Journal of Research

of the

National Bureau of Standards

✦

Volume 23, Number 3
September 1939

Published with approval of the Director of the Budget

UNITED STATES
GOVERNMENT PRINTING OFFICE
WASHINGTON : 1939

For sale by the Superintendent of Documents, Washington, D. C. - - - - - - Price 30 cents
$3.50 per year on subscription

The prices of the separate Research Papers appearing in this JOURNAL are given on the front cover page. If 100 or more copies of any separate are ordered, a discount of 25 percent is allowed. Those who desire copies of separate Research Papers should send their orders and remittances without delay to the Superintendent of Documents, U. S. Government Printing Office, Washington, D. C. This will aid him to determine the number of copies to be printed for sale. Research Papers are not printed from electrotypes, and usually no more reprints can be had when the first and only printing is exhausted.

U. S. DEPARTMENT OF COMMERCE NATIONAL BUREAU OF STANDARDS

RESEARCH PAPER RP1237

Part of Journal of Research of the National Bureau of Standards, Volume 23, September 1939

EFFECTS OF HUMIDITY AND COMPOSITION ON STRENGTH AND YOUNG'S MODULUS OF ENAMELS

By Dwight G. Moore and William N. Harrison

ABSTRACT

Both Young's modulus and the modulus of rupture of eight types of enamel frit were determined under constant conditions of temperature and humidity, by transverse loading of annealed fibers about three-fourths millimeter in diameter. Also, one enamel fired on metal specimens was tested under varying conditions of humidity for resistance to chipping in torsion. Fibers of two of the frits were tested in air under different humidities at constant temperature, immersed in different liquids at constant temperature, and immersed in water-free kerosene at different temperatures. The most noteworthy effect observed was that of humidity upon the modulus of rupture of the frit fibers and also upon the resistance of enameled-iron specimens to chipping in torsion.

CONTENTS

	Page
I. Introduction	329
II. Preparation of specimens	330
III. Modulus of rupture tests	330
1. Methods of testing and treatment of data	330
(a) Sustained-load tests	330
(b) Tests with uniformly increasing load	331
2. Effect of humidity on modulus of rupture	332
(a) Effect of humidity in sustained-load tests	332
(b) Effect of humidity in tests with uniformly increasing load	333
3. Effect of immersion in different liquids on modulus of rupture	333
4. Effect of temperature on modulus of rupture	335
5. Variation in modulus of rupture with type of frit	335
6. Discussion of results	336
IV. Torsion tests on enameled-iron specimens	338
1. Method of testing	338
2. Effect of humidity on resistance to chipping by torsion	338
3. Discussion of results	339
V. Modulus of elasticity tests	340
1. Method of testing and treatment of data	340
2. Effect of humidity on modulus of elasticity	340
3. Variation in Young's modulus with type of frit	341
4. Discussion of results	341
VI. Conclusions	342
VII. References	343

I. INTRODUCTION

This report is the third in a series concerning the various properties of eight typical commercial enamel frits. The papers already published relate to consistency [1][1] and surface tension [2]. A study of the thermal expansion and refractoriness of these enamels has been

[1] Figures in brackets indicate the literature references at the end of this paper.

completed but is not yet published. Both the method of selection and the composition of the frits have been previously reported [1]. The types of enamel represented are as follows:

Frit 1, a "soft" sheet-iron ground-coat frit, to be mixed with a harder frit before use.

Frit 11, a "hard" sheet-iron ground-coat frit, used with admixture of a softer frit.

Frit 6, an acid-resisting type of white cover-coat frit for sheet iron.

Frit 25, an "ordinary" white cover-coat frit for sheet iron.

Frit 35, a "super-opaque" white cover-coat frit for sheet iron.

Frit 65, a leadless dry-process frit for cast iron.

Frit 72, a high-lead (40 percent of PbO) wet-process frit for cast iron.

Frit 85, a lead-bearing (10 percent of PbO) dry-process frit for a cast iron.

II. PREPARATION OF SPECIMENS

The specimens used for both strength and elasticity determinations were drawn by hand as fibers from molten frit contained in platinum. The fibers were started with a round nickel rod, the temperature during drawing being adjusted to give fibers between 0.65 and 0.85 mm in diameter. Such specimens were chosen as approximating in thickness the enamel on normally coated ware. The length of the specimens for the modulus-of-elasticity tests was about 12 cm and for the strength tests about 4 cm. Only straight fibers which were either of round cross section or but slightly out-of-round were chosen. These fibers were annealed in a laboratory electric furnace by heating for not less than 15 min at about 5° C (9° F) above the interferometer softening point [3] and cooling at a rate of approximately 2° C (4° F) per minute through the critical range.

Frit 6 was applied as an enamel coating on blanks of 20-gage iron, 8 in. (20 cm) long and 2 in. (5 cm) wide, which had been bent, before enameling, to form 1-in. (2.5 cm) angle-iron specimens having a $\frac{1}{16}$-in. (2 mm) radius of curvature (outside) at the apex. Each specimen was first ground-coated and then coated with enamel 6 on the outer surface. Before firing, the dried cover coat was brushed off a distance of $\frac{1}{4}$-in. (6 mm) from the edges and 2 in. (5 cm) from the ends of the specimen.

III. MODULUS OF RUPTURE TESTS

1. METHODS OF TESTING AND TREATMENT OF DATA

One of the more important variables in strength tests on brittle materials is the rate at which load is applied. The strength of glass, for example, has been shown to vary widely with the loading rate [4]. It, therefore, seems necessary either to control the loading rate closely or to eliminate this variable as far as possible by the use of sustained loads. In this investigation both methods were used.

(a) SUSTAINED-LOAD TESTS

The procedure used in the sustained-load tests, which has been previously described [5], may be easily understood by reference to

figure 1. Using a 2.35-cm span, 20 specimens were tested independently at each specified stress, never less than 5 separate stresses (100 specimens) being used for each determination. Each of the first set of 20 specimens was calipered and loaded at the center to give a maximum fiber stress of 8 kg/mm². After a lapse of 20 hr, two specimens, or 10 percent of the set, had failed. Twenty new specimens were then similarly tested at 9 kg/mm² and 20 percent of these failed. This procedure was repeated with stress increments of 1 kg/mm² until at least 80 percent of the specimens failed (95 percent in fig. 1). The median stress, that is, the stress required to break 50 percent of the specimens (approximately 11.5 kg/mm² in fig. 1), and the statistical error of the determination were computed from the data by the method of C. I. Bliss [6]. Throughout the investigation, the statistical 95-percent-confidence error was used [7, 8].

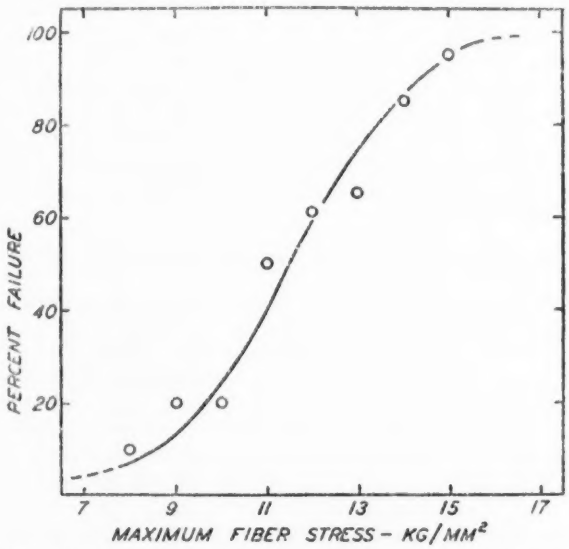

FIGURE 1.—*Typical data obtained in a determination of modulus of rupture by sustained loading.*

Each point indicates the percentage of a 20-specimen sample which failed within 20 hours under sustained load at the indicated stress. The computed stress required for 50 percent failure was reported.

(b) TESTS WITH UNIFORMLY INCREASING LOAD

In the tests with uniformly increasing load, the stress was applied at the center of the specimen on a span of 2.35 cm. The center knife-edge was attached to the base of a modified pan balance and remained stationary. The two end supports were suspended from one arm of the balance, and moved upward as the load was applied to the opposite arm by allowing water to run into a vessel supported therefrom. The water in the reservoir was kept at a constant head by use of a Mariotte bottle and hence flowed at a constant rate. This rate was 1.354 ± 0.003 g/sec, and the applied loads were obtained to an accuracy of ± 1 percent by means of a stop watch. In these tests the rate of stress

application varied from a minimum of 0.132 (kg/mm²)/sec to a maximum of 0.295 (kg/mm²)/sec, depending on the diameter of the specimens. Twenty-five to fifty specimens were tested in each determination, and the statistical error was computed by ordinary methods [7].

2. EFFECT OF HUMIDITY ON MODULUS OF RUPTURE

In a period of relatively high humidity, frit 85 gave 50 percent failures under sustained loading at a stress of 9 kg/mm². Later, under the same conditions, except for lower humidity, this same frit gave only 15 percent failures. However, when a small drop of water was placed gently on the midpoint of each specimen, the 17 test rods remaining unbroken out of the original 20 began breaking almost immediately and within 40 min showed 65 percent failures instead of the original 15 percent. Calculations indicated that the weight of the water drops could not have increased the maximum fiber stress by more than 0.03 kg/mm². To determine whether or not it is necessary to control the humidity fairly closely in order to obtain comparable results, further experiments were made to determine the effect of variations in humidity on the strength of the specimens broken by sustained and by increasing loads. Frits 1 and 6, which represented two distinct degrees of fusibility, or hardness, were selected for this study.

(a) EFFECT OF HUMIDITY IN SUSTAINED-LOAD TESTS

A box in which both the temperature and the humidity could be controlled was constructed to contain the apparatus used for the sustained-load tests. The temperature was maintained at 36° C (97° F) and tests were made at 56- and 90-percent relative humidity. The 90-percent humidity resulted from placing pans of water on the floor of the box, while the 56-percent humidity resulted when a saturated solution of cobalt chloride was substituted for the water, it being possible to maintain both humidities to ±3 percent in this way. A wet- and a dry-bulb thermometer placed in the path of a circulating fan were used for the humidity determinations. The results given in table 1 show significantly greater strength [2] at 56- than at 90-percent relative humidity. Frit 1 had the lower modulus of rupture and showed a greater effect resulting from humidity change, the strength being about 53 percent greater at the lower humidity. The strength of frit 6 was about 15 percent greater at 56- than at 90-percent relative humidity.

---

[2] A difference was considered significant if there was a 95-percent or greater probability that it was not caused by chance fluctuations in sampling or in test conditions. To determine whether or not this requirement was fulfilled, the following ratio was used:

$$\frac{d}{\sqrt{e_1^2+e_2^2}}$$

In this ratio, e_1 and e_2 are the 95-percent-confidence errors of two determinations, as computed by the method of Bliss (see reference [6]), and d is the difference between the two determinations. If this ratio equaled or exceeded unity, the difference was considered significant, on a basis of 95-percent confidence.

TABLE 1.—*Modulus of rupture of fibers of frits 1 and 6 by sustained-load and by increasing-load tests*

Test method	Frit number	Relative humidity	Number of specimens	Modulus of rupture *
		Percent		*kg/mm²*
Twenty-hour sustained loading at 36° C (97° F)	1	90	100	4.7±0.8
	1	56	100	7.2±0.6
	6	90	100	8.4±0.7
	6	56	100	9.7±0.6
Uniformly increasing load at 21° C (70° F)	1	98	52	17.6±0.9
	1	65	51	18.0±1.5
	1	35	52	19.0±0.8
	6	98	52	22.2±1.3
	6	65	52	24.8±1.6
	6	35	52	27.2±1.9

* Limits given are for 95-percent confidence. See references [6, 7, 8].

(b) EFFECT OF HUMIDITY IN TESTS WITH UNIFORMLY INCREASING LOAD

To study the effect of humidity on strength as determined by the increasing-load tests, frits 1 and 6 were tested in constant-temperature, constant-humidity rooms. The three rooms available for this purpose were held at 21° ±0.5° C (70° ±1° F), the relative humidities being 35, 65, and 98 percent (in each case ±2 percent), respectively. The specimens were stored in the rooms for not less than 20 hr before testing. Table 1 includes a summary of the results of these tests, the trend of the data being shown graphically in figure 2. With both frits, the difference in strength, when tested at 35- and at 98-percent relative humidity, is definitely significant.[3] Computations indicate about 97-percent confidence that the variation in strength with humidity is real for frit 1, and well over 99-percent confidence for frit 6. The strengths are, respectively, about 8 and 22 percent greater at 35- than at 98-percent relative humidity.

The two curves in figure 2 show definitely the downward trend of modulus of rupture as the relative humidity is increased. These curves are drawn as straight lines merely to show the trend, as the data do not necessarily establish a straight-line relationship.

3. EFFECT OF IMMERSION IN DIFFERENT LIQUIDS ON MODULUS OF RUPTURE

Since variations in atmospheric humidity affected the modulus of rupture, tests were made to determine the effect of immersion in various liquids, such as water, ethyl alcohol, and kerosene. For these tests, the increasing-load apparatus was modified slightly so that the specimens could be completely immersed in liquid during testing. In one experiment, specimens dried at 110° C were given a very thin moisture-repellent coating by dipping in molten paraffin before the test.

The results of these experiments are given in table 2. For some tests not all of the desirable information concerning storage conditions is available. The information gained from these tests was considered adequate, however, for the purposes of this investigation. Frit 1,

[3] For these data, Fisher's "*t* test" was used to determine the significance of differences (see reference [8]). This treatment of data is preferred by the authors but was not used for the sustained-load test, because data of that type are not susceptible of such treatment.

when dried over $CaCl_2$ and tested under kerosene containing sodium to eliminate water (test 4), was about 30 percent stronger than when tested under water after storage in open air (test 1). When tested in air and in alcohol after storage in open air (tests 2 and 3), the strengths were practically equal and were intermediate between those obtained under the first-mentioned conditions. This intermediate strength is significantly lower than that for dry specimens in kerosene but not significantly higher than that for specimens tested under

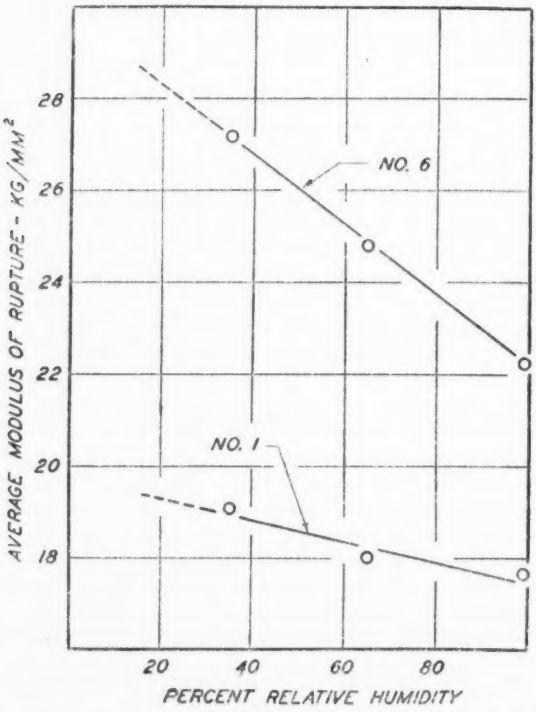

FIGURE 2.—*Graph showing trend towards increasing modulus of rupture with decreasing relative humidity for fibers of frit 6 and frit 1, when tested at 21° C (70° F) under uniformly increasing load.*

water. Comparable conditions of storage and test for frit 6 (tests 5, 6, 7, and 8) showed the same trend of results but more positively, the two intermediate values being significantly different from both extremes.

The strength of the dried specimens of frit 6 under kerosene was about 49 percent greater than that of the specimens tested under water, as compared with 30 percent for frit 1. The strength of specimens of frit 6 tested in air at 65-percent relative humidity (test 6) was not significantly different from that of specimens stored at "room humidity" prior to testing under alcohol (test 7)[4] nor from

[4] Weather Bureau reports indicate that the atmospheric humidity at the time of the latter test was in or near the 60- to 65-percent range.

that of specimens stored in air at 60-percent relative humidity prior to testing in kerosene (test 9). Drying the specimens at 110° C (230° F) prior to testing in kerosene (test 10) gave nearly the same results as drying them over $CaCl_2$ (test 8).

TABLE 2.—*Modulus of rupture of frits 1 and 6 when stored under various conditions and tested in different media and at different temperatures, under constantly increasing load*

Test number	Frit number	Storage conditions prior to testing	Surrounding medium during test	Temperature of surrounding medium		Number of specimens	Modulus of rupture [a]
				°C	°F		kg/mm²
1	1	Room temperature and humidity	Water	26	79	50	17.0±1.0
2	1	65-percent relative humidity, room temperature.	Air	21	70	51	18.0±1.5
3	1	Room temperature and humidity	Alcohol [b]	22	72	51	18.4±1.4
4	1	Dried over $CaCl_2$ for 36 hours at 26° C (79° F).	Kerosene [c]	27	81	31	22.1±1.8
5	6	Room temperature and humidity	Water	21	70	52	19.2±1.4
6	6	65-percent relative humidity, room temperature.	Air	21	70	52	24.8±1.6
7	6	Room temperature and humidty	Alcohol [b]	24	75	52	24.3±1.8
8	6	Dried over $CaCl_2$ for 36 hours at 26° C (79° F).	Kerosene [c]	27	81	32	28.7±1.9
9	6	60-percent relative humidity, room temperature.	do.[c]	22	72	52	25.4±1.3
10	6	Dried at 110° C (230° F) for 48 hours	do.[c]	22	72	29	27.6±1.7
11	6	Dried over $CaCl_2$ for 36 hours at 26° C (79° F).	do.[c]	62	144	33	29.5±1.9
12	6	Dried at 110° C (230° F). Dipped in paraffin at 80° C (176° F).	Paraffin coating	22	72	25	33.8±1.8

[a] Limits given are for 95-percent confidence. See references [7, 8].
[b] Absolute ethyl alcohol denatured with about 5-percent absolute methyl.
[c] Water-free kerosene containing metallic sodium.

The strength of specimens dried at 110° C (230° F) and dipped in molten paraffin (test 12) was significantly greater than that resulting from any other treatment. The paraffin film was about 0.01 mm thick.

4. EFFECT OF TEMPERATURE ON MODULUS OF RUPTURE

In order to establish standard testing conditions, it was desired to determine the effect of temperature on the modulus of rupture of the frit fibers. Since humidity influences the strength, it was necessary to eliminate this variable. This was done by breaking the fibers under water-free kerosene after the specimens had been previously dried by storage for 36 hr over $CaCl_2$.

Tests 8 and 11, made at 27° C (81° F) and 62° C (144° F), respectively (see table 2), show no significant difference in strength and indicate that temperature of itself does not appreciably influence the modulus of rupture of the frit fibers within the range of temperatures studied.

5. VARIATION IN MODULUS OF RUPTURE WITH TYPE OF FRIT

From the data presented in the previous sections, it is obvious that, to obtain reproducible results with modulus of rupture tests on fibers of enamel frit, it is essential to make the determinations under controlled humidity conditions. Inasmuch as determinations by the increasing-load tests could be carried out in about one-fourth of the

time required for the sustained-load tests, and with fewer specimens for approximately the same percentage of error, this method was chosen for comparing the strengths of the frits. The data are summarized in table 3.

TABLE 3.—*Modulus of rupture and modulus of elasticity of enamel-frit fibers*

Frit number	Type of enamel [a]	Modulus of rupture [b]		Modulus of elasticity	
		Number of specimens	Average value [c]	Number of specimens	Average value [c]
			kg/mm²		*kg/mm²*
1	Soft ground coat	51	18.0 ±1.5	35	8,250 ±70
11	Hard ground coat	52	20.1 ±1.1	78	8,420 ±50
25	Ordinary cover coat	53	24.6 ±1.6	36	8,010 ±110
35	Superopaque cover coat	54	23.2 ±1.3	30	8,030 ±130
6	Acid-resisting cover coat	52	24.8 ±1.6	41	8,470 ±130
65	Leadless dry process	54	16.9 ±1.0	36	8,100 ±80
85	Lead-bearing dry process	54	19.0 ±1.0	54	7,620 ±110
72	High lead, cast iron [d]			8	6,120 ±470

[a] Wet process, except where otherwise stated.
[b] Modulus-of-rupture values are for annealed specimens broken in air at 70° F and 60-percent relative humidity (65 percent for frits 1 and 6) by increasing-load test, after at least 20 hours of storage under the test conditions.
[c] Limits given are for 95-percent confidence. See references 7 and 8.
[d] Because of peculiar consistency of high-lead cast-iron enamel, fibers were formed only with difficulty and were covered with surface imperfections.

The data obtained at 21° C (70° F) and 60- to 65-percent relative humidity indicate that the three sheet-iron cover coats (6, 25, and 35) were significantly stronger than both the sheet-iron ground coats (1 and 11) and the cast-iron enamels (65 and 85). The "hard" ground coat 11 was significantly stronger than the "soft" ground coat 1. No data were obtained on the high-lead cast-iron enamel 72, since no fibers satisfactory for this test could be drawn from the molten frit.

6. DISCUSSION OF RESULTS

The large difference in average modulus of rupture obtained with the sustained-load and with the increasing-load tests, indicated in table 1, could be caused in some degree by the greater moisture content of the air for the same relative humidity at the higher temperature used in the sustained-load tests. However, the large difference in apparent strength under the two conditions of test conforms with well-known experience on a number of other materials, and has been reported previously for enamel frits [5].

From the lower modulus-of-rupture values obtained in sustained loading, it may be concluded that vitreous enamel should withstand briefly applied stresses involving no plastic flow of the metal, better than it should withstand stresses of the same magnitude which are sustained over a considerable period of time. Delayed chipping may well be a manifestation of delayed fracture under constant stress. Assuming that a sustained tensile stress is introduced at some edge or corner of an enamel shape during processing or assembling, it is conceivable that the ware might require several hours or even days to chip, depending on the magnitude of the stress. In a border-line case the chipping might not occur until a period of high atmospheric humidity prevailed. Likewise, in a border-line case, humidity might

determine whether a given briefly applied stress would cause failure or not.

The fact that humidity has a significant effect on the modulus of rupture of enamel is not surprising in view of results obtained in some previous investigations of other ceramic products. A. C. Harrison [9], describing a falling-sand abrasion test for whiteware glazes, reported, in 1927, as follows:

"Early in the investigation unaccountable variations were noted in the resistance of the same glazes upon testing them on different days. Finally, a series of tests extending over a period of two weeks were made on the same brand of hotel chinaware. Contemporary records of atmospheric conditions showed the resistance of the glaze to be proportional to the percent relative humidity of the atmosphere * * *."

Milligan [10], in 1929, reported that scratched-glass bars that would sustain transverse loads for several days without failure in dry air would fail in from 1 to 30 hours under the same loads in air saturated with water vapor. Schurkow [11] worked with fused-quartz filaments from 2 to 10 microns in diameter and found that the tensile strength was on the order of 50 percent greater when tested in air dried with $CaCl_2$ than when tested in "room air." He found no difference between the strength of fused-quartz filaments in "room air" and the strength under water. In the present study, however, the strength of enamel frit 6 was found to be almost 30 percent greater in air at 65-percent relative humidity than when immersed in water (see tests 5 and 6, table 2). The strength in air at 98-percent relative humidity was intermediate (see table 1). Frit 1 was somewhat stronger in air at 65-percent relative humidity than it was in air at 98-percent relative humidity, or in water, but the differences in this case were not statistically significant.

Schurkow also found the strength of fused-quartz fibers which had been preheated in a vacuum, and which were tested in a vacuum, to be several times greater than the strength of similar fibers tested in "room air" or in water. Some of his results were later confirmed by Reinkober [12].

The large decreases in strength noted by Griffith [13] on aged fibers of soda-lime-silica glass as compared with freshly drawn specimens might possibly have been caused by the effect of atmospheric moisture.

Grebenchikov, who is quoted by Jurkov [14], explains the effect of humidity and also the effect of various liquids on the strength of silicate glasses by postulating the presence of a thin colloidal film (silica gel) on the surface of the specimen, which swells or contracts, depending on the conditions to which the specimen is exposed. The film is assumed to be present also in surface cracks or discontinuities and to produce a concentration of stress at these points, which varies with the physical state of the gel. Thus, in the presence of an increased concentration of moisture, the gel would swell, causing an increase in the localized stresses at the flaw so that less externally applied force would be required to cause failure. When moved from a damp to a dry atmosphere, the gel would contract and relieve some of the localized stress, thus requiring more applied load to cause failure.

Even though the silica gel postulated by Grebenchikov were not present, specimens immersed in water would tend to draw the water into any cracks or surface flaws through capillary attraction. The

air entrapped in a flaw would be compressed by the advancing water and thereby increase the localized stresses. If such a mechanism is effective, it should operate for any liquid which wets the specimen, and its effect should be a function of the surface tension of the liquid. The same mechanism might conceivably operate in the open air if the amount of moisture absorbed in the flaws increased with increasing humidity. It is the authors' opinion, however, that this explanation accounts, at most, for only a part of the observed phenomena, it being particularly weak in explaining the atmospheric-humidity effects.

Another possible explanation is that the water which is dissolved in the glass [15] (or enamel), and which might be expected to vary in concentration with the humidity of the atmosphere, actually reduces the strength of the material to an extent dependent upon the concentration of the dissolved water. For such changes in dissolved water to be effective, it would be sufficient if the moisture content changed in the surface layer only, since the maximum stress and the beginning of failure occur at the surface.

IV. TORSION TESTS ON ENAMELED-IRON SPECIMENS

Having found that variation in atmospheric humidity affects the modulus of rupture of enamel-frit fibers, it was desired to determine whether or not it also affects the resistance to chipping of enamel applied to metal specimens. For this purpose, the angular specimens previously described under section II were enameled and tested.

1. METHOD OF TESTING

The specimens were tested by inserting one end 1½ in. (3.8 cm) into a fixed right-angle clamp, and the opposite end 1½ in. into a free right-angle clamp having a horizontal lever arm with pointer attached. Load was applied at the end of the lever at a uniform rate to give an angular deflection of about 2° per min. The angle of twist required to cause the first chip at any point along the 4-in. (10 cm) cover-coated apex of the specimen was observed.[5] The thickness of the enamel immediately adjacent to the chip was measured to ±0.0002 in. (0.005 mm) with a Brenner magnetic thickness gage [16].

2. EFFECT OF HUMIDITY ON RESISTANCE TO CHIPPING BY TORSION

Determinations were made at 70° F in atmospheres of 35- and 98-percent relative humidity, after prior storage under the conditions of test for not less than 24 hr. Some of the specimens were dipped in molten paraffin immediately after firing and before completely cooling to room temperature. These were stored and tested at 98-percent relative humidity.

Figure 3 shows the results obtained. Each point in this figure represents a different specimen. If comparisons are made at a thickness of 15 mils (0.38 mm), the angle required to cause chipping at 35-percent humidity is about 15 percent greater than at 98 percent. The

[5] This test was developed in connection with the work of Paul L. Smith for the Porcelain Enamel Institute Research Associateship at the National Bureau of Standards.

paraffin treatment, which presumably kept the specimens dry even though the atmosphere was at 98-percent relative humidity when they were tested, increased the resistance about 30 percent. The

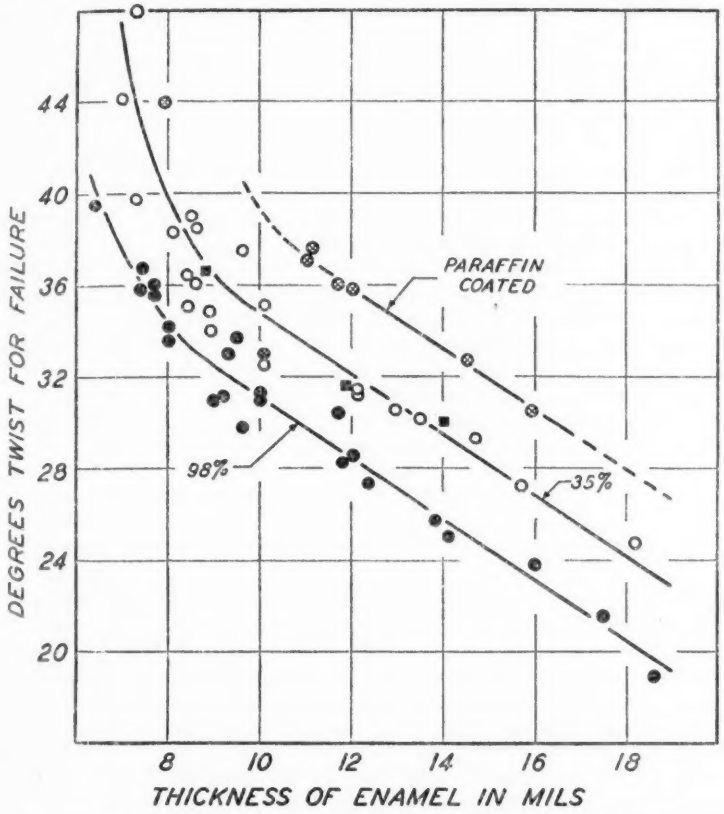

FIGURE 3.—*Angle of twist required to cause chipping of enameled-iron specimens, plotted against thickness of enamel.*

The three curves are for tests made at 98-percent and at 35-percent relative humidity, respectively, on untreated specimens and on specimens given a moisture-repellent coating of paraffin before completely cooling after firing.

three solid squares on the 35-percent humidity curve represent specimens stored 72 hr at 98-percent humidity and then returned to 35-percent relative humidity, stored 24 hr, and tested.

3. DISCUSSION OF RESULTS

It is evident that a decrease in humidity increases the chipping resistance of enameled-iron specimens in torsion, a result which is in agreement with the modulus-of-rupture tests on frit fibers.

The data represented by the squares in figure 3 show that under the conditions of test the effect of varying humidity is reversible; that is, the lowering of strength at 98-percent relative humidity did not persist after the specimens were returned to an atmosphere of 35-

percent relative humidity. This reversibility is in accord with the findings of Milligan [10] and Anderegg [17] that glass weakened by immersion in water regained its strength when dried.

That the mechanism of capillary attraction discussed in connection with the tests on enamel fibers may, under some conditions, be quite important is suggested by the following qualitative experiment:

The enameled-metal specimen is first twisted about 90° at room humidity, causing a permanent strain which is of sufficient magnitude to chip the enamel considerably. In several hours the continued chipping off of the small fragments will have practically stopped. However, when the same specimen is subsequently placed in a pan of water, additional chipping will immediately set in, and within 15 min the specimen may show as much as 50 percent more chipping than had taken place during several hours in the open air.

Since numerous crevices undoubtedly exist in the enamel after the specimen is chipped by twisting, but prior to immersion, and since the effect of immersion is very rapid, the mechanism of capillary attraction may be of importance under the conditions of this experiment. Even so, its action might merely supplement that of the gel film postulated by Grebenchikov or of the dissolved water mentioned by the authors as a possible contributory explanation of the effect of moisture on the strength of enamels and similar materials.

V. MODULUS OF ELASTICITY TESTS

1. METHOD OF TESTING AND TREATMENT OF DATA

Modulus of elasticity was determined by a method similar to that used in a previous study [5]. The specimens were measured with a dial micrometer to the nearest 0.005 mm. A small flag consisting of a gummed label was fixed to one end of each specimen for identification purposes and also to indicate the least diameter in specimens of slightly elliptical cross section. Ten readings, evenly spaced along the axis of the specimen, were averaged for the minimum diameter and another 10 were taken at right angles thereto for the maximum diameter. No specimens were used with maximum deviations from the average greater than 0.045 mm. During a test a micrometer microscope, which could be read to 0.005 mm, was mounted to focus on the midspan of the enamel fiber. The fiber rested on fixed knife-edges separated by a span of 91.23 mm. A small aluminum pan, giving a tare of 5 g, was suspended by a fine wire from the midpoint of the span. The load, either 5 or 10 g, depending on the diameter of the specimen, was applied by placing calibrated weights on the pan. By rotating the specimen through an angle of 90° after each deflection reading, four measurements were obtained for each fiber, and the average of the four was used for computing the modulus.

The data were treated statistically by the procedure used in the increasing-load tests for strength.

2. EFFECT OF HUMIDITY ON MODULUS OF ELASTICITY

Several tests were made to determine the effect of humidity on the modulus of elasticity of enamel-frit fibers. Frits 1 and 65 were chosen for study, and determinations were made at 22° C (72° F) in

atmospheres at 98- and 50-percent relative humidities, respectively. The data showed no change in Young's modulus, and therefore humidity was not controlled for the tests reported in table 3.

3. VARIATION IN YOUNG'S MODULUS WITH TYPE OF FRIT

Table 3 includes a summary of the data obtained on the eight frits. Tests for differences in the averages showed Young's modulus of the "soft" ground-coat frit 1 to be significantly lower than that for the "hard" ground-coat frit 11. Cover coats 25, 35, and 65 had lower moduli than the acid-resisting cover-coat frit 6. The lead-bearing enamels, frits 85 and 72, have lower moduli than the other types, that of the high-lead composition (frit 72) being lowest.

Figure 4 is a frequency histogram prepared from the data on frit 11. A total of 78 specimens of this frit were tested to establish whether or not the determined values were approximately normally distributed. Visual examination of figure 4 suggests an approximately normal distribution, and calculated skewness is only +0.10 [7].

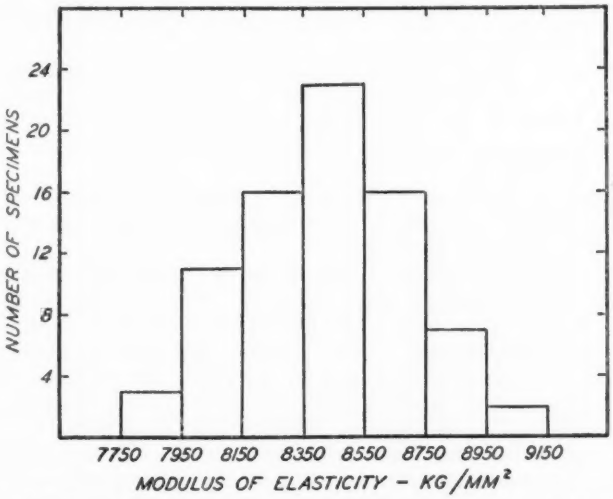

FIGURE 4.—*Frequency histogram showing distribution of 78 modulus-of-elasticity determinations with ground-coat frit 11.*

4. DISCUSSION OF RESULTS

The average moduli in table 3 are of about the same order of magnitude as those reported previously by Harrison, Shelton, and Wadleigh [5], and are about 8 percent higher on the average than the results given by Stong [18] for a special bulb-glass composition. The values approximating 4,000 kg/mm² reported by Anderegg [17] for glass fibers are in fair agreement with those reported by Reinkober [12]. However, subsequent results by Jurkov [14], using more precise methods of measuring deflections, did not agree with Reinkober's data. The average modulus given by Jurkov is 8,000 kg/mm². The results of Fetterolf and Parmelee [19] are considerably lower, approxi-

mating 5,000 to 6,000 kg/mm². Their results, however, were obtained on rods of much larger cross section loaded as cantilevers.

VI. CONCLUSIONS

1. The modulus of rupture of enamel-frit fibers increased with decreasing atmospheric humidity. The maximum change observed was in the sustained-load test, in which a "soft" sheet-iron ground-coat frit (1) was 53 percent stronger at 56-percent relative humidity than at 90 percent, the temperature being 36° C (97° F). Under the same conditions an acid-resisting sheet-iron frit (6) was 15 percent stronger at the lower humidity.

2. In the increasing-load test the gains in strength of these frits were 8 and 22 percent, respectively, when the relative humidity was decreased from 98 to 35 percent at 21° C (70° F).

3. The modulus of rupture of enamel-frit fibers was substantially greater when they were dried over $CaCl_2$ and immersed in water-free kerosene than when they were immersed in water, the acid-resisting frit (6) showing a 49-percent increase and the ground coat (1) a 30-percent increase. Tests of immersed specimens were made by the increasing-load method only.

4. Specimens stored in air at about 60- to 65-percent relative humidity and tested while immersed in alcohol, and similarly stored specimens tested in air, had about equal strength, which was intermediate between the strengths for the two conditions described in the preceding conclusion.

5. Specimens dried over $CaCl_2$ and immersed in kerosene did not vary significantly in strength when the temperature was raised from 27° C (81° F) to 62° C (144° F).

6. The moduli of rupture of frit fibers of the sheet-iron cover coats were significantly greater than those of both the sheet-iron ground coats and the cast-iron frits when tested by the increasing-load test as used in this investigation. The leadless cast-iron enamel frit (65) was significantly weaker than any of the other compositions tested.

7. The modulus of elasticity of two frits (1 and 65) was not significantly affected by changes in atmospheric humidity.

8. The acid-resisting sheet-iron cover coat (6) and the "hard" sheet-iron ground-coat frit (11) under the test conditions used in this investigation, had the highest Young's modulus, approximately 8,400 kg/mm². The other sheet-iron cover coats and the leadless cast-iron enamel gave average moduli of about 8,000 kg/mm², while the lead-bearing cast-iron enamels were significantly lower, the high-lead composition being lowest.

9. When applied to 20-gage metal, the resistance of an acid-resisting enamel (6) to chipping in torsion increased about 15 percent with a decrease in relative humidity from 98 to 35 percent. A thin paraffin coating over the enamel surface, applied before the specimens were quite cool after firing, increased the resistance of these specimens to chipping in torsion by about 30 percent, even though the surrounding air was at 98-percent relative humidity.

VII. REFERENCES

[1] W. N. Harrison, R. E. Stephens, and S. M. Shelton, J. Research NBS **20,** 39 (1938) RP1063.
[2] W. N. Harrison and D. G. Moore, J. Research NBS **21,** 337 (1938) RP1133.
[3] W. N. Harrison and B. J. Sweo, BS J. Research **10,** 189 (1933) RP524.
[4] L. V. Black, Bul. Am. Ceram. Soc. **15,** 274 (1936).
[5] W. N. Harrison, S. M. Shelton, and W. H. Wadleigh, J. Am. Ceram. Soc. **18,** 100 (1935).
[6] C. I. Bliss, Ann. Applied Biol. **22,** 134 (1935).
[7] Am. Soc. Testing Materials Manual on Presentation of Data (March 1937).
[8] R. A. Fisher, Statistical Methods for Research Workers (Oliver and Boyd, London; 1936 edition).
[9] A. C. Harrison, J. Am. Ceram. Soc. **10,** 77 (1927).
[10] L. H. Milligan, J. Soc. Glass Tech. **13,** 351 (1929).
[11] S. Schurkow, Physik. Z. Sowjetunion **1,** 123 (1932).
[12] O. Reinkober, Physik. Z. **38,** 112 (1937).
[13] A. A. Griffith, Phil. Trans. Roy. Soc. (London) [A] **221,** 163 (1920).
[14] S. Jurkov, Tech. Phys. USSR **1,** 392 (1935).
[15] C. Hahner, G. Q. Voigt, and A. N. Finn, J. Research NBS **19,** 95 (1937) RP 1014.
[16] A. Brenner, J. Research NBS **20,** 357 (1938) RP1081.
[17] F. O. Anderegg, Ind. Eng. Chem. **31,** 290 (1939).
[18] G. A. Stong, J. Am. Ceram. Soc. **20,** 16 (1937).
[19] L. D. Fetterolf and C. W. Parmelee, J. Am. Ceram. Soc. **12,** 3 (1929).

WASHINGTON, July 14, 1939.

168819—39——2

U. S. DEPARTMENT OF COMMERCE NATIONAL BUREAU OF STANDARDS

RESEARCH PAPER RP1238

Part of Journal of Research of the National Bureau of Standards, Volume 23, September 1939

SATURATION OF GASES BY LABORATORY WET TEST METERS

By Francis A. Smith and John H. Eiseman

ABSTRACT

A laboratory wet test meter registering $\frac{1}{10}$ cubic foot per revolution has been studied by the National Bureau of Standards, at the request of a committee of the American Society for Testing Materials, to determine: (*a*) how nearly the gas passing through the meter becomes saturated with water from the meter, (*b*) the error in the indicated volume resulting from a lack of complete saturation at different rates of flow, and (*c*) the error in the indicated volume resulting from failure to level the meter.

Saturation of dry air was found to be over 98 percent complete at all practicable rates of flow. The directly observed error in the indicated volume was found to be less than 0.2 percent. Errors resulting from failure to level the meter were found to be less than 0.1 percent, provided the quantity of water in the meter was the same as at calibration.

CONTENTS

	Page
I. Introduction	345
II. Degree of saturation of gas in a wet test meter	346
III. Error resulting from incomplete saturation	349
IV. Effect of tilting a meter on the indication of gas volume	351
V. Discussion of results	353

I. INTRODUCTION

In January 1937, at the request of the American Society for Testing Materials (Committee D–3 on Gaseous Fuels, Subcommittee II on Measurement of Gaseous Samples), the National Bureau of Standards undertook to determine (*a*) how nearly the gas passing through a laboratory wet test meter becomes saturated with water from the meter, (*b*) to what extent the volume indicated by such a meter might be in error as a result of failure to saturate the gas completely at different rates of flow, and (*c*) to what extent the volume indicated might be in error as a result of failure to level the meter when moved after proving.

The method chosen for (*a*) necessitated a sensitive means of determining water vapor in air which is nearly saturated. A gas interferometer was chosen for the purpose, preliminary tests having indicated that it would permit the determination of the water vapor to approximately ± 0.05 percent.

The methods chosen for (*b*) and (*c*) involved the observation of differences in the indications of the meter. Consequently, the accuracy of the results reported is dependent not on an accurate calibration of the meters but only on their ability to give consistent results when the tests were repeated under identical conditions.

The two meters used were calorimeter meters each of which indicated 0.1 cu ft per revolution. These meters were adjusted and calibrated by the Gas Measuring Instruments Section by comparison with a 5-cu ft oil-sealed meter prover before the beginning of the tests, at rates of flow ranging from 1.4 to 11.4 cu ft per hour. The range used in the tests was 0.7 to 12.4 cu ft. per hour.

II. DEGREE OF SATURATION OF GAS IN A WET TEST METER

The equipment used in this determination is shown diagrammatically in figure 1.

Air from the laboratory compressed-air line entered through cock *A*,

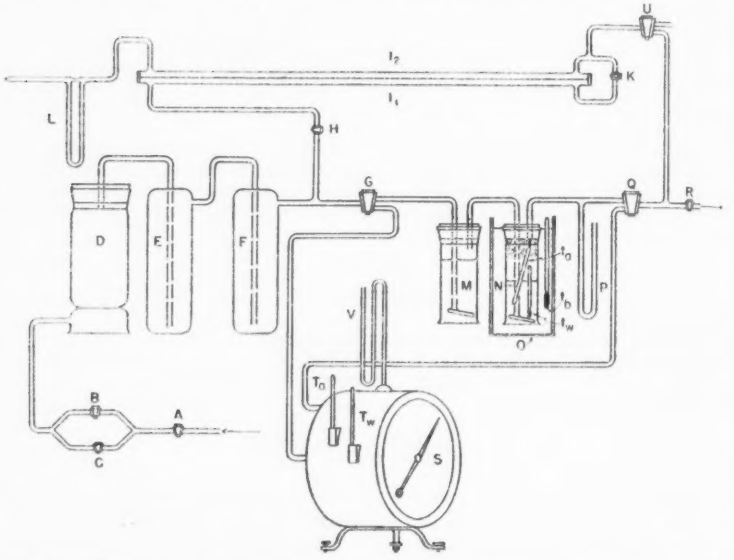

FIGURE 1.—*Diagram of apparatus used to test completeness of saturation of air passing through a wet test meter.*

opened fully, and passed through cocks *B* and *C* in parallel. *B* alone gave the desired low rate. *B* and *C* together gave the desired high rate. Alternate changes from one to the other were then accomplished without readjustment by completely opening or closing cock *C*. The air then passed through a tower of calcium chloride (*D*) for preliminary drying and then through two tubes of dehydrated alumina gel (*E* and *F*), which reduced the water vapor in the effluent air to less than 0.01 percent.

From this point (cock *U* being closed) the dried air was divided, part passing through cock *G* and part through cock *H*. Cock *H* was set to give an arbitrary small flow (as indicated by flowmeter *L*) through tube I_1 of the gas interferometer, through cock *K*, through tube I_2 of the interferometer, and out through the flowmeter. Cock *H* was then closed, isolating in the two tubes of the interferometer a sample of dried air at atmospheric pressure. The reading of the inter-

ferometer scale under a typical set of conditions was 418.0, which corresponded to 0 percent of water vapor in tube I_2, as compared with that in tube I_1 as a standard for reference.

Cock K was then closed, which isolated the standard of reference in tube I_1. All the dried air then passed through cock G to saturator M, where most of the water was added, and thence to saturator N, where equilibrium was established. N was immersed in a tall bath of water, O, whose temperature was measured by thermometer t_b. In both M and N the air bubbled into distilled water through a sintered glass frit at the end of the bubbling tube, which produced a large number of very small bubbles and insured complete saturation. The temperature of the water was determined at the level of the frit by thermometer t_w. The top of the bottle was filled with glass wool to catch the droplets thrown by the bursting bubbles; and the temperature of the moist glass wool was determined by a third thermometer, t_a, which temperature was taken as the temperature of saturation.

From this point the moist air passed a manometer, P, through cock Q and out through cock R. After equilibrium had been established, a portion was passed through cock U and through tube I_2 of the interferometer. When I_2 had been thoroughly purged with the moist air, cock U was again closed and K opened to bring I_1 and I_2 to the same, as well as to atmospheric, pressure. The reading of the interferometer scale was 345.0, which corresponded to complete saturation under the conditions observed in the saturator.

The barometric pressure (765.7 mm) plus the pressure indicated by manometer P (8.9 mm) gave the total pressure (774.6 mm) of the mixture of air and water vapor leaving the saturator. The temperature of the saturator bath was 22.0° C, of the saturator water 21.9° C, and of the glass wool 22.0° C. The latter was taken as the temperature of saturation; and, since the temperature of the room was 24.9° C, no loss of water from the air through condensation could occur. The partial pressure of water vapor at 22.0° C is 19.84 mm, which is 2.56 percent of the total pressure at saturation.

The interferometer-scale reading of 345.0 thus corresponded to 2.56 percent of water vapor, and the above steps have sufficed to determine two points on a curve constituting an empirical calibration of the interferometer. Figure 2 shows the two points on the interferometer calibration curve, indicated by circles, with a straight line drawn through them.

Cocks G and Q were then reversed, which sent the dried air through the wet test meter S. Cock R was adjusted to make the pressure on meter manometer V approximately equal to that indicated by P when the air was passed through the saturator. This made the pressure of saturation approximately the same in both cases, and, after determining the rate of flow by timing the meter, the same rate could be assumed without significant error for the flow through the saturator.

After equilibrium had again been established, a portion of the flow was again diverted through tube I_2 of the interferometer by opening U, and the temperatures of the water and air in the meter were read on thermometers T_w and T_a. After closing U and opening K, the interferometer scale was read as before.

In the present illustrative case, the barometric pressure (765.5 mm) plus the meter pressure (8.9 mm) gave a total pressure of 774.4 mm.

The temperature of the air in the meter was 23.8° C, of the water 23.0° C, and of the room 24.7° C. The temperature of the water was taken as the temperature of the unknown degree of saturation. The partial pressure of water vapor at 23.0° C is 21.09 mm, which was 2.72 percent of the total pressure. However, the interferometer scale read 342.2. This scale reading, on the interferometer calibration in figure 2, corresponded to 2.70 percent of water vapor, as indicated by the cross.

This indicated that only 2.70 percent of water actually was in the air from the wet test meter, while 2.72 percent would have been present had the air been completely saturated. Thus, on passing

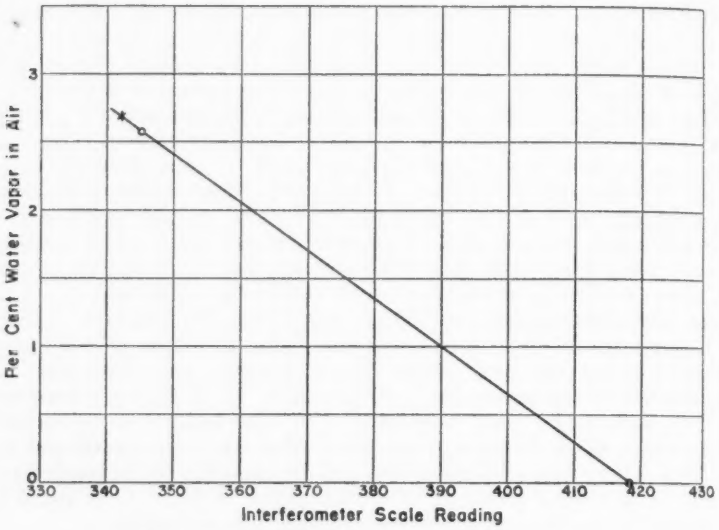

FIGURE 2.—*Calibration of gas interferometer.*

through the wet test meter, saturation of the dried air was 2.70/2.72= 99.4 percent complete at a rate of flow of 12.4 cu ft per hour.

The procedure described above was repeated alternately at high and low rates of flow, with the results shown in table 1.

TABLE 1.—*Extent of saturation of dried air at high and low rates of flow*

Rate of flow (cu ft per hr)	Completeness of saturation
	Percent
12.42	99.4
0.82	97.2
12.30	97.9
0.80	98.7
12.20	99.4
0.86	97.3

The completeness of saturation at the high rates of flow averaged 98.9 percent, whereas at the low rates of flow the average was 97.7. This was unexpected, and investigation disclosed the fact that, at low rates of flow, only the tip of the bulb of the water thermometer in the meter projected below the surface of the water. At high rates of flow the water level rose and about half of the bulb was immersed. These circumstances account for the observations of lower water-thermometer readings at high rates of flow than at low rates and indicate that all the thermometer readings of water temperature were probably slightly high. Because the thermometers were enclosed, bulb and all, in metal shields, it was impossible to alter their position with respect to the water. The regular thermometer was then replaced by a laboratory thermometer inserted through a rubber stopper far enough to immerse the bulb completely at all times, and this was used in the tests reported in section III. An estimated correction was applied to the thermometer readings observed at the low rates, with the result that the computed completeness of saturation was raised to a few tenths over 100 percent.

It is concluded that the completeness of saturation of dry air is at least 98 percent at any practicable rate of flow. Since the water vapor involved will usually amount to less than 3 percent of the total indicated volume, the error, as a result of incompleteness of saturation, will be less than 0.06 percent of the volume indicated by the meter, provided the degree of saturation at the moment the measured volume of gas is sealed off in the rotating measuring chamber is equal to the degree of saturation when the gas finally leaves the meter. However, the measured gas has considerable opportunity to become more nearly saturated within the meter after it has been sealed off, and it seemed necessary, for this reason, to make a further test by comparing the relative volumes indicated by the meter when supplied with dry and with saturated air.

III. ERROR RESULTING FROM INCOMPLETE SATURATION

The conclusion from the tests described in section II was checked by direct observation of the volumes indicated by the meter, in the following manner. The two meters used in this investigation were connected as indicated in the diagram in figure 3.

Air from the laboratory compressed-air line entered through cock *A*, had its flow controlled by *B* and *C*, and was dried in *D*, *E*, and *F*, as described in section II. Cocks *G* and *Q* were turned to pass the dried air through saturators *M* and *N*, indicated in figure 3 and described in section II. The air from the saturator passed through meter *T*, on which the variations were observed, and then through meter *S*, which was used as a standard for comparison.

Air was passed through the apparatus (with cock *C* open to give high rate of flow) until temperature equilibrium had been established, when the flow was stopped by closing *A*. The reading of each meter was observed, the flow started and continued until meter *S* had made five revolutions, when the flow was again stopped and the meters read. Observations of temperature and pressure of both meters were made while the gas was flowing. Cock *C* was then closed to give a low rate of flow and the procedure repeated.

Then with cock C open, cocks G and Q were turned to pass the dried air directly into meter T, and the steps described in the above paragraph repeated. This gave four sets of readings, two at a high rate of flow, one with the air entering meter T wet and the other with it dry, and two similar ones at a low rate of flow. All the observed volumes were placed on a comparable basis by correcting each to the arbitrary standard condition of 760 mm and 25.0° C. This represents approximately the average of the temperatures and pressures existing during the tests. The observed temperatures were all within 1° C and the pressures within 2 mm of these conditions. In addition, the corrected volumes passing meter T have been multiplied by the factor required to bring the corrected volume passing meter S to 0.5000 cu ft.

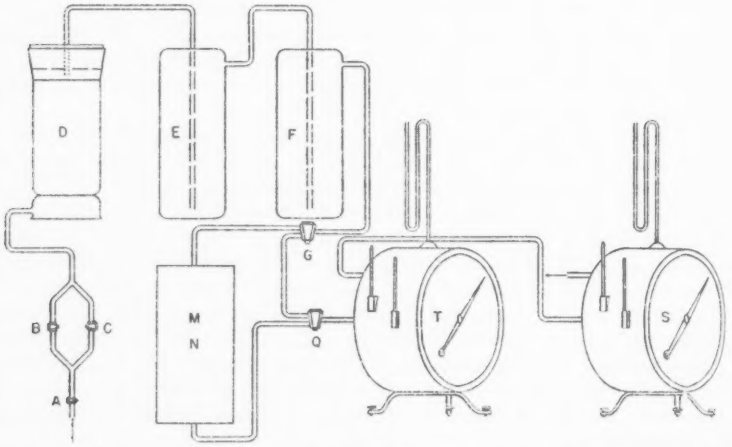

FIGURE 3.—*Diagram of apparatus used to detect variations in indication of a wet test meter when supplied with saturated as compared with dried air.*

The essential data from four series of observations made as described are shown in table 2. This procedure was repeated three times and comparisons made between the "wet" and "dry" indications of meter T at both high and low rates of flow. A summary of the results is presented in table 3.

TABLE 2.—*Data illustrating the method used in computing the results obtained by comparing the indicated volume of saturated air with the volume indicated when dry air entered the meter*

[It will be noted that the volume of air passed by meter S corrected to 25° C and 760 mm (shown in line 4) is not 0.5000 cu ft. The corrected volume passing meter T (line 6) has therefore been multiplied by the factor required to bring the volumes of line 4 to 0.5000 and the result entered in line 7]

Rate of flow (cu ft/hr)	10.46	10.77	0.77	1.20
Air entering meter T	Wet	Dry	Wet	Dry
Volume indicated by meter S (cu ft)	0.5000	0.4996	0.5000	0.5003
Volume indicated by meter S corrected to 25° C, 760 mm	.5016	.4990	.5009	.4997
Volume indicated by meter T (cu ft)	.4882	.4876	.4886	.4885
Volume indicated by meter T corrected to 25° C, 760 mm	.4908	.4876	.4898	.4877
Volume of meter T equivalent to 0.5000 cu ft through meter S	.4892	.4886	.4889	.4880
Difference between wet and dry (cu ft)	.0006		.0009	
Difference (percent)	.12		.18	

TABLE 3.—*Summary of results showing direct effect of incomplete saturation on the volume indicated by a one-tenth cubic foot wet test meter*

Rate of flow	Condition of air entering meter T	Difference in indication (wet−dry)	Difference in indication	
cu ft/hr		*cu ft*	*Percent*	
10.94	Wet	0.0009	0.18	
10.67	Dry			
0.81	Wet	−.0007		−0.14
1.21	Dry			
10.67	Dry	.0008	.16	
10.46	Wet			
1.21	Dry	.0000		.00
0.77	Wet			
10.46	Wet	.0006	.12	
10.77	Dry			
0.77	Wet	.0009		.18
1.20	Dry			
10.77	Dry	.0008	.16	
9.38	Wet			
1.20	Dry	.0012		.24
0.73	Wet			
9.38	Wet	.0008	.16	
11.03	Dry			
0.73	Wet	.0008		.16
1.26	Dry			
Average for high rate of flow			0.16	
Average for low rate of flow				0.09

It will be noted that in 9 of the 10 comparisons the meter under test indicated a greater volume with wet air than with dry air, with a maximum difference of 0.24 percent. The negative difference seems to indicate the possibility of a random error of the order of 0.3 percent superposed on a smaller effect caused by lack of saturation. The consistency of the positive differences, especially those associated with the higher rates of flow, indicates a real effect of the order of 0.15 percent which might be attributed to lack of saturation. The one negative difference is associated with a low rate of flow, under which conditions the relative indications of the two meters had previously been found to differ by as much as 0.5 percent from their relative indications at higher rates of flow. The data of this report do not permit a determination of the cause of this behavior, but it undoubtedly will result in much larger errors than those caused by lack of saturation of the gas with water vapor.

In spite of the variability of the differences associated with low rates of flow, there is little to indicate that there is any real difference which is attributable to rate of flow in the effect of saturation on the indication of the meter.

IV. EFFECT OF TILTING A METER ON THE INDICATION OF GAS VOLUME

In these tests the arrangement of apparatus was the same as that described in section III. The drying equipment was dispensed with and all the air entering the meter to be tested passed through the saturator. The meter to be tilted was fitted with a plumb line, and a scale was mounted horizontally 500 mm below the point of support of the plumb line. The angle of tilt could readily be determined from the deflection of the plumb line on the scale.

In all these tests the deflection was 6.5 mm, making the tangent of the angle 6.5/500 = 0.0130, which corresponds to an angle of 0°45′. This angle resulted when the meter was tilted sufficiently to move the bubble in the spirit level on the meter through one half its length. The tilt was easily noticeable and probably represents even worse than careless use of a meter with respect to leveling.

The tests were arranged in a sequence in which three series of observations were made with the meter level, three with the meter tilted but without any readjustment of water level, three with the tilt unchanged but with the water level adjusted to the mark in the gage, and finally, three with the meter again level and with the water restored to its original position in the gage. The rate of flow was kept approximately in midrange between the extremes previously used, that is, between 5.5 and 6.5 cu ft per hour. The meter was tilted both clockwise and counterclockwise about the axis of the drum, keeping it level from front to back, and both forward and backward while keeping it level from side to side. For brevity, only the data from the clockwise and forward tilts are presented here. The data have been treated in the manner indicated in table 4.

TABLE 4.—*Data illustrating the method of computing results of tests of the effect of tilting 0°45′ on the indication of a one-tenth cubic foot wet test meter*

	Meter *T* level			Meter *T* tilted clockwise, no adjustment of water level		
Volume indicated by meter *S* (cu ft)	0.5000	0.5000	0.5000	0.5000	0.5000	0.5000
Volume indicated by meter *S* corrected to 25 °C, 760 mm	.5057	.5057	.5055	.5052	.5052	.5050
Volume indicated by meter *T* (cu ft)	.4909	.4907	.4910	.4910	.4905	.4908
Volume indicated by meter *T* corrected to 25°C, 760 mm	.4973	.4968	.4971	.4966	.4961	.4959
Volume indicated by meter *T* equivalent to 0.5000 cu ft through meter *S*	.4917	.4912	.4917	.4915	.4910	.4910
Averages		.4915			.4912	
Difference, level minus tilted (no adjustment of water)		0.0003				
Difference (percent)		.06				

TABLE 5.—*Summary of results of tilting tests*

Condition	Averages of runs (clockwise tilt)	Difference 1—2	Difference 4—3	Averages of runs (forward tilt)	Difference 1—2	Difference 4—3
1. Level	0.4915	0.0003 cu ft; 0.06%.		0.4905	−0.0003 cu ft; −0.06%.	
2. Tilted (no adjustment of water).	.4912			.4908		
3. Tilted (adjustment of water).	.4875		0.0033 cu ft; 0.66%.	.4896		0.0014 cu ft; 0.28%.
4. Level (original water adjustment).	.4908			.4910		

Table 5 presents a summary of the results obtained in the "clockwise" and "forward" tilting tests. From these results, it appears that a relatively large and easily noticeable departure from level introduced no consistent or significant error in the indication of the meter tested, as long as the correct volume of water, determined at the time of calibration, was maintained in the meter. The differences between the volumes shown in lines 1 and 2 of the table are very small, and probably are not much larger than the reproducibility of the tests. On the other hand, after the proper volume of water had been determined by calibration and its position marked in the gage, setting the water level to the mark, when the meter was not accurately leveled, involved changing the quantity of water in the meter by 50 ml in the case of the clockwise tilt and by 13 ml in the case of the forward tilt. The corresponding errors introduced were 0.66 and 0.28 percent, respectively. Tilts in the counterclockwise and backward directions resulted in errors equal in magnitude and opposite in sign to those shown. Tilting in the clockwise direction may introduce an error in the reading of the water temperature by lifting the thermometer entirely out of the water, if its depth of immersion is as slight as that mentioned in section II.

V. DISCUSSION OF RESULTS

The direct determination of the completeness of saturation of the air leaving the wet test meter, when translated into terms of error in the volume indicated, showed that the meter indicated a maximum volume about 0.06 percent less than would have been the case had the gas been saturated. In most cases the gas being measured probably will not enter the meter completely dried as in this case, and the error, if any, would be correspondingly smaller.

The direct observation of the difference of the volume registered when wet air entered the meter, as compared with dry air, indicated the maximum error to be about 0.15 percent. While this is two and one-half times the error arrived at by the other method, the two are of the same order of magnitude and, when considered together, give a better idea of the behavior of the meter under these conditions than would the result of either method alone.

The tests of the effect of tilting the meter on the volume indicated show that when the meter has been once calibrated while accurately level, it is apparently not subject to appreciable error because of any failure to level it which is not obvious, provided the weight of water in the meter is the same as at the time of calibration. However, if the amount of water in the meter is judged by filling to a gage mark, accurate leveling is essential.

In general, the tests described herein show that errors in the indication of small wet test meters arising from incomplete saturation of the gas, or from inaccurate leveling, are small. They are probably negligible as compared with larger errors arising from other causes, such as calibrating a meter at one rate of flow and assuming that the calibration is the same at any other rate.

These conclusions result from tests made on a single meter of the type and size used with manual calorimeters. They do not necessarily apply to meters of other types or sizes.

WASHINGTON, April 18, 1939.

U. S. DEPARTMENT OF COMMERCE NATIONAL BUREAU OF STANDARDS

RESEARCH PAPER RP1239

Part of Journal of Research of the National Bureau of Standards, Volume 23, September 1939

METHOD OF DESIGNATING COLORS [1]

By Deane B. Judd [2] and Kenneth L. Kelly [3]

ABSTRACT

In 1931 the first chairman of the Inter-Society Color Council, E. N. Gathercoal, proposed on behalf of the United States Pharmacopoeial Revision Committee the problem of devising a system of color designations for drugs and chemicals. He said, "A means of designating colors in the United States Pharmacopoeia, in the National Formulary, and in general pharmaceutical literature is desired; such designation to be sufficiently standardized as to be acceptable and usable by science, sufficiently broad to be appreciated and used by science, art, and industry, and sufficiently commonplace to be understood, at least in a general way, by the whole public." With the assistance of the American Pharmaceutical Association, and following plans outlined in 1933 by the Inter-Society Color Council, there has been worked out a solution for this problem, which substantially fulfills the requirements laid down by Dr. Gathercoal.

CONTENTS

	Page
I. History	356
II. Scope	356
III. Logic of the designations	356
1. Surface-color solid	356
2. Basic plan of forming the designations	358
3. Divisions of the hue circle	359
4. Pink, orange, brown, and olive	359
5. Some unavoidable disadvantages	359
IV. Definition of the color ranges	360
V. Hue boundaries for various ranges of Munsell value and chroma	361
VI. Color designations for opaque powders	361
1. Preparation of sample	361
2. Lighting and viewing conditions	362
3. Procedure	362
4. An example	363
VII. Color designations for whole crude drugs	363
1. Comparison with Munsell color standards	363
2. Lighting and viewing conditions	363
3. Ways of using the color designations	364
VIII. Color designations for any object	364
1. For opaque nonmetallic materials	364
(a) With matte surfaces	364
(b) With glossy surfaces having no regular detailed structure	364
(c) With glossy surfaces made up of cylindrical elements	364
2. For metallic surfaces	365
3. For materials which transmit but do not scatter light	365
4. For translucent materials	365
IX. Summary	365
X. References	366
How to use the color name charts 1 to 34	367

[1] Recommended by the Inter-Society Color Council, June 1939, for drugs and chemicals, and tentatively suggested for general use.

[2] Physicist, National Bureau of Standards, and chairman of the Committee on Color Problems of the Inter-Society Color Council.

[3] Research Associate at the National Bureau of Standards, representing the American Pharmaceutical Association.

I. HISTORY

The problem was referred by the Inter-Society Color Council to its Committee on Measurement and Specification which, under the chairmanship of I. H. Godlove, presented several reports surveying available methods of color designation. The 1933 annual report of this committe included the outline of a recommended system of color designations. These recommendations were approved by the Council and have been followed by the authors, who have developed this system of color designations, have set the color boundaries, and have worked out methods of applying the system to drugs and chemicals in various forms. The Inter-Society Color Council in 1939 formally approved by letter ballot and recommended to the United States Pharmacopoeial Convention the method now to be described.

Member bodies of the Council whose voting delegates have approved this method of designating the colors of drugs and chemicals are: [4]

American Association of Textile Chemists and Colorists.
American Ceramic Society.
American Psychological Association.
American Society for Testing Materials.
Illuminating Engineering Society.
National Formulary, American Pharmaceutical Association.
Optical Society of America.
Technical Association of the Pulp and Paper Industry.
United States Pharmacopoeial Convention.

II. SCOPE

The recommended color designations apply to powdered drugs and chemicals and to whole crude drugs viewed in daylight. The Council is now engaged in a study of the general applicability of these designations to colors of opaque, nonmetallic surfaces with a view to official adoption for all such surfaces.

The recommended system does not give suitable color designations in its present form for liquids and solids viewed by transmitted light. An extension of the system to cover such samples has been undertaken by the Council. (See also section VIII, 3.)

III. LOGIC OF THE DESIGNATIONS

The designation for all but very grayish colors consists of a hue name (*red*, *green*, *blue*, *purple*, etc.) preceded by appropriate modifiers (such as *weak*, *moderate*, *strong*, *light*, and *dark*). The designation for very grayish colors consists of a noun (*white*, *gray*, or *black*), with modifiers appropriate to the lightness and hue of the colors (such as *dark reddish gray* or *yellowish white*).

1. SURFACE-COLOR SOLID

The relationships between the names can best be understood by a consideration of the psychological color solid. The dimensions of this solid are hue, lightness, and saturation (see fig. 1); the color of any

[4] A majority of the voting delegates representing the individual members of the Council also approved. Textile Color Card Association of the United States (not voting).

matte, opaque surface in daylight is represented by some point in it; hence it is often called the surface-color solid. Lightness starts at zero for black, represented at the bottom of the figure, and is measured by distance from the base plane, being a maximum for white represented at the top of the figure. Hue is represented by angle about the black-white axis, giving the closed series red, yellow, green, blue,

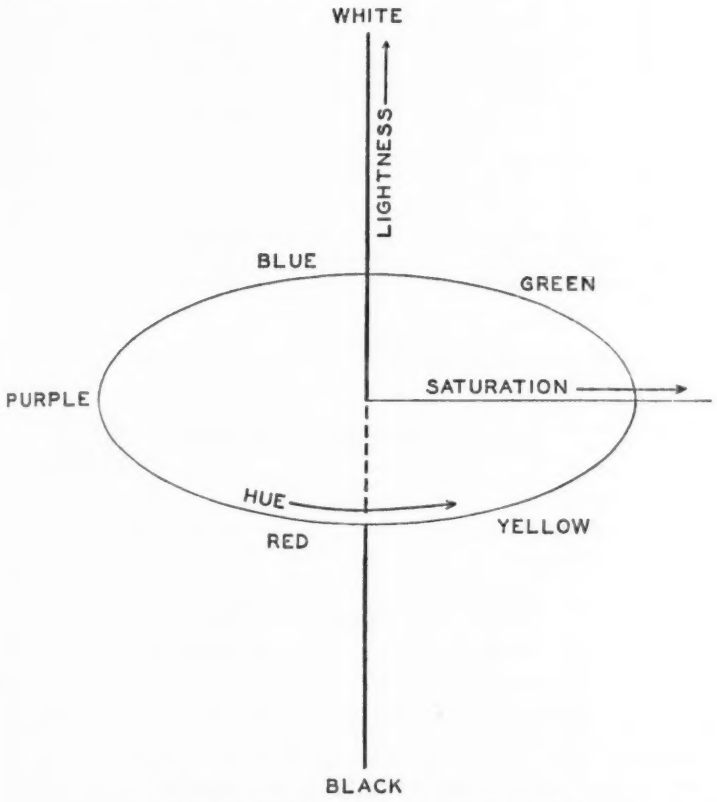

FIGURE 1.—*Dimensions of the surface-color solid.*

purple, red, with their intermediates. Saturation is represented by distance from the black-white axis, being zero for black, white and the intermediate grays, and increasing toward the boundary of the surface-color solid on which would be represented the most vivid colors producible from surfaces [1].[5]

Colors of one hue are therefore represented in the solid by points falling in a single one of the vertical planes intersecting at the black-white axis. Colors of one lightness are represented by points in any one horizontal plane; and colors of one saturation are represented by points in any one of the series of right circular cylinders concentric about the black-white axis.

[5] Figures in brackets indicate the literature references at the end of this paper.

2. BASIC PLAN OF FORMING THE DESIGNATIONS

The hue name of the color designation is intended to indicate a range of hue angle in the color solid, and other words in the designation are to indicate ranges of lightness and saturation for this hue range. The system of modifiers is indicated in figure 2. Deviations

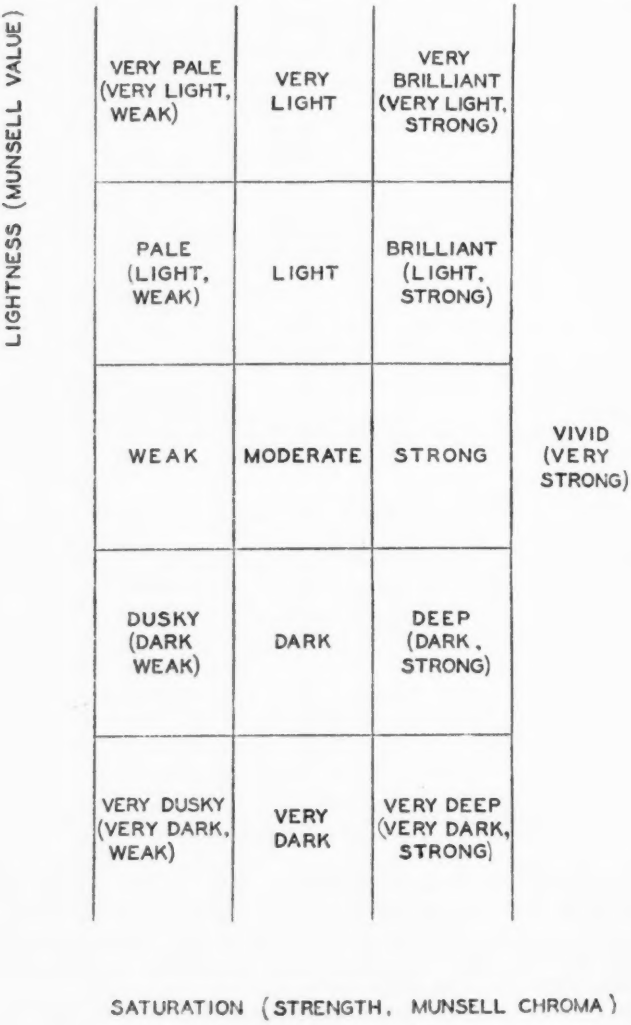

FIGURE 2.—*System of modifiers.*

The color designation, except for very grayish colors, consists of a hue name combined with one of these modifiers.

from the moderate range in lightness are indicated by the terms, *light* and *dark;* deviations in saturation by the terms *weak, strong,* and *vivid;* and deviations in both lightness and saturation by the terms *pale, deep, dusky,* and *brilliant.* The whole color designation, hue

name and modifiers, therefore, defines a block of the surface-color solid bounded by vertical planes of constant hue, horizontal planes of constant lightness, and cylindrical sufaces of constant saturation. The surface-color solid is divided into 314 such blocks, with 5 cylindrical blocks for black, grays, and white, making 319 blocks in all.

3. DIVISIONS OF THE HUE CIRCLE

The 1933 recommendations by Dr. Godlove included a 20-point division of the hue circle for colors of moderate saturation, a 10-point division for weak colors and a 5-point division for very weak colors. By adhering to the principle of this recommendation it has been possible to make each color designation refer more nearly to the same-sized color range than would otherwise have been possible. Deviations from the 1933 recommendations have been introduced to make the color designations accord more closely with present usage, particularly usage in the United States Pharmacopoeia and National Formulary. Most of these deviations arise from our introduction of the color terms *pink*, *brown*, and *olive*, and our change to a more restricted color range for *orange*.

4. PINK, ORANGE, BROWN, AND OLIVE

Unlike the terms *green* and *blue*, which are hue names applying to all lightnesses and saturations, the term *yellow* is commonly used to designate not only a certain hue range, but also a high-lightness range within this hue range. Dark colors of the same hue as yellow are commonly called *olive* or *olive brown*. Common usage limits the term *orange* even more strictly; it is taken to refer not simply to a range of yellow-red hues but also to a medium-lightness range and a high-saturation range. Colors of the same hue but of lower lightness and saturation than the orange range are called *browns* or *reddish browns*.

To follow common usage in this respect, there is included a series of hue names applicable to dark colors only, as follows: *reddish brown*, *brown*, *yellowish brown*, *olive brown*, *olive*, and *olive green*. As a further concession to common usage, there is also included the following series of hue names applicable to very light colors only: *purplish pink*, *pink*, and *orange pink*. The chief series of hue names to which these two subsidiary series have been fitted follows closely the 20-point division recommended by Dr. Godlove; the chief series includes the names *red*, *reddish orange*, *orange*, *yellowish orange*, *yellow*, *greenish yellow*, *yellow green*, *yellowish green*, *green*, *bluish green*, *blue green*, *greenish blue*, *blue*, *purplish blue*, *bluish purple*, *purple*, *reddish purple*, *red purple*, and *purplish red*.

5. SOME UNAVOIDABLE DISADVANTAGES

A frequent objection to this system of color designations is that each designation refers to a group of distinguishable colors rather than to a single color. Since there are about ten million surface-colors distinguishable in daylight by the trained human eye and only 319 color designations in this system, it is obvious that the average color range denoted by a single designation must contain about 30,000 distinguish-

able colors. If it is important to make distinctions among some of these thousands of colors bearing by this system identical designations, resort must be had to one of the many numerical systems of color specification available. Preeminent among these is the colorimetric coordinate system recommended in 1931 by the International Commission on Illumination [2].

A corollary to this objection is that there are many pairs of easily distinguishable colors which receive by this system the same designation, while there are also many pairs that can scarcely be distinguished which receive different designations. This property is, of course, an unavoidable result of dividing the color solid into an arbitrary number of blocks, one for each of the 319 designations. Analogous disadvantages result from identifying the time of events according to date; two events occurring on the same date may be separated by many hours, but on the other hand two scarcely separable midnight events may have to be assigned different dates. Just as identifying the time of an event by giving the date has proved to be useful, so it is anticipated that a system of color designations such as this will find many uses.

IV. DEFINITION OF THE COLOR RANGES

The adjustment of the boundaries defining the 319 color ranges has been carried out by the committees of the Inter-Society Color Council with reference to the color standards of the Munsell Book of Color [3]. These standards are arranged according to Munsell hue, Munsell value, and Munsell chroma, which are intended to be practical evaluations of the surface-color attributes: hue, lightness, and saturation, respectively. That is, all Munsell standards bearing the same Munsell hue notation are intended to have colors of the same hue; likewise, Munsell value is intended to indicate, and does closely, the lightness of the color; and Munsell chroma corresponds well with saturation. For the present, therefore, the definition of the color ranges is given in terms of Munsell hue, value, and chroma. (See the 34 name charts which form the major part of this paper.)

Ultimately, it will be desirable to supplement this practical definition of the color designations by giving the equivalent definition in terms of the 1931 colorimetric coordinate system [2], which does not depend upon the integrity of material standards of color. Any small uncertainty in the boundaries arising from disagreement among the various sets of Munsell color standards, or from their impermanence, will be resolved through spectrophotometric specifications, already partially available, of two sets of master standards deposited at the National Bureau of Standards in 1935 by the Munsell Color Co. A set of smoothed interpolation curves based upon spectrophotometric measurements of a set of Munsell standards by J. J. Glenn and J. T. Killian in A. C. Hardy's laboratory at the Massachusetts Institute of Technology already permits a fairly reliable transfer from Munsell notation to ICI specification to be made. These interpolation curves are available through Dorothy Nickerson, color technologist, Agricultural Marketing Service, Washington, D. C. The Maerz and Paul Dictionary of Color [4] was used to test the suitability of many of the boundaries, and because of its large number (7,056) of colors, well distributed throughout the surface-color solid, it forms the basis for a very satisfactory possible definition of the

boundaries for practical use. The determination of the color names of only a few of this large number of samples has so far been completed.

V. HUE BOUNDARIES FOR VARIOUS RANGES OF MUNSELL VALUE AND CHROMA

Although the systematically arranged and graded standards of the Munsell Book of Color have proved to be invaluable aids in the choice of color-designation boundaries to accord with common usage, it has been found that best agreement with such usage is obtained by deviating in many cases from constant Munsell hue. One deviation from constant Munsell chroma has also been made (*3Y* to *8Y*, inclusive, change from 1.5 to 2.0 chroma). These deviations are shown on charts 35 and 36 which consist of the hue boundaries for various chroma ranges. Chart 35 refers to dark and medium colors; chart 36, to all light colors having hue boundaries different from the corresponding dark and medium colors. The hues are indicated by abbreviations such as *pR* for *purplish red*, *R* for *red*, *rO* for *reddish orange*, *r-Br* for *reddish brown*, *Ol-Br* for *olive brown*, *p-Pk* for *purplish pink*, *O-Pk* for *orange pink*, and so on. Munsell hue is indicated on the 100-point scale on the outer circle. These charts show at a glance for all Munsell chromas what ranges of Munsell hue are referred to by the various hue names of this system; this information is of course also obtainable from the name charts (1 to 34), themselves, but less conveniently. The central circle marked *N* for *neutral* refers to Munsell chromas less than 0.5. The 6-point division on chart 35 refers to the chroma range (with the exception noted above) 0.5 to 1.5, and yields color designations involving the hue adjectives, *reddish*, *brownish*, *olive*, *greenish*, *bluish*, and *purplish*, such as *reddish gray* and *reddish black*. The 5-point division on chart 36 similarly refers to color designations involving the hue adjectives, *pinkish*, *yellowish*, *greenish*, *bluish*, and *purplish*. The 10-point division on chart 35 refers to the chroma range 1.5 to 3.0 and involves the hue names: *red*, *brown*, *olive brown*, *olive green*, *green*, *blue green*, *blue*, *purplish blue*, *purple*, and *red purple*. The similar ring on chart 36 has 11 divisions: *pink*, *orange pink*, *orange*, *yellow*, *yellow green*, *green*, *blue green*, *blue*, *purplish blue*, *purple*, and *purplish pink*. The 19-point division on chart 35 refers to chromas greater than 3.0, and it will be noted that within the two chroma ranges, 3.0 to 5.0, and greater than 5.0, the hue boundaries for simplicity are kept at constant Munsell hue. As mentioned above, however, it has been found possible to increase agreement of these color designations with common usage by adopting in 5 out of 19 cases a different hue boundary for the chroma range 3.0 to 5.0 than is used for the chroma range 5.0 up. Many of the hue boundaries for the inner rings are also shifted in a corresponding way for the same reason.

VI. COLOR DESIGNATIONS FOR OPAQUE POWDERS

1. PREPARATION OF SAMPLE

The sample is placed slightly heaped up in a clean aluminum holder at least 2 mm deep. Over it is placed an optical-glass cover of 1 mm thickness, which is pressed down with a rotary motion, and two small

rubber bands are snapped across underneath the sample holder between the opposite hooks on the back of the cover glass; see figure 3.

2. LIGHTING AND VIEWING CONDITIONS

The illumination to be used in the color-comparison work is daylight. A table placed by a window so that light reaches the table top from the operator's left or right chiefly from the sky and chiefly at an angle of 45° from the horizontal is recommended. A north window is best because no special precautions are usually required to eliminate direct sunlight, but windows facing in any direction may be used if equipped with suitable diffusing curtains. A canopy of black cloth (preferably black velvet) should be hung above the sample on the side opposite the operator in such a position as to be imaged in the mirror surfaces of the cover glass; such an arrangement eliminates errors from unwanted admixture of light reflected only from the cover glass. The sample and standard placed on the table top are viewed nearly perpendicular to the surfaces, that is, just enough off the perpendicular to avoid having the operator's face mirrored in the cover glass. Illumination at 45° and perpendicular viewing are recommended by the International Commission on Illumination [2]. A skylight or source of artificial daylight located above the sample may also be used, but in such a case the angle of view should be approximately at 45° from the horizontal, and the black cloth should be hung vertically beside the sample opposite the observer. Perpendicular illumination with viewing at 45° gives results equivalent to the recommended ICI method.

It is important that the illumination of sample and working standard be closely the same both in amount and quality; otherwise different Munsell notations will be found by interchanging them. Even with illumination of good uniformity it is best practice to make this interchange as a check during the comparison.

In any computations involving the spectral energy distribution of the illuminant, that of standard illuminant *C* recommended by the International Commission on Illumination [2] as representative of average daylight is to be used.

3. PROCEDURE

Select the two adjacent Munsell constant-hue charts between which the hue of the sample falls. Place these on each side of the sample and cover each with a small gray shield, or if using the large triple-aperture shield (shown in fig. 4), place them under the holes in the side flaps and the sample under the central rectangular opening. The Munsell hue, value, and chroma notations for a sample are found by interpolation among the standards of the Munsell charts; most operators prefer to interpolate first for value, then chroma, and finally hue. For detailed suggestions on this interpolation consult the Munsell Book of Color, Standard edition [3].

Once the Munsell notation is found for the sample, select the color-name chart referring to the hue of the sample (see Munsell hue designations near upper right-hand corner of each name chart). Plot the value and chroma of the sample on this chart, noting that chroma from 0 up to 1.5 has, for convenience, been plotted to a more open scale than the remainder (see vertical double line dividing the two scales

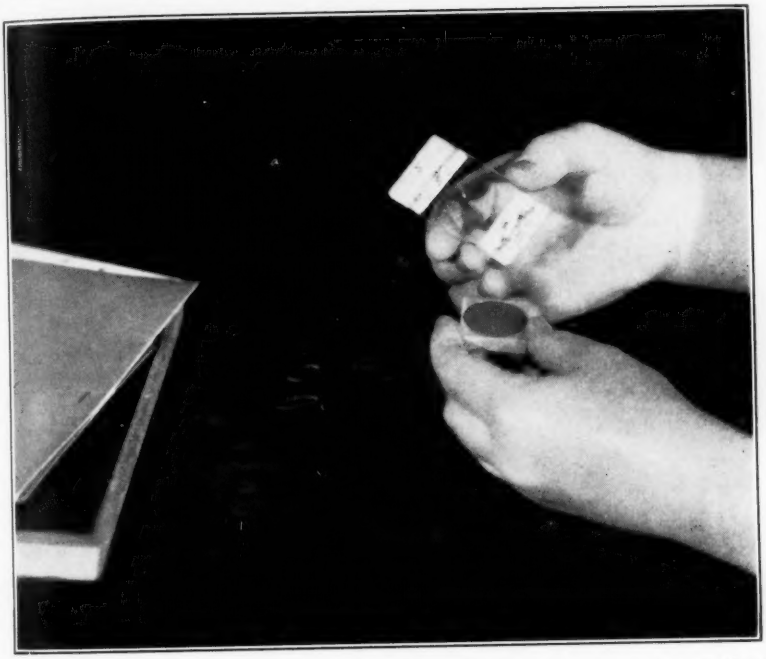

FIGURE 3.—*Preparation of an opaque-powder sample for comparison with the Munsell color standards.*

Note the hooks on the under side of the cover glass, which is attached thereby to the sample holder by means of rubber bands.

UNIV. OF MICH.

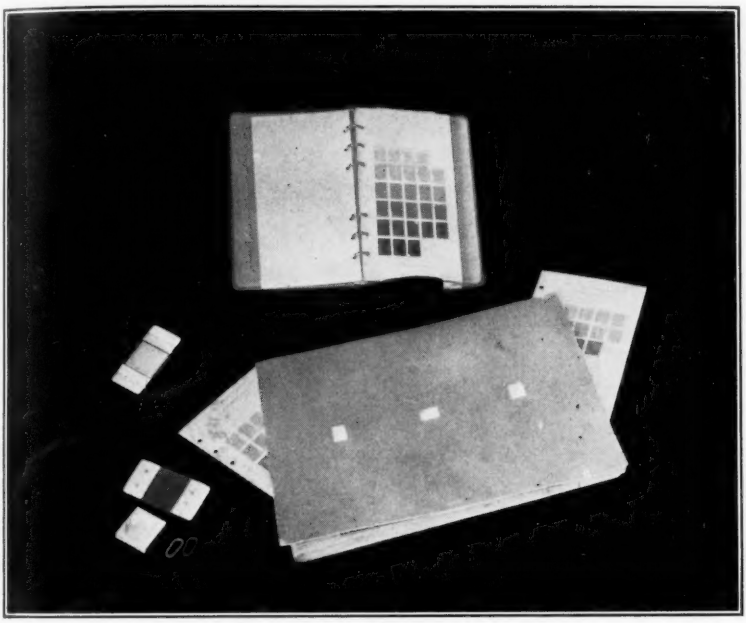

FIGURE 4.—*Triple-aperture shield.*

Sample aperture in center, apertures for Munsell color standards on each side. The abridged edition of the Munsell Book of Color is also shown, together with two sample holders, one assembled, the other taken apart.

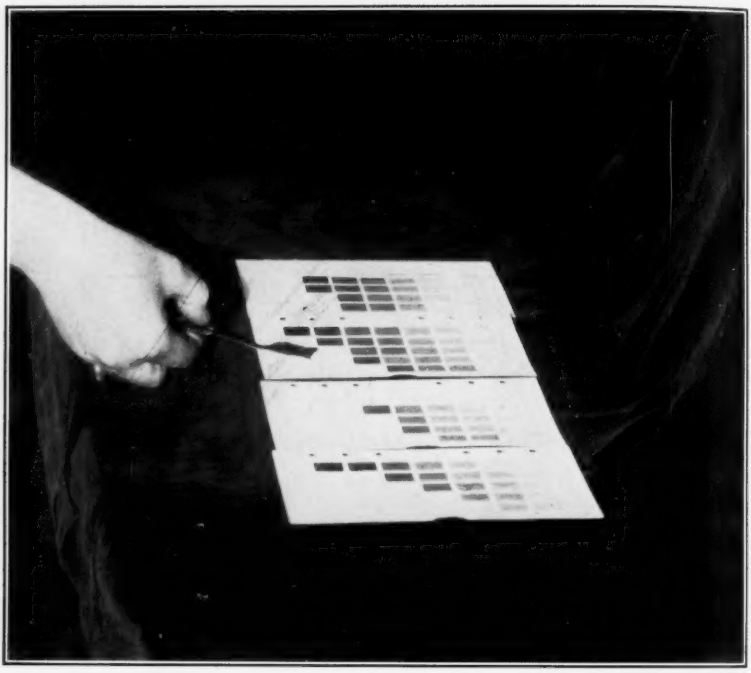

FIGURE 5.—*Comparison of whole crude drugs with the Munsell color standards.*
The crude drug shown is a leaf and is held by the tweezers a few inches above the color standards.

on each name chart). Record the name of the block in which this point falls as the color designation of the sample. If, however, the point falls on a value or chroma boundary, or if the hue notation falls exactly between successive charts yielding different color names, the names of all of the blocks touching the point apply to the sample.

4. AN EXAMPLE

Suppose that the hue of the sample falls between the *YR* (*5YR*) and the *YR–Y* (*10YR*) charts, and that its value falls between 7 and 8 value, but nearer 7, and is estimated as 7.2. Suppose, further, that its chroma is found to be closer to 4 than to 6 and is estimated as 4.5. Now compare the sample with the two Munsell 7/4 standards. Suppose that its hue is seen to be nearer to that of the *YR–Y* chart than the *YR* chart, say 4/5 of the hue difference between the charts or four hue steps from the *YR* and one from the *YR–Y* chart. Now interchange the positions of the charts and check the Munsell notation. If these are found to be unchanged, the final notation is *9YR* 7.2/4.5. Now look through the name charts until the one for *9YR* is found (chart 8, see hue designation near upper right-hand corner). Plot 7.2 value and 4.5 chroma on this chart. It falls in the block named *weak orange;* so the color designation of the sample is *a weak orange.*

VII. COLOR DESIGNATIONS FOR WHOLE CRUDE DRUGS

1. COMPARISON WITH MUNSELL COLOR STANDARDS

Hold the sample in the fingers, or in tweezers if the sample is small, a short distance above the chart or charts and move it about for comparison with the Munsell color standards. Care should be taken not to cast a shadow on the standard with which the sample is being compared; on this account the larger samples should be held higher above the charts than the small (see fig. 5). The time required for the comparison, and consequent soil and wear on the standards, will be saved if the charts are arranged in hue sequence on the table top so that each chart covers the 8- and 10-chroma columns on the preceding chart.

2. LIGHTING AND VIEWING CONDITIONS

The samples are to be illuminated at 45° by daylight (see section VI, 2), and viewed along the perpendicular to the surface. Since the samples are held above the plane of the color standards, it is important that the illumination on the two horizontal planes be the same in amount and quality. Care should be taken to hold the surface of the sample as nearly in the horizontal plane as possible; errors in Munsell value by as much as a whole step are possible through inadvertent tilting of the sample surface. If a source of artificial daylight is used giving a diffused even illumination over a large area from above, or if the comparison is made out of doors by diffuse light from a large part of the sky, the angle at which the sample is held with respect to the light source is less critical.

For minimizing the troubles due to uneven illumination on samples (such as roots) having approximately cylindrical surfaces, it is recommended that the axis of the cylinder be held horizontal and pointed in

the direction of the light source so that neither side of the sample is shaded.

For samples having glossy surfaces the use of a black canopy or curtain will be required as described in section VI, 2.

3. WAYS OF USING THE COLOR DESIGNATIONS

The color of a crude drug may be designated either by giving the name of the average color found in the lot, if the range of color is small, or by giving the color names corresponding to the maximum range of color. This range may be of hue, lightness, or saturation, or a combination of two or all of these. Departures from such a range will frequently be an indication of deterioration or impurity. Color ranges involving chiefly variations in lightness and saturation can often be conveniently indicated by the unmodified hue name, such as *orange*, by which would be meant the color range covered by the designations, *brilliant orange, vivid orange, strong orange, moderate orange, weak orange, light orange, pale orange, dark orange,* and *deep orange* (see charts 4 to 6).

VIII. COLOR DESIGNATIONS FOR ANY OBJECT

The main purpose of this paper is to provide information required for obtaining color designations of powdered crude drugs, whole crude drugs, and chemicals of small particle size. To this end, specific instructions have been given in sections VI and VII. A secondary purpose, however, is to facilitate study of the suitability of these color designations to any object. Detailed procedures applicable to this wider use of the system have yet to be formulated; but some general instructions can be given.

1. FOR OPAQUE NONMETALLIC MATERIALS

(a) WITH MATTE SURFACES

Proceed as in section VI or VII. The recommended angles of illumination and viewing need not be strictly followed, because the appearance of a matte surface does not change importantly with small variations in these angular conditions.

(b) WITH GLOSSY SURFACES HAVING NO REGULAR DETAILED STRUCTURE

Samples of vitreous enamel and smooth paint films are often found with glossy surfaces having no regular detailed structure. Proceed as in section VI and VII, giving particular attention to the prescribed angles of illumination and viewing. The characteristic color of the sample is obtained only when specularly reflected light is prevented from reaching the eye of the observer.

(c) WITH GLOSSY SURFACES MADE UP OF CYLINDRICAL ELEMENTS

Samples of satin-finish textiles and glossy brush-marked paint films may be considered as made up of cylindrical elements. Proceed as in section VII, 2 for cylindrical surfaces. It is not always possible to prevent light from being specularly reflected from such glossy surfaces into the eye of the observer; but by so orienting the sample in its own

plane that the specular component is reduced to a minimum, the most characteristic color of the sample is usually obtained. Particular attention is being devoted to choice of angular conditions of illuminating and viewing the satin-finish and ribbed-finish standards issued by the Textile Color Card Association of the United States with a view to obtaining designations for the characteristic colors of these standards. Some textiles require more than one angle of view or illumination to bring out the characteristic color or colors; changeable silks are extreme examples of such textiles.

2. FOR METALLIC SURFACES

The characteristic color of a metallic surface is obtained from the specularly reflected light. Proceed, therefore, as in section VI or VII, but obtain, in addition, the hue name for the specularly reflected light. These two names may possibly yield a useful designation of the color of the metallic surface, but they will not correspond well with common usage which involves color terms that apply characteristically to metallic appearance (silver, brass, gold, copper, and so on).

3. FOR MATERIALS WHICH TRANSMIT BUT DO NOT SCATTER LIGHT

Samples of liquids, glass and gelatins are often encountered which transmit but do not scatter light. The transmitted light, of course, yields the characteristic color of such materials, but the color designations of the present system are not all applicable to such materials; for example, *white* is a color designation applying characteristically to materials which *do* scatter light. The Council has undertaken an extension of the present system of color designations to colors of materials viewed by transmitted light. It is planned to compare the appearance of a white surface illuminated by daylight and viewed through a prescribed thickness of the material with the appearance of the Munsell standards similarly illuminated but viewed directly. About 25 of the 319 designations will have to be changed; for example, *white* will have to be supplanted by some such term as *colorless* or *clear*. Similarly, *pinkish white* would have to be changed to some term like *light pinkish* (*color*); and *light gray*, perhaps, to *light smoky* (or to *light smoke* if the noun form is desired). In this way it is hoped that a system in fair accord with common usage will result, but the color terms (*amber, claret* and so on) characteristic of materials viewed by transmitted light will not be a part of the system.

4. FOR TRANSLUCENT MATERIALS

Translucent materials both transmit some light and scatter some. The characteristic color for some of such materials is obtained by reflected light, and for others by transmitted light; if in doubt, get both.

IX. SUMMARY

A method of designating the colors of powdered drugs and chemicals and crude whole drugs has been described; this method has, furthermore, been devised with the thought of its applicability to colors of opaque, nonmetallic surfaces generally. Suggestions for its ex-

tension to the color designations of transparent and translucent media have also been given. This method is dedicated to everyone who has found it difficult to make his color descriptions intelligible, in the hope that it will eventually be elaborated into a successful system of color designation for the general use of science, art, and industry.

X. REFERENCES

[1] D. MacAdam. *The theory of the maximum visual efficiency of colored materials*, J. Opt. Soc. Am. **25,** 249 (1935); *Maximum visual efficiency of colored materials* **25,** 361 (1935).

[2] Proceedings of the Eighth Session, Commission Internationale de l'Éclairage, Cambridge, Eng., p. 19–29 (September 1931).
D. B. Judd, *The 1931 ICI standard observer and coordinate system for colorimetry*, J. Opt. Soc. Am. **23,** 359 (1933).
A. C. Hardy, Handbook of Colorimetry (Technology Press, Cambridge, Mass., 1936).

[3] Munsell Book of Color, Standard and abridged editions (Hoffman Bros., Baltimore, Md., 1939). Available also through the Munsell Color Co., 10 East Franklin Street, Baltimore, Md.

[4] A. Maerz and M. Rea Paul, A Dictionary of Color (McGraw-Hill Book Co., Inc., New York, N. Y., 1930).

WASHINGTON, July 14, 1939.

HOW TO USE THE COLOR NAME CHARTS 1 TO 34[a]

Given: Munsell notation of the sample.

Required: The color designation.

First, turn to the particular name chart referring most closely to the Munsell hue notation of the sample (see numbers at top of chart); or, if the hue is equally close to two successive charts, use them both.

Second, find the point on the chart defined by the Munsell value and Munsell chroma of the sample; or, if two charts are to be used, plot the point on both of them. Note that the chroma scale is expanded for chromas less than 1.5; see vertical double line on each chart.

Third, read the color designation of the block within which the point falls. If the point falls on a boundary between blocks, read color designations of all blocks touching the point. If, when two charts are to be used, the second chart yields a different designation from the first, read them both.

[a] Acknowledgment is made to Miss Dorothy Nickerson, individual member of the Inter-Society Color Council, for suggesting the present simple form of these name charts.

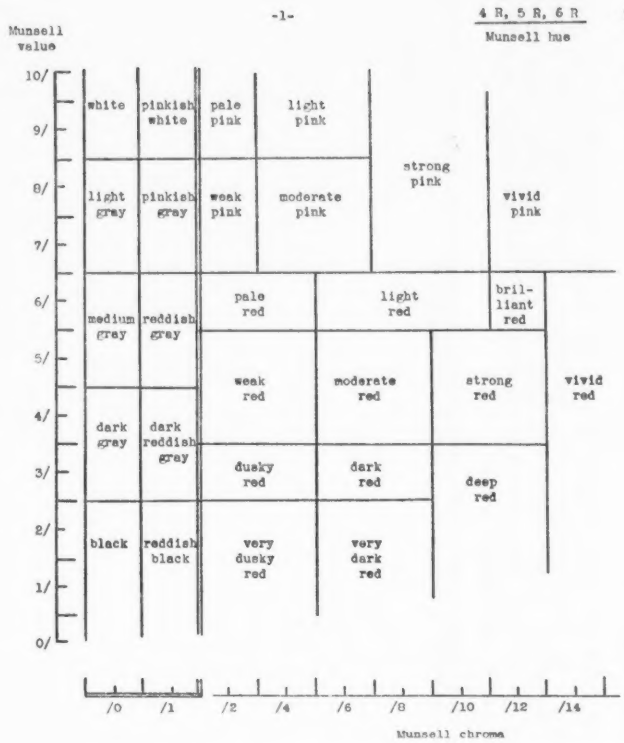
-1-
4 R, 5 R, 6 R
Munsell hue
Munsell value
10/
9/
8/
7/
6/
5/
4/
3/
2/
1/
0/
white
pinkish white
pale pink
light pink
strong pink
vivid pink
light gray
pinkish gray
weak pink
moderate pink
pale red
light red
brilliant red
medium gray
reddish gray
weak red
moderate red
strong red
vivid red
dark gray
dark reddish gray
dusky red
dark red
deep red
black
reddish black
very dusky red
very dark red
/0
/1
/2
/4
/6
/8
/10
/12
/14
Munsell chroma

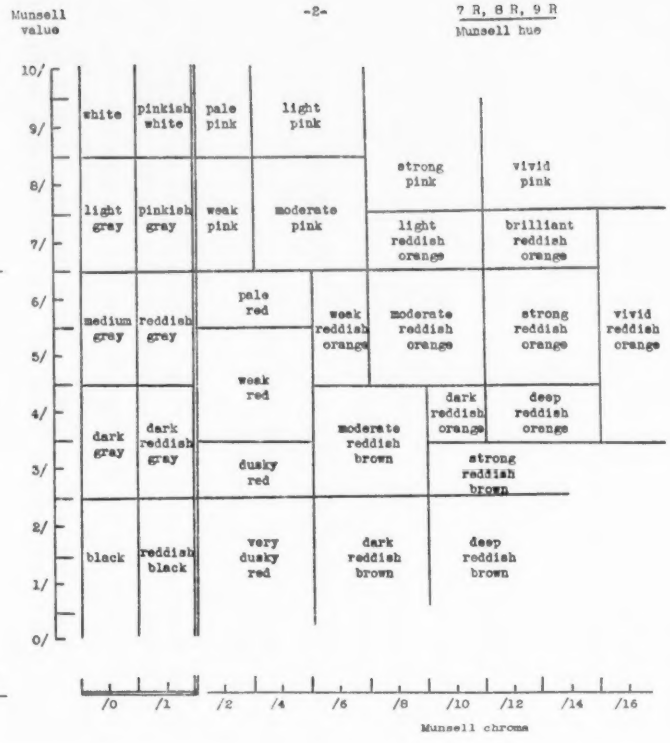
-2-
7 R, 8 R, 9 R
Munsell hue
Munsell value
10/
9/
8/
7/
6/
5/
4/
3/
2/
1/
0/
white
pinkish white
pale pink
light pink
strong pink
vivid pink
light gray
pinkish gray
weak pink
moderate pink
light reddish orange
brilliant reddish orange
pale red
weak reddish orange
moderate reddish orange
strong reddish orange
vivid reddish orange
medium gray
reddish gray
weak red
dark reddish orange
deep reddish orange
dark gray
dark reddish gray
moderate reddish brown
strong reddish brown
dusky red
black
reddish black
very dusky red
dark reddish brown
deep reddish brown
/0
/1
/2
/4
/6
/8
/10
/12
/14
/16
Munsell chroma

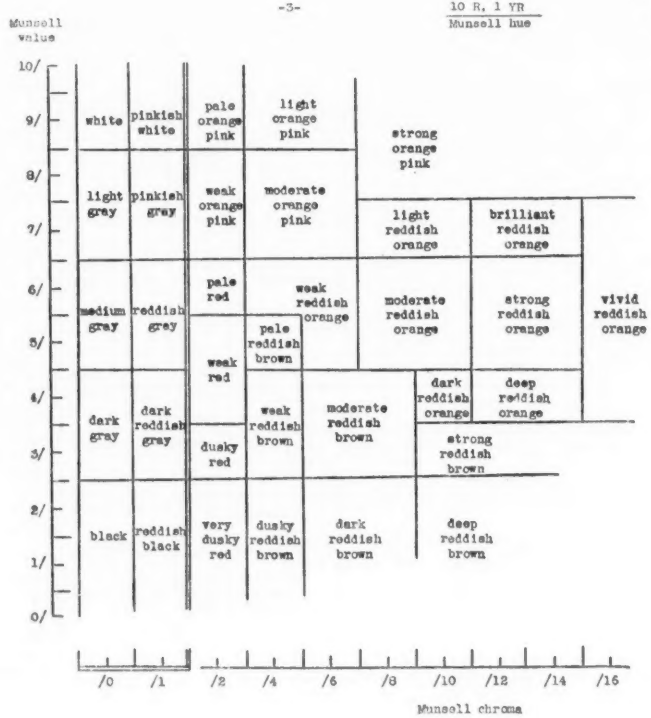
-3-
10 R, 1 YR
Munsell hue
Munsell value
10/
9/
8/
7/
6/
5/
4/
3/
2/
1/
0/
white
pinkish white
pale orange pink
light orange pink
strong orange pink
light gray
pinkish gray
weak orange pink
moderate orange pink
light reddish orange
brilliant reddish orange
pale red
weak reddish orange
moderate reddish orange
strong reddish orange
vivid reddish orange
medium gray
reddish gray
pale reddish brown
weak red
dark reddish orange
deep reddish orange
dark gray
dark reddish gray
weak reddish brown
moderate reddish brown
strong reddish brown
dusky red
black
reddish black
very dusky red
dusky reddish brown
dark reddish brown
deep reddish brown
/0
/1
/2
/4
/6
/8
/10
/12
/14
/16
Munsell chroma

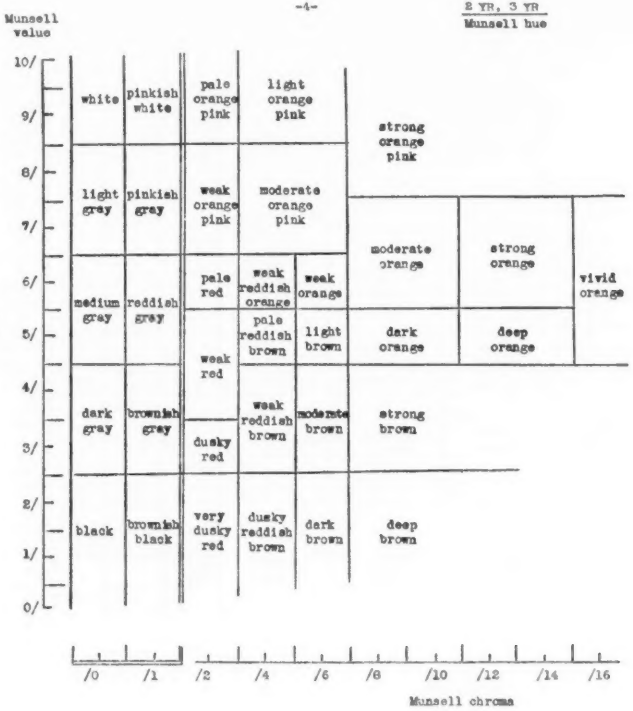
-4-
2 YR, 3 YR
Munsell hue
Munsell value
10/
9/
8/
7/
6/
5/
4/
3/
2/
1/
0/
white
pinkish white
pale orange pink
light orange pink
strong orange pink
light gray
pinkish gray
weak orange pink
moderate orange pink
moderate orange
strong orange
vivid orange
pale red
weak reddish orange
weak orange
medium gray
reddish gray
pale reddish brown
light brown
dark orange
deep orange
weak red
dark gray
brownish gray
weak reddish brown
moderate brown
strong brown
dusky red
black
brownish black
very dusky red
dusky reddish brown
dark brown
deep brown
/0
/1
/2
/4
/6
/8
/10
/12
/14
/16
Munsell chroma

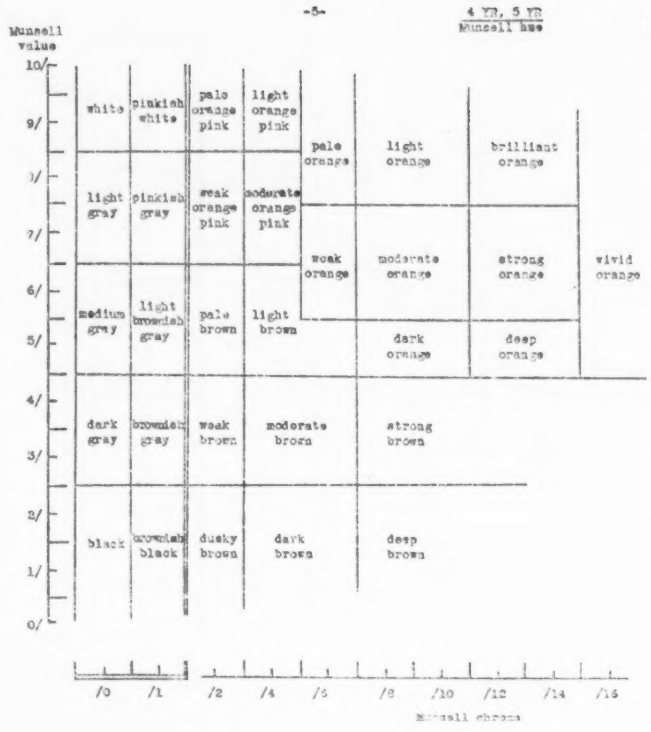
-5-
4 YR, 5 YR
Munsell hue
Munsell value
10/
9/
8/
7/
6/
5/
4/
3/
2/
1/
0/
white
pinkish white
pale orange pink
light orange pink
pale orange
light orange
brilliant orange
light gray
pinkish gray
weak orange pink
moderate orange pink
weak orange
moderate orange
strong orange
vivid orange
medium gray
light brownish gray
pale brown
light brown
dark orange
deep orange
dark gray
brownish gray
weak brown
moderate brown
strong brown
black
brownish black
dusky brown
dark brown
deep brown
/0
/1
/2
/4
/6
/8
/10
/12
/14
/16
Munsell chroma

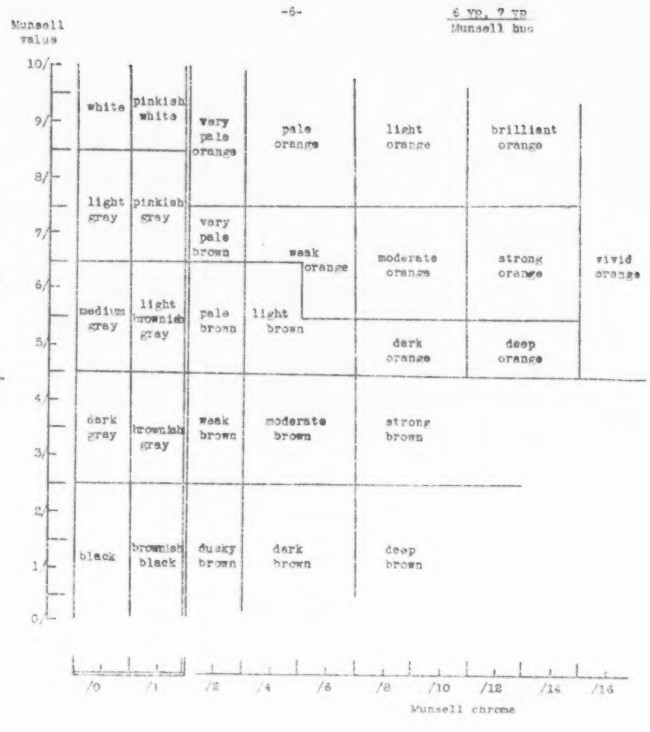
-6-
6 YR, 7 YR
Munsell hue
Munsell value
10/
9/
8/
7/
6/
5/
4/
3/
2/
1/
0/
white
pinkish white
very pale orange
pale orange
light orange
brilliant orange
light gray
pinkish gray
very pale brown
weak orange
moderate orange
strong orange
vivid orange
medium gray
light brownish gray
pale brown
light brown
dark orange
deep orange
dark gray
brownish gray
weak brown
moderate brown
strong brown
black
brownish black
dusky brown
dark brown
deep brown
/0
/1
/2
/4
/6
/8
/10
/12
/14
/16
Munsell chroma

-7-

8 YR
Munsell hue

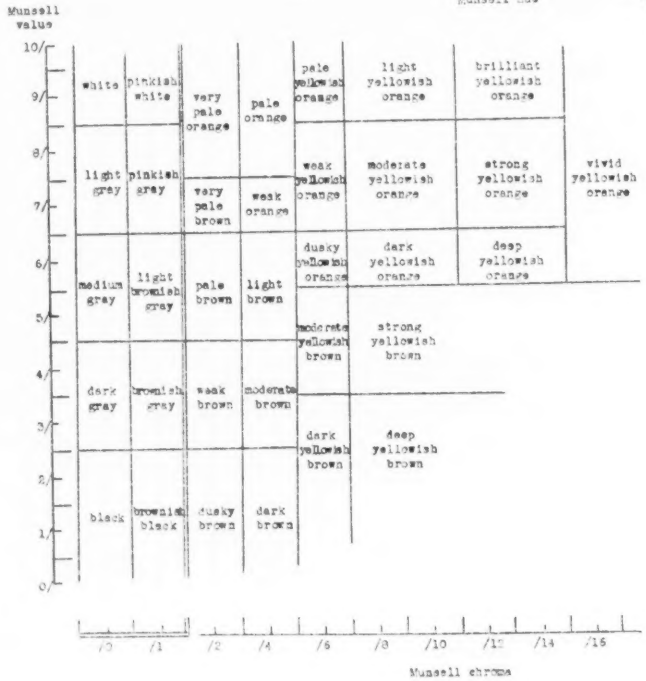

-8-

9 YR
Munsell hue

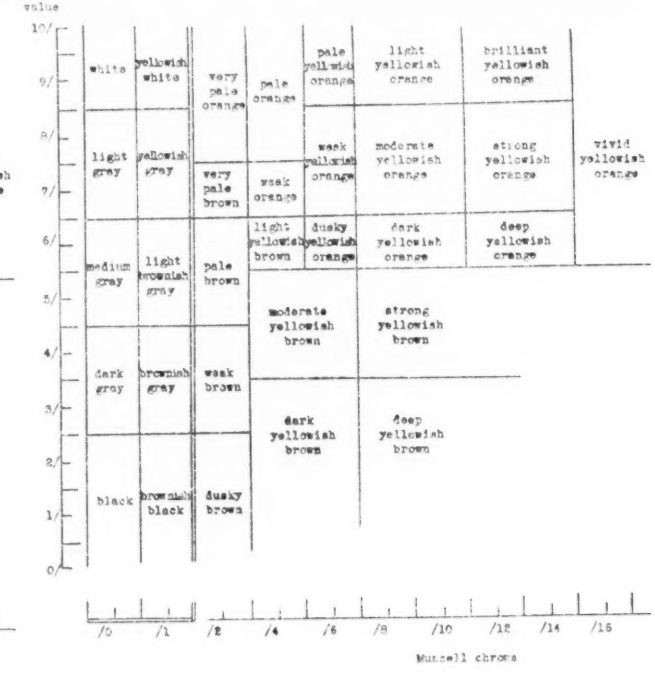

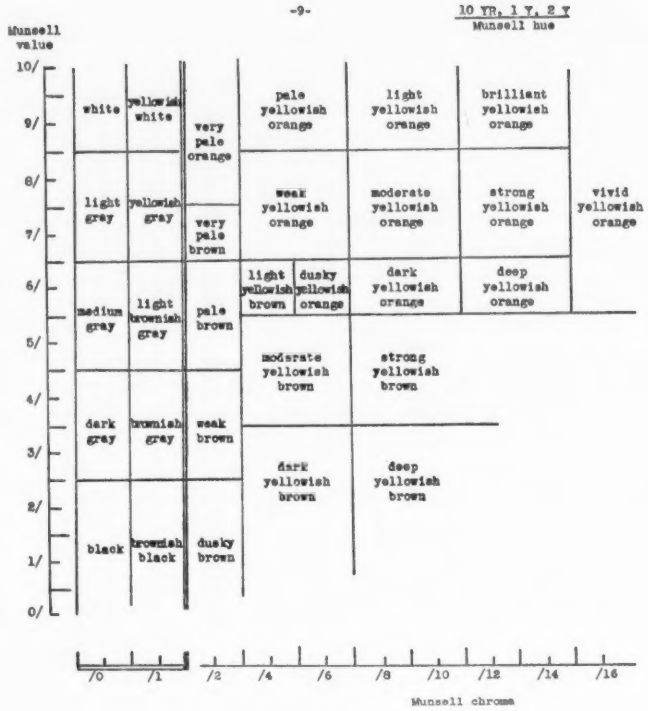
-9-
10 YR, 1 Y, 2 Y
Munsell hue
Munsell value
10/
9/
8/
7/
6/
5/
4/
3/
2/
1/
0/
white
yellowish white
very pale orange
pale yellowish orange
light yellowish orange
brilliant yellowish orange
light gray
yellowish gray
very pale brown
weak yellowish orange
moderate yellowish orange
strong yellowish orange
vivid yellowish orange
light yellowish brown
dusky yellowish orange
dark yellowish orange
deep yellowish orange
medium gray
light brownish gray
pale brown
moderate yellowish brown
strong yellowish brown
dark gray
brownish gray
weak brown
dark yellowish brown
deep yellowish brown
black
brownish black
dusky brown
/0
/1
/2
/4
/6
/8
/10
/12
/14
/16
Munsell chroma

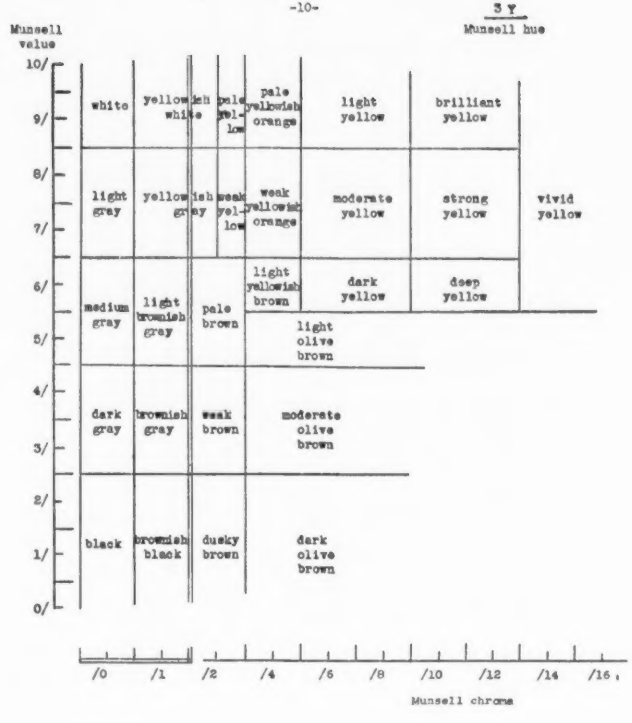
-10-
5 Y
Munsell hue
Munsell value
10/
9/
8/
7/
6/
5/
4/
3/
2/
1/
0/
white
yellowish white
pale yellow
pale yellowish orange
light yellow
brilliant yellow
light gray
yellowish gray
weak yellow
weak yellowish orange
moderate yellow
strong yellow
vivid yellow
light yellowish brown
dark yellow
deep yellow
medium gray
light brownish gray
pale brown
light olive brown
dark gray
brownish gray
weak brown
moderate olive brown
black
brownish black
dusky brown
dark olive brown
/0
/1
/2
/4
/6
/8
/10
/12
/14
/16
Munsell chroma

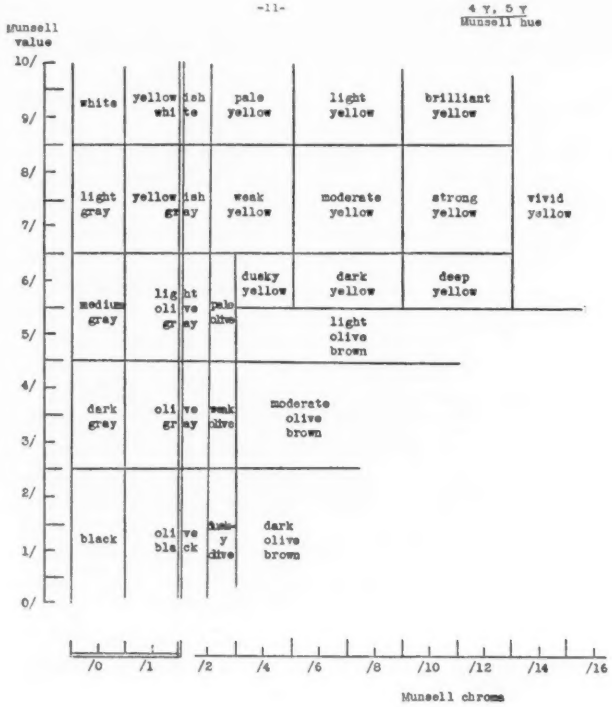
-11-
4 Y, 5 Y
Munsell hue
Munsell value
10/
9/
8/
7/
6/
5/
4/
3/
2/
1/
0/
white
yellowish white
pale yellow
light yellow
brilliant yellow
light gray
yellowish gray
weak yellow
moderate yellow
strong yellow
vivid yellow
dusky yellow
dark yellow
deep yellow
medium gray
light olive gray
pale olive
light olive brown
dark gray
olive gray
weak olive
moderate olive brown
black
olive black
dusky olive
dark olive brown
/0
/1
/2
/4
/6
/8
/10
/12
/14
/16
Munsell chroma

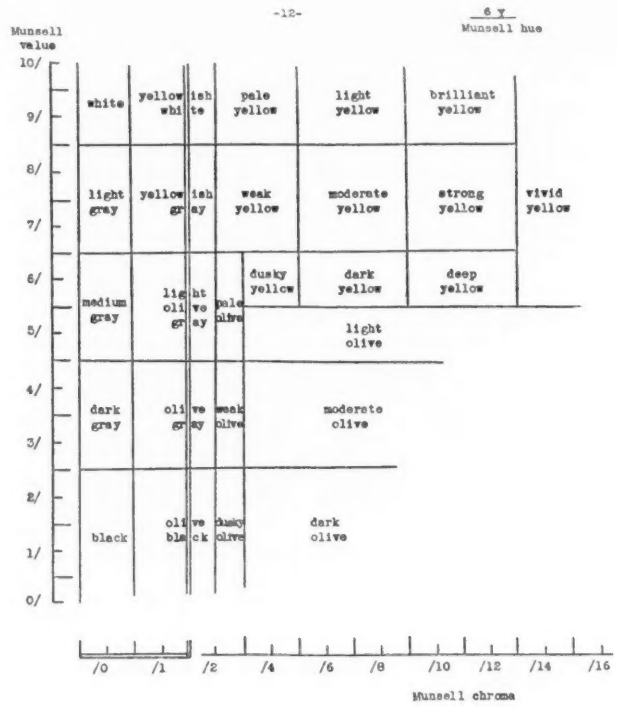
-12-
6 Y
Munsell hue
Munsell value
10/
9/
8/
7/
6/
5/
4/
3/
2/
1/
0/
white
yellowish white
pale yellow
light yellow
brilliant yellow
light gray
yellowish gray
weak yellow
moderate yellow
strong yellow
vivid yellow
dusky yellow
dark yellow
deep yellow
medium gray
light olive gray
pale olive
light olive
dark gray
olive gray
weak olive
moderate olive
black
olive black
dusky olive
dark olive
/0
/1
/2
/4
/6
/8
/10
/12
/14
/16
Munsell chroma

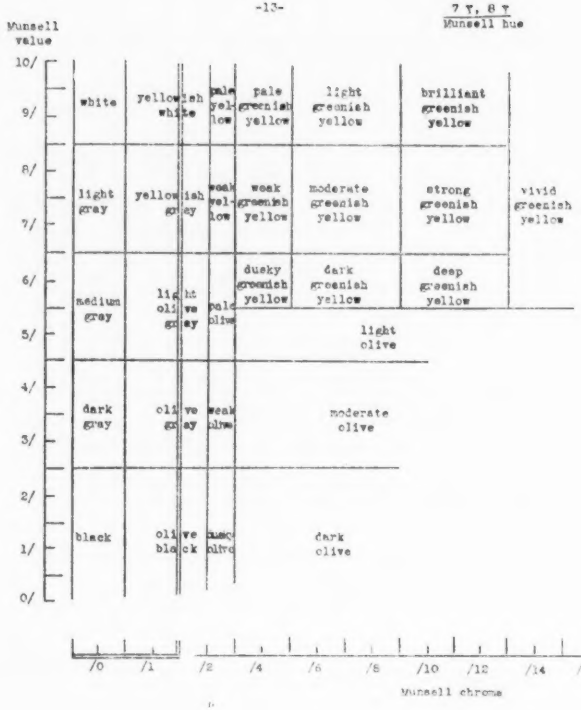
-13-
7 Y, 8 Y
Munsell hue
Munsell value
10/
9/
8/
7/
6/
5/
4/
3/
2/
1/
0/
white
yellowish white
pale yellow
pale greenish yellow
light greenish yellow
brilliant greenish yellow
light gray
yellowish gray
weak yellow
weak greenish yellow
moderate greenish yellow
strong greenish yellow
vivid greenish yellow
medium gray
light olive gray
pale olive
dusky greenish yellow
dark greenish yellow
deep greenish yellow
light olive
dark gray
olive gray
weak olive
moderate olive
black
olive black
dark olive
/0
/1
/2
/4
/6
/8
/10
/12
/14
/16
Munsell chroma

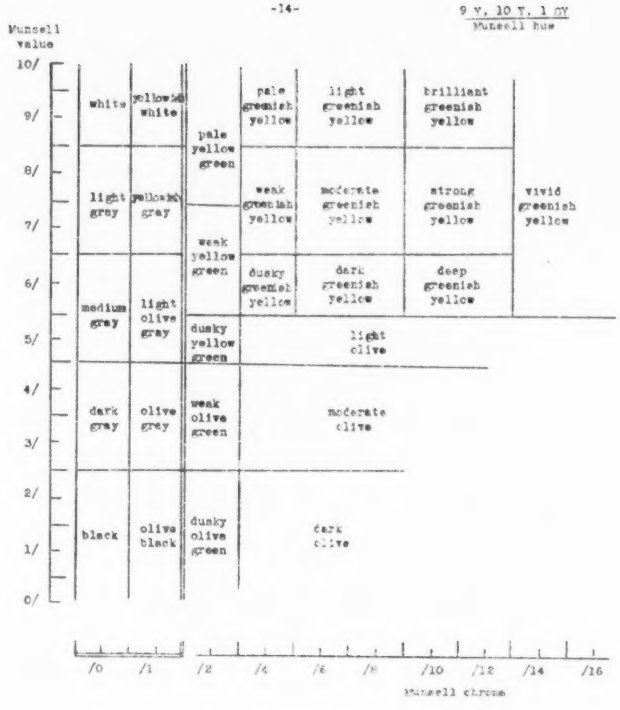
-14-
9 Y, 10 Y, 1 GY
Munsell hue
Munsell value
10/
9/
8/
7/
6/
5/
4/
3/
2/
1/
0/
white
yellowish white
pale yellow green
pale greenish yellow
light greenish yellow
brilliant greenish yellow
light gray
yellowish gray
weak greenish yellow
moderate greenish yellow
strong greenish yellow
vivid greenish yellow
weak yellow green
medium gray
light olive gray
dusky greenish yellow
dark greenish yellow
deep greenish yellow
dusky yellow green
light olive
dark gray
olive gray
weak olive green
moderate olive
black
olive black
dusky olive green
dark olive
/0
/1
/2
/4
/6
/8
/10
/12
/14
/16
Munsell chroma

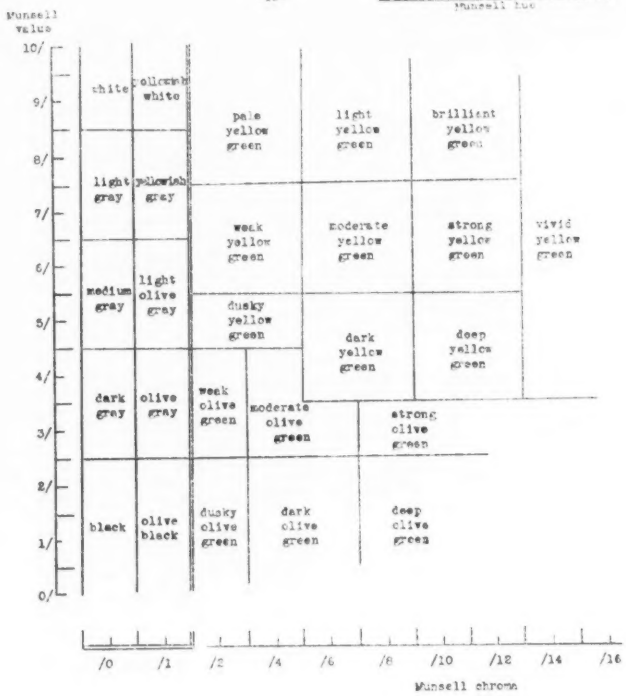
Munsell value
10/
9/
8/
7/
6/
5/
4/
3/
2/
1/
0/
white
yellowish white
light gray
yellowish gray
medium gray
light olive gray
dark gray
olive gray
black
olive black
pale yellow green
light yellow green
brilliant yellow green
weak yellow green
moderate yellow green
strong yellow green
vivid yellow green
dusky yellow green
dark yellow green
deep yellow green
weak olive green
moderate olive green
strong olive green
dusky olive green
dark olive green
deep olive green
/0
/1
/2
/4
/6
/8
/10
/12
/14
/16
Munsell chroma

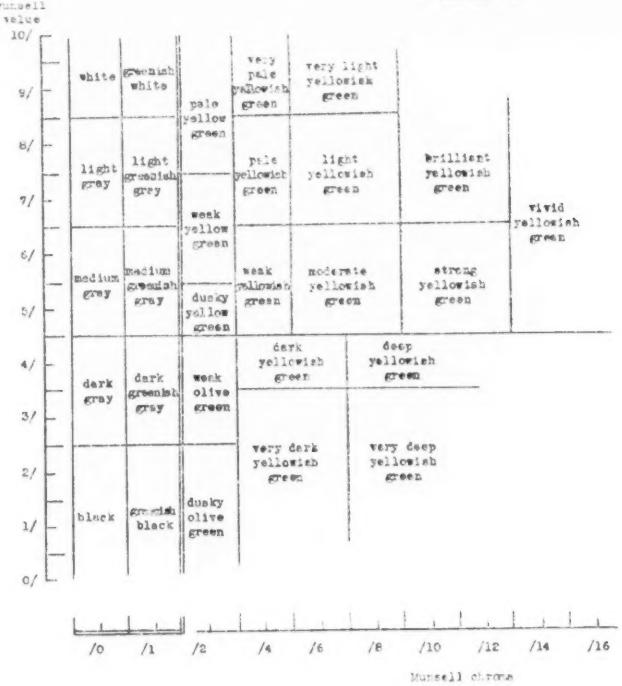
Munsell value
10/
9/
8/
7/
6/
5/
4/
3/
2/
1/
0/
white
greenish white
light gray
light greenish gray
medium gray
medium greenish gray
dark gray
dark greenish gray
black
greenish black
pale yellow green
weak yellow green
dusky yellow green
very pale yellowish green
very light yellowish green
pale yellowish green
light yellowish green
brilliant yellowish green
vivid yellowish green
weak yellowish green
moderate yellowish green
strong yellowish green
weak olive green
dark yellowish green
deep yellowish green
very dark yellowish green
very deep yellowish green
dusky olive green
/0
/1
/2
/4
/6
/8
/10
/12
/14
/16
Munsell chroma

-17-

10 GY, 1 G, 2 G
Munsell hue

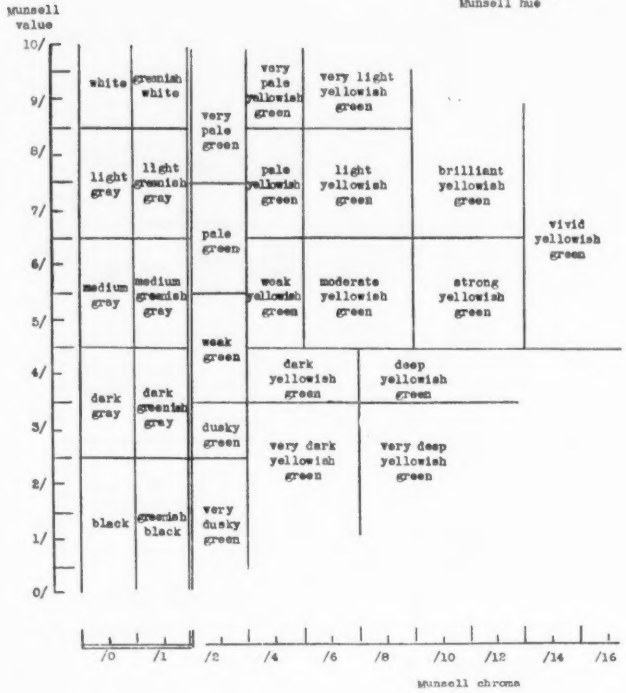

-18-

3 G, 4 G, 5 G
Munsell hue

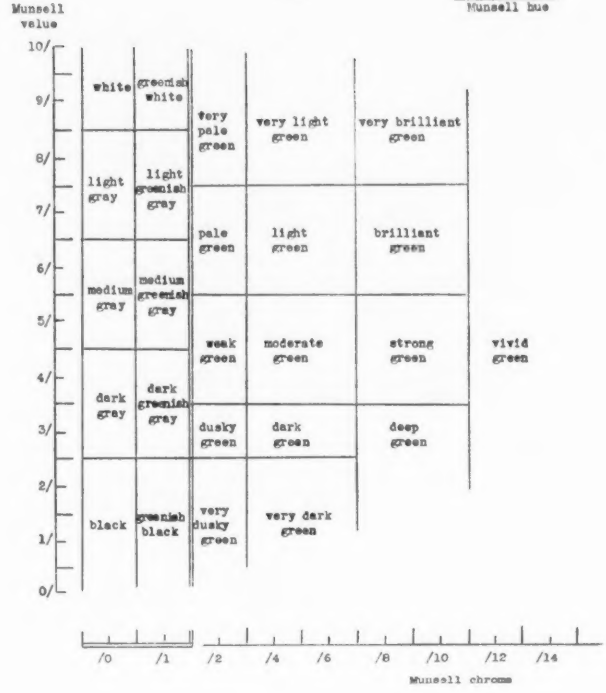

5 G, 7 G
Munsell hue

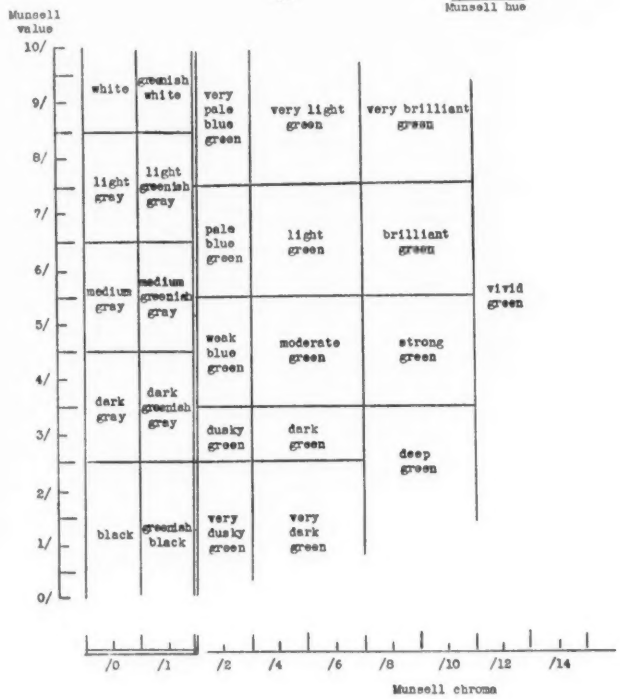

8 G, 9 G
Munsell hue

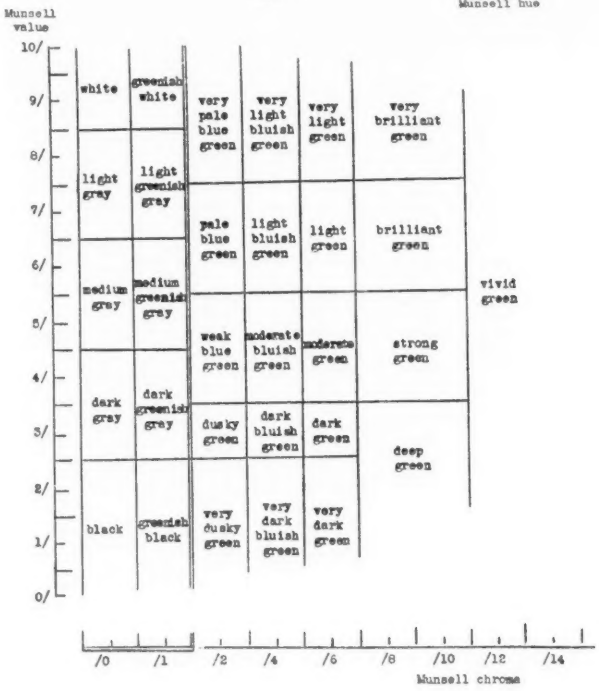

-21-
10 G, 1 PB, 2 B
Munsell hue
Munsell value
10/
9/
8/
7/
6/
5/
4/
3/
2/
1/
0/
white
light gray
dark gray
black
greenish white
light greenish gray
medium greenish gray
dark greenish gray
greenish black
very pale blue green
pale blue green
weak blue green
dusky green
very dusky green
very light bluish green
light bluish green
moderate bluish green
dark bluish green
very dark bluish green
brilliant bluish green
strong bluish green
deep bluish green
vivid bluish green
/0 /1 /2 /4 /6 /8 /10 /12 /14
Munsell chroma
-22-
5 BG, 4 B
Munsell hue
Munsell value
10/
9/
8/
7/
6/
5/
4/
3/
2/
1/
0/
white
light gray
medium gray
dark gray
black
greenish white
light greenish gray
medium greenish gray
dark greenish gray
greenish black
very pale blue green
pale blue green
weak blue green
dusky blue green
very dusky blue green
very light blue green
light blue green
moderate blue green
dark blue green
very dark blue green
brilliant blue green
strong blue green
deep blue green
vivid blue green
/0 /1 /2 /4 /6 /8 /10 /12 /14
Munsell chroma

5 BG, 6 BG, 7 BG, 8 BG
Munsell hue

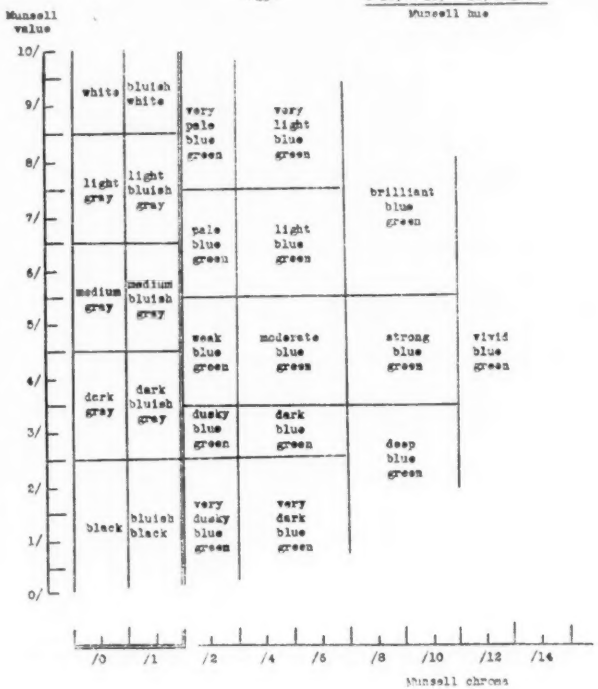

9 BG, 10 BG, 1 B, 2 B, 3 B
Munsell hue

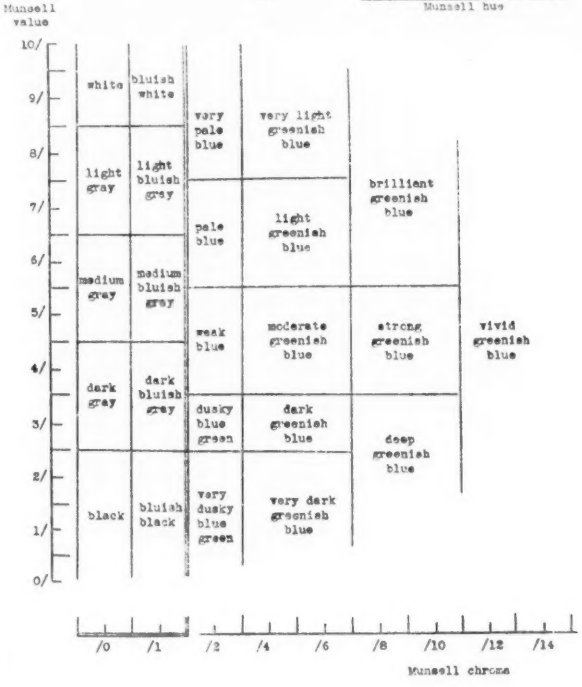

-25-

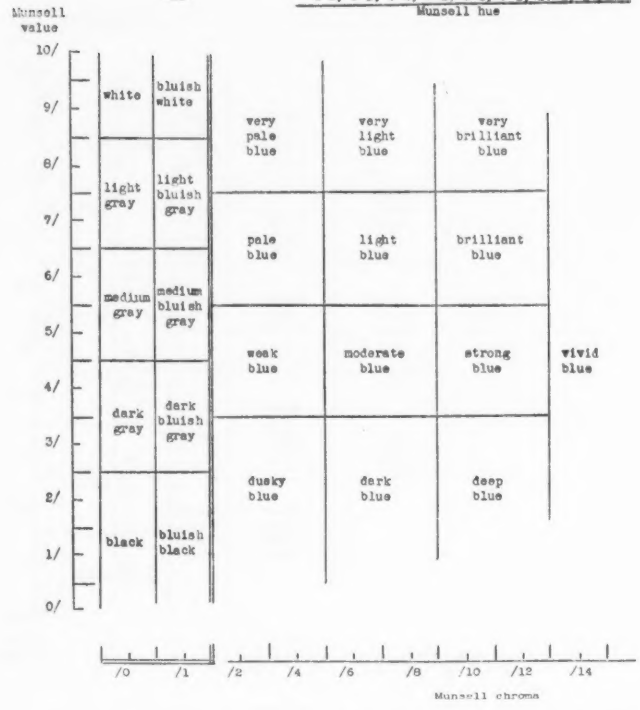
4 B, 5 B, 6 B, 7 B, 8 B, 9 B, 10 B, 1 PB
Munsell hue
Munsell value
10/
9/
8/
7/
6/
5/
4/
3/
2/
1/
0/
white
bluish white
light gray
light bluish gray
medium gray
medium bluish gray
dark gray
dark bluish gray
black
bluish black
very pale blue
very light blue
very brilliant blue
pale blue
light blue
brilliant blue
weak blue
moderate blue
strong blue
vivid blue
dusky blue
dark blue
deep blue
/0
/1
/2
/4
/6
/8
/10
/12
/14
Munsell chroma

-26-

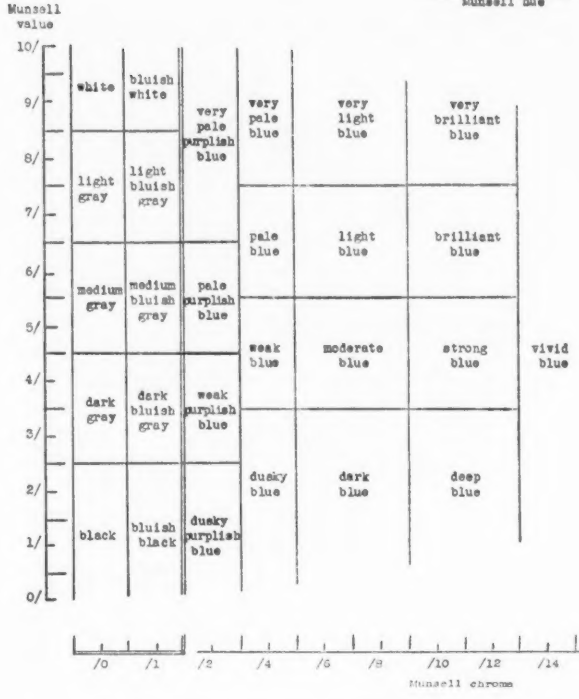
2 PB, 3 PB
Munsell hue
Munsell value
10/
9/
8/
7/
6/
5/
4/
3/
2/
1/
0/
white
bluish white
light gray
light bluish gray
medium gray
medium bluish gray
dark gray
dark bluish gray
black
bluish black
very pale purplish blue
pale purplish blue
weak purplish blue
dusky purplish blue
very pale blue
very light blue
very brilliant blue
pale blue
light blue
brilliant blue
weak blue
moderate blue
strong blue
vivid blue
dusky blue
dark blue
deep blue
/0
/1
/2
/4
/6
/8
/10
/12
/14
Munsell chroma

-27-

4 PB, 5 PB, 6 PB, 7 PB
Munsell hue

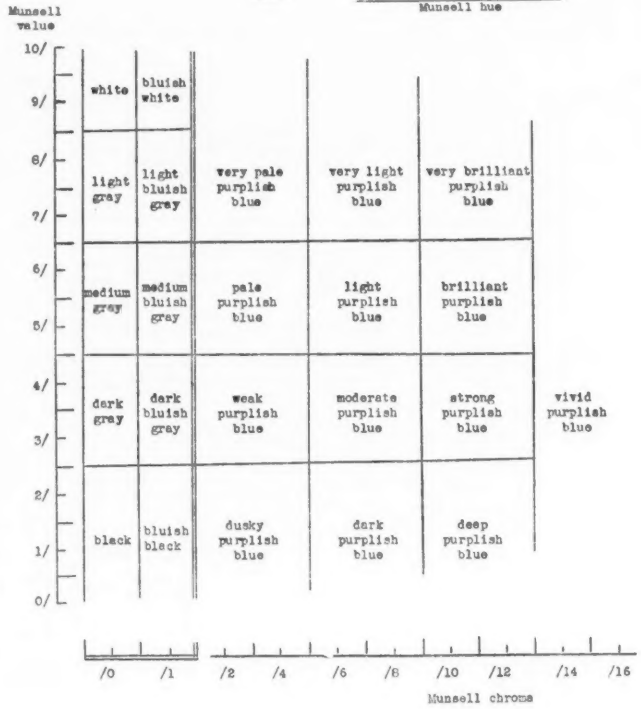

-28-

8PB, 9PB, 10PB
Munsell hue

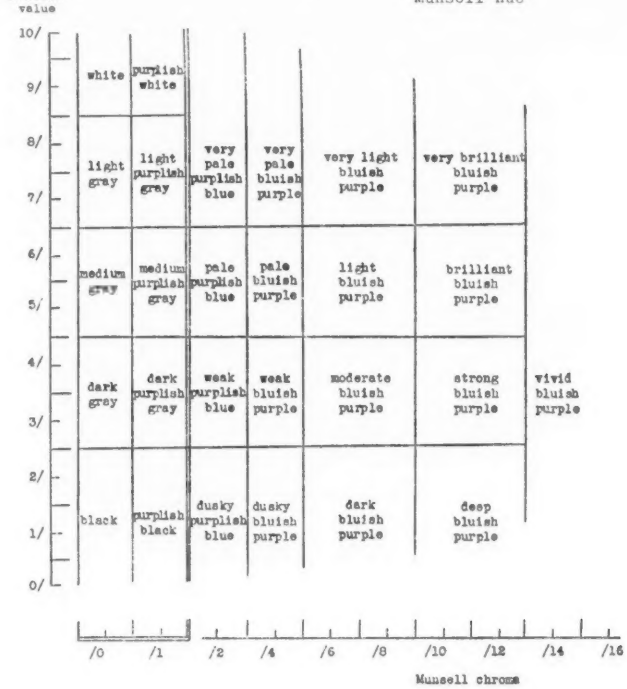

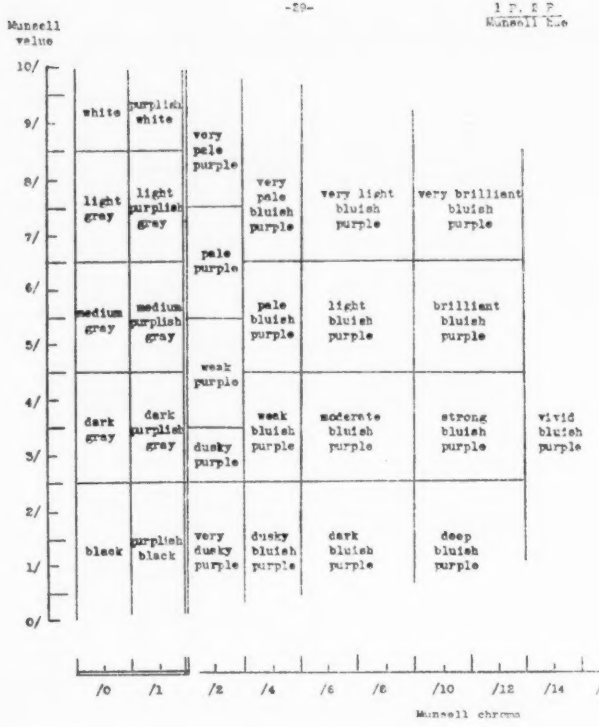
-29-
1 P, 2 P
Munsell Hue
Munsell value
10/
9/
8/
7/
6/
5/
4/
3/
2/
1/
0/
white
purplish white
light grey
light purplish gray
medium gray
medium purplish gray
dark gray
dark purplish gray
black
purplish black
very pale purple
pale purple
weak purple
dusky purple
very dusky purple
very pale bluish purple
pale bluish purple
weak bluish purple
dusky bluish purple
very light bluish purple
light bluish purple
moderate bluish purple
dark bluish purple
very brilliant bluish purple
brilliant bluish purple
strong bluish purple
deep bluish purple
vivid bluish purple
/0
/1
/2
/4
/6
/8
/10
/12
/14
/16
Munsell chroma

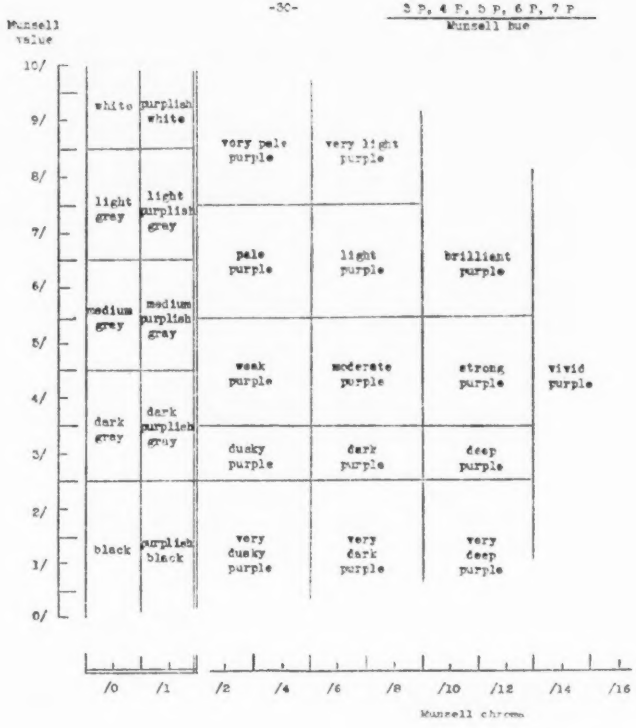
-30-
3 P, 4 P, 5 P, 6 P, 7 P
Munsell Hue
Munsell value
10/
9/
8/
7/
6/
5/
4/
3/
2/
1/
0/
white
purplish white
light grey
light purplish gray
medium grey
medium purplish gray
dark gray
dark purplish gray
black
purplish black
very pale purple
very light purple
pale purple
light purple
brilliant purple
weak purple
moderate purple
strong purple
vivid purple
dusky purple
dark purple
deep purple
very dusky purple
very dark purple
very deep purple
/0
/1
/2
/4
/6
/8
/10
/12
/14
/16
Munsell chroma

-31-

9 P, 9 P, 10 P, 1 RP
Munsell hue

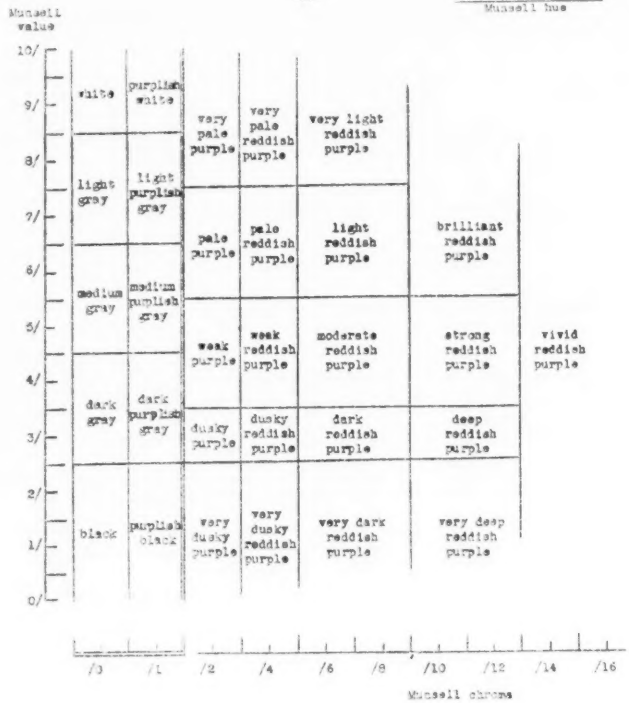

-32-

2 RP, 3 RP, 4 RP
Munsell hue

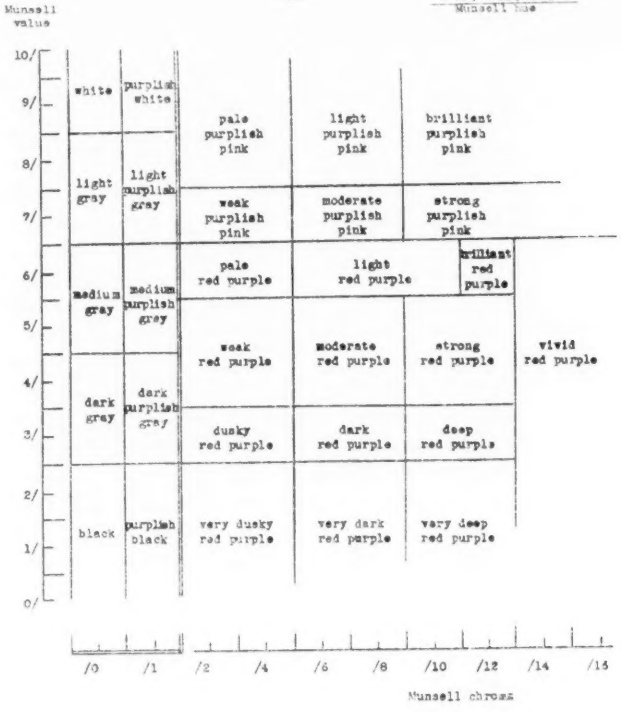

-33-

5 RP, 6 RP, 7 RP
Munsell hue

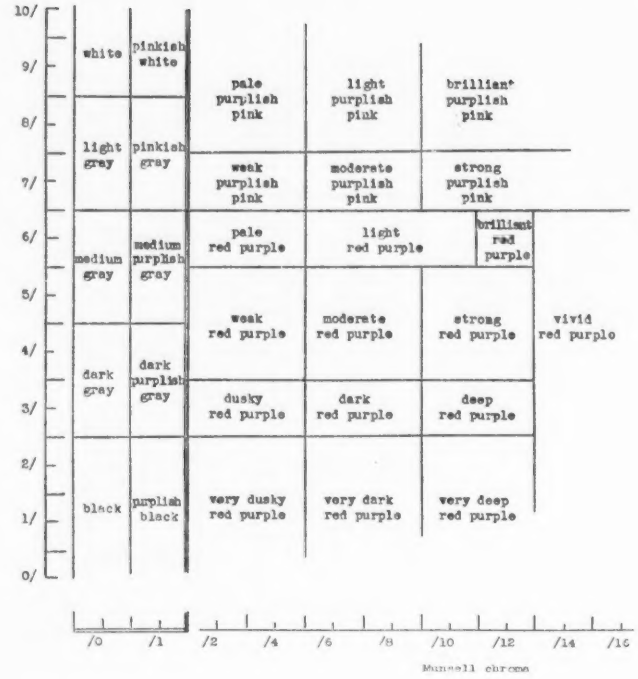

-34-

8 RP, 9 RP, 10 RP, 1 R, 2 R, 3 R
Munsell hue

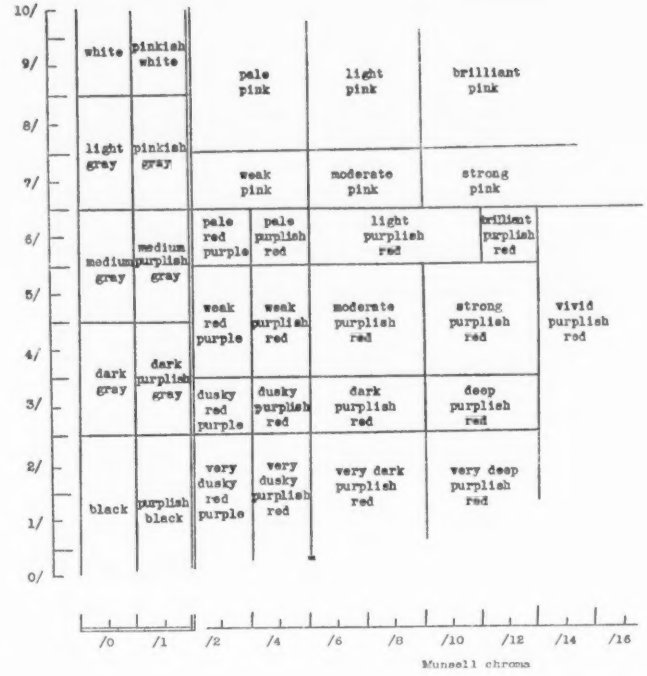

-36-

10Y
5GY
10GY
5G
5Y
10YR
5YR
10R
5R
10RP
5RP
10P
5P
Z
gY
YG
Y
YO
O
O-Pk
Pk
P-Pk
P
pB
B
bG
G

-35-

10Y
5GY
10GY
5G
10G
5BG
10BG
5B
10B
5PB
10PB
5P
10P
5RP
10RP
5R
10R
5YR
10YR
5Y
Z
O1
O1-G
YG
G
bG
BG
cB
B
pB
bP
P
RP
rP
R
rO
R-Br
Br
Y-Br
O1-Br

U. S. DEPARTMENT OF COMMERCE NATIONAL BUREAU OF STANDARDS

RESEARCH PAPER RP1240

Part of Journal of Research of the National Bureau of Standards, Volume 23, September 1939

DROPPING TESTS FOR MEASURING THE THICKNESS OF ZINC AND CADMIUM COATINGS ON STEEL

By Abner Brenner

ABSTRACT

The dropping test was reinvestigated because of reported difficulties with the end point. Improvements were made in the apparatus, which permitted a more constant rate of dropping of the reagent. For comparison, some thickness tests were also made by the jet, magnetic, and microscopic methods. The ammonium nitrate dropping-test reagent did not give a satisfactory end point with zinc-mercury coatings and did not dissolve different types of bright cadmium coatings at the same rate. A chromic acid reagent, containing 200 g/liter of chromic acid and 50 g/liter of sulfuric acid, overcame these difficulties and had the additional advantage that only one reagent was required for testing different types of zinc and cadmium coatings. On commercial specimens, this reagent gave an average error of ±12 percent and maximum errors of about ±20 percent. The jet method and the microscopic method are not very satisfactory for measuring the thickness of zinc and cadmium coatings. The magnetic method usually yields errors less than ±15 percent, and appears satisfactory except for thin coatings on rough basis metals.

CONTENTS

	Page
I. Introduction	388
II. Test methods	389
1. Stripping methods	389
2. Dropping tests	389
(a) Apparatus and procedure	389
(b) End points	390
(c) Determination of thickness factors	390
3. Jet test	395
4. Magnetic thickness measurements	395
5. Testing commercial articles	395
III. Results of tests	395
1. Zinc coatings	395
(a) Electroplated	395
(1) Dropping tests	395
(2) Jet tests	397
(3) Magnetic measurements	397
(4) Miscellaneous tests	397
(b) Hot-dipped	397
(1) Dropping tests	397
(2) Magnetic measurements	398
(c) Sherardized	399
(1) Dropping tests	399
(2) Magnetic measurements	399
2. Cadmium coatings	400
(a) Dropping tests	400
(b) Magnetic measurements	401
3. Microscopic method for zinc and cadmium coatings	401
IV. Conclusions	401
1. Dropping tests	401
2. Jet test	402
3. Magnetic measurements	402
V. Recommendations	402

I. INTRODUCTION

The increasing adoption of specifications for the minimum thickness of plated coatings has stimulated interest in rapid methods for determining thickness. The microscopic method, which is standard, has the disadvantage of requiring expensive equipment and considerable time and does not always give satisfactory results on zinc and cadmium coatings. Often the testing of a larger number of specimens by a more rapid method would give more accurate information about an entire shipment than testing more accurately a relatively few specimens. The Preece test, in spite of its admitted shortcomings, has been used extensively for determining the minimum thickness of zinc coatings. The dropping test, developed to replace the less accurate Preece test, has been incorporated in a number of commercial and Federal specifications.

The dropping test consists in dropping a corrosive solution onto a zinc or cadmium coating until the latter is penetrated. The thickness of coating is obtained by multiplying the number of seconds required for penetration by a factor previously determined for that reagent and coating. The test was devised by S. G. Clarke,[1] who used a solution of iodine in potassium iodide. It was modified by Hull and Strausser,[2] who substituted acidified ammonium nitrate solutions for the iodine. The test was rapidly adopted by industry, because the apparatus could be cheaply constructed from ordinary laboratory equipment, and the test could be performed by operators lacking extensive laboratory experience.

Experience with the method in general use showed that the end points were unsatisfactory for some commercial materials, especially those with coatings deposited on rough basis metals. Hull[3] attempted to improve the end point by adding potassium ferricyanide to the reagent. When the coating was penetrated, enough iron was dissolved to produce a blue color with the potassium ferricyanide.

Because of the reported difficulties with the end point it was decided to study critically the dropping tests:

1. To improve the end point, if necessary by the use of a different reagent.
2. To determine whether the method of deposition of a zinc or cadmium coating affected its rate of solution in the reagent.
3. To determine the accuracy of the test, especially when applied to commercial materials.

The use of another solution, containing 200 g/liter of chromic acid and 50 g/liter of concentrated sulfuric acid, was investigated. This solution has some advantages over ammonium nitrate solutions, as regards end point and accuracy. Both the ammonium nitrate and the chromic acid reagents were used in the following studies.

For comparison with the dropping tests, some measurements were made by the microscopic method, the jet[4] method, and the magnetic[5] method. The latter two methods were developed more recently than the dropping test.

---

[1] J. Electrodepositors' Tech. Soc. **8**, Paper No. 11 (May 1933).
[2] Monthly Rev. Am. Electroplaters' Soc. **22**, 9 (March 1935); J. Research NBS **16**, 209 (1936) RP867.
[3] Unpublished communications.
[4] S. G. Clarke, J. Electrodepositors' Tech. Soc. **12**, 1 and 157 (1936-37).
[5] A. Brenner, J. Research NBS **20**, 357 (1938) RP1081.

II. TEST METHODS

1. STRIPPING METHODS

The average thickness of zinc or cadmium was determined by dissolving the coating from a measured area with a solution consisting of 20 g of antimony trioxide dissolved in 1 liter of concentrated hydrochloric acid. This reagent does not appreciably attack the steel basis metal. The average thickness of coating was calculated from the weight per unit area and the density. In general, the thickness given by the stripping method was taken as the standard with which the other results were compared. In a few cases, microscopic measurements were also made at points adjacent to those tested by other methods.

The hot-dipped and sherardized zinc coatings contain a small amount of iron which is dissolved by the stripping and dropping reagents and hence is included in the thickness of the coating. No attempt was made to determine the amount of iron in the coating.

The stripping method gives average thickness, whereas the other methods to be described give the local thickness of the coating at the points tested. To compare them with the stripping method, it is necessary that the coatings examined have a fairly uniform thickness, or that enough measurements of local thickness be made to get an average value.

2. DROPPING TESTS

(a) APPARATUS AND PROCEDURE

The dropping test is performed by dropping the reagent at a definite rate, that is, 100 drops per minute, onto the surface, which is inclined at an angle of about 45° to the horizontal. The time required for the end point to appear is measured with a stop watch. The room temperature should be noted, as the rate of solution of the coating usually varies with temperature.

The original apparatus of Clarke consisted of a separatory funnel and two stopcocks, one of which was used to adjust the rate of dropping and the other to turn the flow of liquid on and off. It is difficult to regulate the rate of flow by a stopcock, and, after the stopcock is adjusted, the small orifice frequently clogs. In the modified apparatus (see fig. 1) this difficulty is overcome by using a capillary tube, *B*, for securing the required rate of dropping. One stopcock is provided for starting the flow. A capillary tube with a bore of approximately 0.025 in. (0.63 mm) and a length of 5.5 in. (14 cm) is satisfactory. Between the capillary and the stopcock of the funnel there is from 3 to 5 in. (7.5 to 12.5 cm) of wide-bore tubing, to increase the head of liquid, so that the proper rate of flow is obtained. The capillary is connected to the stem of the separatory funnel by rubber tubing, in which a space of about 0.5 in. (13 mm) is left, so that the rubber tubing can be compressed when it is desired to force air bubbles or foreign matter from the glass tubes. The chromic acid reagent slowly attacks rubber tubing, and the connections must be replaced occasionally. The stopcock is lubricated with petroleum jelly, which is not attacked by chromic acid.

The volume of the drops used in these tests was about 0.05 ml. To obtain drops of this size, the end of the capillary was tapered for

about 0.5 in. (1 cm) to a tip which had an outside diameter of about 0.14 in. (3.3 mm). The glass tube, *A*, inside the funnel serves to maintain a constant head of liquid. By moving this tube up or down, small adjustments can be made in the rate of dropping. There was no difficulty in keeping the rate of dropping at 100 ± 3 drops per minute.

When tests were made with ammonium nitrate reagents, the tip of the capillary was placed about 0.4 in. (1 cm) above the surface of the specimen. With the chromic acid reagent, the distance was increased to about 0.8 in. (2.0 cm), because at the shorter distance a drop would occasionally bounce off the metal without spreading. A variation of 20 percent in these distances did not appreciably affect the accuracy of the test.

The apparatus shown in figure 1 has a pivoted rod, *C*, which can be turned down to gage the distance from the capillary tip to the metal and then swung up out of the way. The test specimen was inclined at 45° to the horizontal. Although the angle is not critical (a variation of $\pm 15°$ produces an error of ± 10 percent), it should not vary too much from 45° if satisfactory results are desired. The spent solution should drain freely from the specimen. When tests are made near an edge, it is advisable to place a strip of cloth on the edge to act as a wick for drawing off the spent solution. The specimens should be solvent-degreased, then scrubbed with magnesium oxide paste, rinsed, and dried. The specimen and apparatus must be rigidly fixed during the test, so that successive drops strike the same spot.

(b) END POINTS

The end point of the test is the exposure of the basis metal, which usually offers enough contrast of color to be readily distinguished from the surrounding area of etched coating. The exposure of smooth basis metal occurs rather suddenly, and the area rapidly increases as more reagent is added. On rough basis metal, especially on cast iron, the end point is not sharp, and the basis metal may be revealed through a few minute areas before the general breakdown. In such case, the end point was taken when small areas of basis metal had appeared over a total area about ⅛ in. (3 mm) in diameter, although these areas of bare iron were irregularly distributed and were intermingled with areas of incompletely dissolved coating. The test would have to be run about 10 to 20 percent longer to produce a continuous area of bare metal.

(c) DETERMINATION OF THICKNESS FACTORS

The compositions of the dropping test reagents and their "thickness factors" are given in table 1. The thickness factors for each reagent were determined by dividing the known thickness of coating (in hundred-thousandths of an inch) by the number of seconds required for penetration. The thickness of any zinc or cadmium coating, in hundred-thousandths of an inch, is obtained by multiplying the number of seconds required for penetration by the appropriate factor. Hull and Strausser attempted to prepare reagents of such concentrations that the factors would be unity, that is, each second of test would correspond to 0.00001 in. (0.00025 mm) of coating. However, as the rates of attack of several of the solutions have considerable

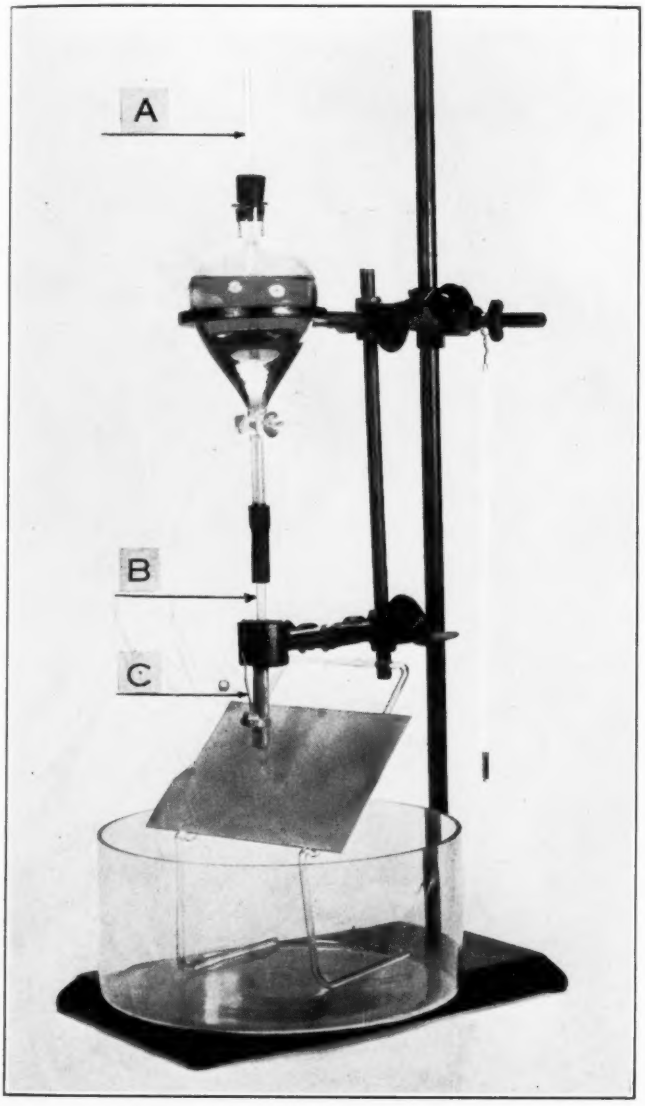

FIGURE 1.—*Dropping-test apparatus.*

A, Glass tube for maintaining a constant head of liquid; *B*, capillary tube; and *C*, device for adjusting the distance between the capillary tip and the specimen.

UNIV OF MICH.

temperature coefficients, the unity factor applies to only one temperature. In the work here reported no attempt was made to devise solutions with a factor of unity at any given temperature. Instead convenient solutions were used and factors were determined for the customary temperature range.

TABLE 1.—*Composition and thickness factors of test solutions*

Reagent symbol [a]	Coating to be tested	Composition of reagent					Thickness factors (hundred thousandth of an inch per second)	
		Oxidizing agent		Acid				
		Formula	g/liter	Formula	ml/liter (conc.)	Normality in reagent	70° F (21° C)	95° F (35° C)
			g		*ml*			
N_E	Electroplated zinc	NH_4NO_3	100	HNO_3	55	0.85	1.03	1.06
N_H	Hot-dipped zinc	NH_4NO_3	100	HCl	75	.85	0.93	1.01
N_S	Sherardized zinc	NH_4NO_3	100	HCl	125	1.45	1.24	1.64
N_{Cd}	Electroplated cadmium	NH_4NO_3	110	HCl	10	0.12	0.95	1.30
CrO_3-Zn	Electroplated zinc	CrO_3	200	H_2SO_4	50	3.0	.97	1.19
CrO_3-Zn	Hot-dipped zinc	CrO_3	200	H_2SO_4	50	3.0	1.01	1.21
CrO_3-Zn	Sherardized zinc	CrO_3	200	H_2SO_4	50	3.0	.96	1.21
						Average [d]	.98	1.20
CrO_3-Cd	Electroplated cadmium	CrO_3	200	H_2SO_4	50	3.0	1.33	1.60
J	Electroplated zinc	NH_4NO_3	70	HCl	[c] 70	0.07	2.25	3.15

[a] Solutions N_E, N_H, and N_{Cd} were developed by Hull and Strausser. Solution N_S was developed by W. G. Schlecht of this laboratory. Solution *J* was recommended by Clarke for the jet test.
[b] Jet test.
[c] 1.0 Normal acid.
[d] Average of the thickness factors of the chromic acid reagent for zinc coatings.

The factors in table 1 were determined at 70° F (21° C) and 95° F (35° C), and the factors for intermediate temperatures were obtained by linear interpolation between the two points (fig. 2). The factors are not necessarily linear functions of temperature, but the accuracy of the test is not sufficient to determine the shape of the curve over this short range.

The factors for electrodeposited zinc and cadmium, tables 2 and 3, are average values obtained partly by testing flat specimens which had been plated from typical solutions at the National Bureau of Standards under conditions giving coatings of known and uniform thickness. In addition, dropping tests were made on some coatings plated by several commercial firms on smooth steel, using proprietary bright plating baths as well as the ordinary acid and cyanide baths. Each value in tables 2 and 3 is the average of three or more dropping tests, which had a reproducibility of about ±6 percent.

From table 1 it may be seen that the average factor for zinc for the N_E solution (previously recommended) is close to unity and has only a small temperature coefficient, which confirms the work of Hull and Strausser. Table 2 shows that the average deviation of the factor from the mean for different electroplated zinc coatings was ±6 percent

and that the maximum deviation was ±13 percent. These deviations are within the limits of accuracy given by Hull and Strausser for the test. With the chromic acid reagent the factors for the different zinc coatings showed less variation than with the ammonium nitrate reagent.

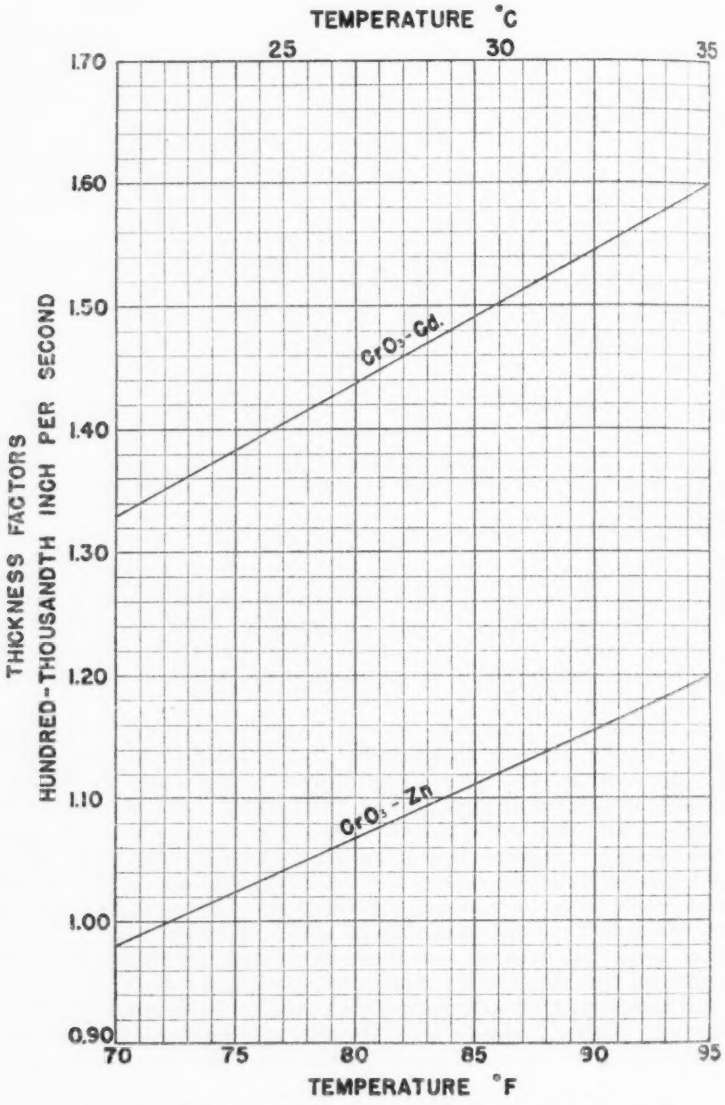

FIGURE 2.—*Thickness factors for the* CrO_3 *dropping-test reagents.*

TABLE 2.—*Thickness factors for zinc coatings*

Manufacturer	Coating: Plating bath	Coating: Thickness	Thickness factors: N_S reagent [a] (75° F)	Thickness factors: CrO_3 reagent: 70° F	Thickness factors: CrO_3 reagent: 95° F	Percentage of error [b]: Jet test	Percentage of error [b]: Magnetic method: Burnished	Percentage of error [b]: Magnetic method: Not burnished
		in.						
E	Acid	0.0005	0.95			+11	0	+6
E	do	.0010	.97			+17		
F1	do	.0005	.96			+10		
F1	do	.0009	1.03			+8	−4	−3
F2	do	.0003	0.87			+4		−5
F2	do	.0012	.97			−2		
F3	Cyanide strike+acid	.0006	.92			+41	−3	−2
F3	do	.0011	.91			+31	−6	−5
G	Acid	.0005	.98	0.96	1.17	+14		
G	do	.0010	.96	.95	1.21	+8	−3	+10
Average			0.95(±3%)	0.96(±1%)	1.19(±2%)	+15±10	−3±1	0±5
Percentage of deviation from general average			−8	−1	0			
E	Cyanide	0.0007	0.88			−4		
E	do	.0010	.95			−3		+3
B1	do	.0004	1.10			−5	−6	+7
B1	do	.0012	1.15	0.95		−2±6	−3	+1±5
G	do	.0002		1.00	1.18			
G	do	.0005	0.92	0.94	1.13	+1±2		
G	do	.0010	1.00	.95	1.22	−8	−4	−3
Average			1.00(±8%)	0.96(±2%)	1.18(±3%)	−4±3	−4±1	+2±4
Percentage of deviation from general average			−3	−1	−1			
H	Cyanide, bright	0.0005	0.95			−4		
H	do	.0010	.96	0.99		−2±4		+2
K	do	.0007	1.08	.98		+4±6		
K	do	.0013	1.12			+12		+1
Average			1.03(±7%)	0.99(±1%)		+3±7		+2
Percentage of deviation from general average			0	+2				
L	Cyanide+Hg	0.0005	1.16	0.95		[c]		
Percentage of deviation from general average			+13	−2				
General average			1.03(±6%)	0.97(±2%)	1.19(±1%)	+5±9	−4±1	+1±4

[a] Since the factor varies little with temperature, most of the tests were made at only one temperature.
[b] Based on stripping test.
[c] Unsatisfactory end point.

TABLE 3.—*Thickness factors for the dropping test on electroplated cadmium coatings*

Coating		70° F (21° C)		95° F (35° C)	
Manufacturer	Thickness	N_{Cd} factor	CrO_3 factor	N_{Cd} factor	CrO_3 factor
	in.				
A	0.0002	1.08	1.40	1.36	1.60
	.0005	1.14	1.31	1.50	1.62
Average		1.11 (±3%)	1.35 (±4%)	1.43 (5±%)	1.61 (±1%)
Percentage of deviation from general average		+17	+2	+10	+1
B	.0002	1.06	1.29	1.50	1.60
	.0004	1.10	1.35	1.45	1.58
	.0010	1.07	1.30	1.44	1.60
Average		1.08 (±2%)	1.31 (±2%)	1.46 (±2%)	1.59 (±1%)
Percentage of deviation from general average		+14	−2	+12	−1
C	.0002	0.68	1.34	0.93	1.53
	.0005	.66	1.28	1.00	1.54
	.0007	.73	1.32	1.16	1.59
Average		0.69 (±4%)	1.31 (±2%)	1.03 (±9%)	1.55 (±1%)
Percentage of deviation from general average		−27	−2	−21	−3
D	.0002	0.92	1.35	1.27	1.53
	.0004	.96	1.31	1.29	1.66
	.0007	.87	1.35	1.30	1.70
Average		0.92 (±3%)	1.34 (±1%)	1.29 (±1%)	1.63 (±4%)
Percentage of deviation from general average		−3	+1	−1	+5
General average		0.95 (±15%)	1.33 (±2%)	1.30 (±11%)	1.60 (±3%)

Table 3 contains the data for four commercial cadmium coatings on which are based the factors in table 1. The N_{Cd} reagent dissolved the cadmium coatings at decidedly different rates. Because of this difference, this reagent cannot be safely used for the general testing of cadmium coatings, although it might be used for plant control of one type of coating. The appreciable temperature variation of the factor for the N_{Cd} reagent (over 1 percent per degree Fahrenheit) was not previously reported. The chromic acid reagent gave about the same factor with all four coatings and the temperature coefficient of the factor is about 1 percent per degree Fahrenheit.

The factors in table 1 for hot-dipped and sherardized coatings were obtained by testing commercial coatings. The results will be discussed in more detail in a later section. The chromic acid reagent has the same factor (0.98 at 70° F) within a few percent for electroplated, hot-dipped, and sherardized zinc, and hence only one factor need be used.

3. JET TEST

The jet test differs from the dropping test in that the reagent strikes the surface in a continuous stream instead of in drops. The dimensions of the jet tube and the head of liquid must meet certain specifications, as defined by Clarke. The apparatus, procedure, and thickness factors used in these tests were in accordance with Clarke's recommendations.

4. MAGNETIC THICKNESS MEASUREMENTS

The thickness of coatings was measured also by a magnetic method, which can be used for any nonmagnetic coating on steel. The method depends on the decrease in the attractive force between a permanent magnet and the steel basis metal when the two are separated by a coating. The instrument, called a "Magne-gage," is calibrated with standard samples having a known thickness of coating plated on steel.

5. TESTING COMMERCIAL ARTICLES

The commercial articles to which the various tests were applied consisted mainly of electrical accessories, such as conduit boxes, utility boxes, and condulets, which were donated by a number of firms. The basis metals consisted of mild sheet steel, malleable iron, and gray cast iron, all of the surfaces of which were usually rough. The coatings included electroplated, hot-dipped, and sherardized zinc, and electroplated cadmium. These articles are representative of commercial products which might be subjected to a dropping test.

The accuracy of the dropping tests on commercial materials was determined by comparison with the antimony trichloride stripping method, which was taken as the standard. The specimens for the stripping test usually had an area of 6 to 20 cm^2 (1 to 3 $in.^2$) and were cut from the center of the sample, where the coating was more likely to be of uniform thickness than near an edge. The test piece was weighed, one side protected with a "stop-off" lacquer, and the other side tested with the Magne-gage and then with two to four dropping tests. The remainder of the coating was dissolved in the antimony trichloride reagent, the lacquer removed, and the loss in weight determined. From the loss in weight, the average thickness was calculated and compared with the results of the other tests. The thickness of the coating did not appreciably affect the accuracy of the dropping test, provided that the coating was at least several ten-thousandths of an inch thick. On thinner coatings the accuracy was less, because each second of error in time produced a relatively large percentage of error in thickness.

III. RESULTS OF TESTS

1. ZINC COATINGS

(a) ELECTROPLATED

(1) *Dropping tests.*—The results of tests on commercial zinc-plated articles are given in table 4. As the basis metals of these articles were rough, the dropping-test end points were not as sharp as those

obtained on smooth steel. The end points given by the Hull-Strausser reagent, N_B, were usually satisfactory on all electrodeposited zinc coatings except those containing mercury.[6] The end points on these coatings were either indistinct or undetectable because the etched zinc coating and the steel had about the same gray color.

The modified reagent suggested by Hull (reagent N_B') was tried on several coatings. The end point consists in the appearance of a blue color. On ordinary zinc coatings, the modified reagent gave results of about the same degree of accuracy as the N_B reagent. On zinc-mercury coatings, however, the results were 10 to 20 percent high for coatings more than 0.0005 in. thick and more than 20 percent high for thinner coatings. Apparently the mercury deposited on the steel and retarded the attack necessary for the formation of the blue color.

TABLE 4.—*Accuracy of thickness measurements of commercial electroplated zinc coatings*

Manufacturers	Basis metal	Coating		Percentage of error [d]					
		Type	Thickness	Dropping-test solutions			Jet solution	Magne-gage	
				N_B	[a]N'_B	CrO_3	J	Burnished	Not burnished
			in.						
M	Sheet steel	Ordinary	0.0004	−12		−7	+5	+10	+25
			.0018	−12	0 ±4	−18			
			.0002		−6±10	−18		+14	+14
N	do	do	.0004 .0008	−11		−7	±9		
	Cast iron	do	.0010 .0017	−11		+7		−12	−10
P	Sheet steel	do	.0005 .0007	−13		−18		−12	−3
Q	Steel tubing	do	.0009 .0012	−9	−5	−5			
R	Malleable iron	do	.0005 .0008	−14		−14		−18	+3
S	Sheet steel	Zn-Hg	.0004 .0005	+36		+1±10	[b]		
			.0006 .0012	[c]−7	0±10	−8			
			.0002 .0003	[c]+6 ±16	+75	+2±13			
T	do	do	.0002 .0004	+12	+70	+3 ±6	[b]		
U	do	do	.0006 .0009	+60	+23	+7	[b]	−7	+5
Average				+2 ±18	+22±29	−6 ±8		−4±11	+6 ±9

[a] The N'_B solution was the N_B solution to which 3.0 g/liter of potassium ferricyanide had beeen added
[b] Reagent dissolved the coating too slowly to permit definite readings.
[c] The N'_B solution was used, but the ordinary end point was observed instead of the appearance of the blue color.
[d] When averages are expressed in the form $A \pm B$, A represents the systematic difference of the measurements from the correct value, and B represents the precision of A.

The chromic acid reagent gave satisfactory end points on all electroplated zinc coatings tested, including zinc-mercury deposits. On ordinary zinc coatings the end point was made visible by contrast of the white steel with the yellow color acquired by zinc. On zinc-mercury coatings, a black color suddenly appeared just before the

[6] The zinc-mercury coatings, deposited from a cyanide bath, may contain up to several percent of mercury.

steel was exposed. Usually a few more drops of reagent dissolved this black layer and revealed the dull gray steel.

(2) *Jet tests.*—Only a small number of measurements were made with the jet test, as it does not offer any advantage over the dropping test for zinc coatings and possesses the following disadvantages:

1. The reagent recommended by Clarke dissolves zinc-mercury coatings at a much slower and less definite rate than other zinc coatings.

2. The end point is difficult to see because the initial penetration of the coating occurs only over a tiny crescent-shaped area. In many cases a hand lens is necessary to detect the end point. This difficulty is increased when the basis metal is rough.

3. As the end point cannot be seen while the test is in progress, the flow of liquid must be stopped at intervals so that the surface can be examined for the end point.

(3) *Magnetic measurements.*—Tests performed with the Magne-gage involve no end point. Since the surfaces of the materials were rough, it was necessary to take the average of a number of readings. Practically all the errors were less than ± 15 percent. Because of the usual roughness of such surfaces, measurements cannot be made on cast iron with this degree of accuracy, unless the coatings are at least 0.0008 in. thick. Measurements with the Magne-gage were also made on the test specimens after burnishing a small area with a half-inch steel ball. This somewhat increased the reproducibility of the readings but tended to make the measurements low. Apparently the burnishing is advantageous if the basis metal is mild steel, but it does not help much if the metal is cast iron.

(4) *Miscellaneous tests.*—A few of the commercial coatings consisted of a layer of cadmium covered by a coating of zinc. These coatings cannot be tested by the dropping method because zinc and cadmium have different rates of solution. The average thickness of each layer can be ascertained by boiling the specimen in a solution of sodium hydroxide, which dissolves the zinc without attacking the cadmium undercoating. The cadmium can then be dissolved with ammonium nitrate solution.

A simple qualitative test for the presence of mercury in a zinc coating is as follows: Dilute nitric acid (1 : 4) is poured onto the surface, which is then rubbed with a piece of clean copper foil. If mercury is present a silvery stain will appear on the copper. The usual procedure of testing a coating by first dissolving it in acid is not successful with zinc-mercury coatings, because the mercury remains on the iron surface and no test for mercury is then obtained in the solution.

(b) HOT-DIPPED

(1) *Dropping tests.*—The factors for the Hull-Strausser dropping test reagent, N_H, and the chromic acid reagent were obtained by testing galvanized sheet from six different sources, with coatings from 0.001 to 0.0015 in. in thickness. The average values of the factors are given in table 1. The factor for the N_H solution is fairly close to unity, which is the value given by Hull and Strausser. For both reagents, the average deviation of the factor from the mean was ± 4 percent and the maximum ± 10 percent. This shows that there was no important difference in the behavior of the coatings from different sources.

The end points of both reagents were satisfactory on the galvanized sheet. With the N_H reagent, the zinc turned black, and at the end point the steel appeared white against the black zinc. The chromic acid reagent also gradually turned the zinc black, but just before the end point the black color gave way to a light gray layer, which was quickly penetrated and revealed the bright steel basis metal.

Table 5 gives the results of some additional tests on hot galvanized electrical fittings. There was no difficulty in obtaining fairly accurate results for coatings on mild steel sheet, as the end point was easily seen. However, the end points of coatings on cast iron were not satisfactory, as the iron had a black color which did not offer a contrast with the black color acquired by the zinc. The N_H reagent gave no evident end point, but apparently when the cast iron was exposed, the zinc began to dissolve with effervescence. This point of effervescence was taken as an approximate end point, but it was not satisfactory. The end point given by the chromic acid reagent did not show sufficient contrast to be seen through the colored reagent. In order to see the end point, the flow of reagent had to be stopped and the solution rinsed from the surface with several drops of water. The end point consisted of a black area of cast iron showing through gray zinc. Whenever there was any doubt of an end point being reached (with either reagent), the surface was tested with a few drops of copper sulfate solution. Bright copper coated any exposed iron, but only a black mossy deposit formed on the zinc surface.

TABLE 5.—*Accuracy of thickness measurements of commercial hot-dipped zinc coatings*

Manufacturer	Basis metal	Coating thickness	Percentage of error		
			Dropping tests		Magne-gage
			Solution N_H	Solution CrO_3	
		in.			
U	Mild steel	0.0030	−4	+2	+3
W	Steel tubing	.0016	−7	−4	−7
		Average	−6	±3	±6
X	Malleable iron	.0045	−8	−18	−5
Y	Cast iron	.0035	−24	−18	−13
Z	do	.0030	−25	+4	−12
		Average	−19	−11 ±10	−10

(2) *Magnetic measurements.*—Tests were made with the Magne-gage on the six specimens of galvanized sheet which had been used for standardizing the drop-test reagents (table 1). The average error was −7 percent and the maximum error −11 percent. The measurements on galvanized fittings, recorded in table 5, are also about 10 percent low. These results check previous magnetic measurements on hot-dipped coatings which showed a systematic error of −10 percent, probably caused by the alloying of the iron and zinc. This error can be eliminated by the use of a correction factor or by standardizing the instrument against hot-dipped zinc coatings of known thickness.

(c) SHERARDIZED

(1) *Dropping tests.*—The thickness factors (table 1) for the N_1 and chromic acid reagents were obtained by testing commercial sherardized coatings from three different sources. The coatings were between 0.001 and 0.003 in. thick and had been applied to mild steel. For each reagent, the average deviation of the measurements from the mean was about ± 7 percent, and the maximum deviation about ± 18 percent. As no additional sherardized samples from other sources were available, the accuracy of the dropping tests could not be determined in general, but from the above results the method is probably reliable within about ± 15 percent.

The end points for sherardized coatings on mild steel appeared rather gradually and were not as distinct as those for hot-dipped coatings. Since the coatings were thick, this did not cause a serious percentage error. The N_1 reagent turned the surface dark, and the end point consisted in the exposure of the white steel. The appearance of the area during the test varied with the specimen and thickness of coating. Some coatings yielded alternate black and silvery layers, and the occurrence of the latter might be mistaken for the steel. In cases of doubt, the test was stopped[7] for a few seconds, whereupon any silver-colored zinc layer immediately turned black, whereas exposed steel darkened but slightly. The chromic acid reagent gave an end point similar to its end point on hot-dipped coatings. The sherardized surface turned dark brown, and the end point occurred when the silvery colored steel appeared. Sometimes, shortly before the end point, the brown color was succeeded by a yellow layer, which was rapidly penetrated to expose the steel.

The end points of the dropping test for sherardized coatings on cast iron are similar to the end points for hot-dipped coatings on cast iron and are not very satisfactory. Hence, the accuracy of the method on this material was not determined.

When dropping tests are to be made on hot-dipped or sherardized coatings, one should make a preliminary test in order to become familiar with the sequence of color changes and not mistake one of them for the end point. The preliminary test should be allowed to proceed long enough to make certain that the steel has been exposed.

To determine the ease of recognizing the end points for hot-dipped and sherardized coatings on mild steel, three different observers performed dropping tests after reading the written instructions. The average error of the tests on galvanized sheet was ± 5 percent for both reagents. On the sherardized coatings, the average error was ± 8 percent for the chromic acid reagent and ± 16 percent for the N_1 reagent.

(2) *Magnetic measurements.*—When measurements were made on sherardized coatings with the Magne-gage, it was necessary to burnish the area tested, as the coatings were rough. The thicknesses given by the Magne-gage were somewhat high as compared with the thickness calculated from the stripping method. The average error was $+8$ percent and the maximum error $+16$ percent. If the surface was not burnished, the errors were about twice as large. The stripping method, using 7.1 for the density of zinc, has been taken as the

[7] The time for tests which were interrupted was measured with a "stop and go" type of stop watch.

standard measure of thickness. However, the sherardized coatings may be thicker than corresponds to the weight of coatings and density of zinc, because they are somewhat porous and may contain oxide.

2. CADMIUM COATINGS

(a) DROPPING TESTS

Table 6 gives the results of tests made on cadmium-coated materials obtained from seven different manufacturers. The N_{Cd} and chromic acid reagents gave sharp end points with cadmium coatings plated on mild steel, especially if the basis metal was smooth. However, the end point for cadmium on rough cast iron surfaces was less satisfactory. With the N_{Cd} reagent, some of the cadmium coatings on cast iron turned dark gray or black, apparently because they contained some impurity, and as the steel was also dark in color, the end point could be distinguished with difficulty, if at all. In these cases, addition of potassium ferricyanide to the N_{Cd} reagent did not improve the accuracy of the test, as apparently the blue color did not appear until the end point was passed. The chromic acid reagent gave a visible end point on all the cadmium-plated cast iron tested. During the test, the cadmium became bright and, at the end point, contrasted with the dull-colored iron. The end point was most easily observed by viewing at the angle which best showed the difference in the reflecting power of the metals.

TABLE 6.—*Accuracy of thickness measurements of commercial electroplated cadmium coatings*

Manufacturer	Basis metal	Coating thickness	Percentage of error				
			Dropping test			Magne-gage	
			N_{Cd}	[a] N'_{Cd}	CrO_3	Burnished	Not burnished
		In.					
G–C	Sheet steel	0.00015	−13		+7	0	0
		.00020	−5		+14	−10	−2
N	do	.0005	−19		−1	−13	−4
	Cast iron	.0008	−17		−16	−1	+7
Z	do	.002	+16		−3	+5	+6
		.001	−3	+17	−15	−4	+9
R	Malleable iron	.0006	+74	+116	−21	−3	+6
U	do	.0006	[b]	+71	−5	−17	+3
		.0007	[b]	+113	−4	−17	+2
Y	do	.0016	[b]		−23	−6	−6
M	Cast iron	.001	[b]		−9	−16	−4
Average					−7 ±9	−9	+2 ±5

[a] Solution N_{Cd}+3 g/liter of $K_3Fe(CN)_6$.
[b] Unsatisfactory end point.

The percentage errors for the N_{Cd} and $N_{C'd}$ solutions are subject to considerable uncertainty, because, as shown in table 3, the factors for four proprietary cadmium deposits were not concordant. In testing cadmium coatings from various sources, it would be necessary to use some value that might be assumed to represent the average cadmium coating. Therefore, the average factors derived from table 3 were used. No such uncertainty is connected with the values for the chromic acid solution.

(b) MAGNETIC MEASUREMENTS

The measurements with the Magne-gage were generally correct within ±15 percent. Burnishing the cadmium coating gave a somewhat low result, probably because the metal is so soft.

3. MICROSCOPIC METHOD FOR ZINC AND CADMIUM COATINGS

The microscopic method of measuring the thickness is not very satisfactory for zinc and cadmium coatings, because these metals are soft and flow when polished. Consequently, it is necessary to employ a special technique and to have considerable experience in order to obtain reliable results.

Several flat specimens, plated with coatings of known uniform thickness were measured microscopically in a laboratory [8] experienced in such measurements. The results were accurate to ±5 percent. In the metallurgical laboratories of this Bureau this accuracy was approached by observers not previously experienced in measuring zinc coatings, only after a number of trials with different polishing procedures. This experience shows that great care is required to obtain reliable values on zinc and cadmium coatings.

IV. CONCLUSIONS

1. DROPPING TESTS

The ammonium nitrate reagents have been found to operate satisfactorily with most types of zinc coatings on mild steel basis metals. Zinc-mercury coatings, however, do not yield a good end point, especially if they are deposited on rough surfaces. If the zinc-mercury coatings are tested with the modified reagent, containing potassium ferricyanide, a large positive error is obtained on coatings several ten-thousandths of an inch thick. The ferricyanide may increase somewhat the sharpness of end point with other coatings, but it is not essential. The ammonium nitrate reagents did not give satisfactory end points for hot-dipped or sherardized zinc coatings on cast iron.

The ammonium nitrate reagent is not satisfactory for cadmium coatings because it does not dissolve coatings from different sources at the same rate. Also the end point for some cadmium coatings on cast iron is indistinct.

The reagent containing 200 g/liter of chromic acid and 50 g/liter of sulfuric acid gave a satisfactory end point with most coatings, including zinc-mercury coatings and cadmium plated on cast iron. The end points for hot-dipped and sherardized zinc coatings on cast iron were not so satisfactory, as the test had to be stopped in order to see the end point. In addition to giving better end points than the ammonium nitrate reagents with some coatings, the chromic acid reagent has the advantage that only one solution is required for testing electroplated, hot-dipped, and sherardized zinc coatings, and electroplated cadmium. Moreover, the application of the reagent is simplified, since the factors for the three kinds of zinc coatings are the same. On the other hand, four different ammonium nitrate solutions have been recommended for the dropping test, one for each type of coating,

[8] New Jersey Zinc Co., through the kindness of E. A. Anderson.

as the original purpose was to develop solutions which had a factor equal to unity. This number of solutions could easily be reduced to three, by using the N_H solution also for testing cadmium, but the number of solutions could not be further decreased without sacrificing either the accuracy or the sharpness of the end points. One advantage of the ammonium nitrate reagents over the chromic acid reagent is that the N_E and N_H solutions have factors with low temperature coefficients.

When satisfactory end points are obtained on coatings thicker than 0.0002 in. the dropping test gives results correct to within ± 15 percent, if the basis metal is fairly smooth. However, if the coatings are deposited on rough surfaces or on cast iron, the measurements may be in error by ± 20 percent. Therefore, if the dropping test is to be used in general testing for example, for compliance with specifications a tolerance of 20 percent should be allowed. When the dropping test is used for plant control, in which case the same type of coating would always be tested, results correct within ± 10 percent can be obtained by making a correction for any systematic error.

2. JET TEST

The jet test was found to be less satisfactory than the dropping test as a general method for electroplated zinc coatings.

3. MAGNETIC MEASUREMENTS

The Magne-gage usually gave results correct within ± 15 percent. Measurements of hot-dipped coatings were consistently about 10 percent low; hence for such coatings more accurate values can be obtained if the direct Magne-gage results are corrected by this amount. Burnishing improves the reproducibility and accuracy of measurements of zinc coatings plated on mild steel and of sherardized coatings. However, it is not necessary on hot-dipped coatings, and does not improve the accuracy of measurements of electroplated coatings on cast iron. The chief limitation of the Magne-gage, when applied to the commercial products, is that it does not accurately measure coatings thinner than 0.0008 in. that are deposited on cast iron.

V. RECOMMENDATIONS

1. The chromic acid reagent is recommended in preference to the ammonium nitrate reagents for testing zinc and cadmium coatings.

2. Even with the chromic acid reagent, a tolerance of -20 percent should be allowed on individual thickness measurements to take care of uncertainties in the end points, especially of coatings from different sources. This tolerance may be included directly in the minimum thicknesses specified.

3. The magnetic method is promising and certainly useful for plant control. Additional commercial experience will be required before it can be included in formal specifications.

4. The use of the microscopic method for umpire tests should be confined to laboratories having experience with these particular measurements.

5. For many purposes the stripping method with hydrochloric acid and antimony trichloride is preferable as an umpire test. A piece

with a total area of from 1 to 4 cm^2 is cut from that portion of the article where the thinnest coating is suspected. It is carefully weighed (to 0.1 mg) and the portion of its surface not to be stripped is coated with an acid-resistant lacquer, which is removed after the stripping and prior to reweighing. This method is usually reliable well within ± 10 percent.

The author expresses his appreciation to W. Blum for his advice and guidance and acknowledges the assistance given by the Metallurgy Division of the Bureau and by W. A. Olson, who performed some of the tests. The author also thanks the following firms for furnishing most of the coated specimens used in the investigation:

Hanson-Van Winkle-Munning Co.; Grasselli Division, Dupont Co.; Udylite Process Co.; Meaker Co.; Thomas & Betts Co.; Steel City Electric Co.; Crouse-Hinds Co.; Appleton Electric Co.; Jefferson Electric Co.; All-Steel Equipment Co.; The Rattan Manufacturing Co.; Benjamin Electric Mfg. Co.; Adalet Manufacturing Co.; Erie Malleable Iron Co.; General Electric Co.; and Bridgeport Switch Co.

WASHINGTON, June 7, 1939.

U. S. DEPARTMENT OF COMMERCE NATIONAL BUREAU OF STANDARDS

RESEARCH PAPER RP1241

Part of Journal of Research of the National Bureau of Standards, Volume 23, September 1939

COMPARISON OF ACCELERATED AGING OF RECORD PAPERS WITH NORMAL AGING FOR 8 YEARS

By B. W. Scribner

ABSTRACT

Various grades of record papers that had been stored under normal conditions for 8 years were tested and the results are compared with test values for their original properties and their properties after accelerated aging by heat at time of storage. The results agree well with a retest made after 4 years of normal aging. The papers had the same relative order of stability, as shown by retention of folding endurance, under both kinds of aging. Their stability was commensurate with the chemical purity of the papers, and the same kind of chemical changes occurred during 8 years of natural aging as under accelerated aging. The cellulose of the stable papers was in good condition, as indicated by high alpha-cellulose content, low copper number, and low or moderate acidity.

CONTENTS

		Page
I.	Introduction	405
II.	Test methods	406
III.	Test data	406
IV.	Discussion	409
V.	Summary	412
VI.	References	413

I. INTRODUCTION

The results of an investigation at the National Bureau of Standards [1],[1] in its early work relating to the standardization and classification of record papers, indicate that the relative stability of such papers under normal storage conditions can be determined satisfactorily by heating the papers and testing for decrease in strength and changes in certain chemical properties. The papers studied in that work were 37 commercial writing and book papers representative of the various grades as produced at the time. The test data showed a good correlation between the retention of folding endurance on heating the papers for 72 hours at 100° C. and the chemical condition of the paper with respect to the purity of the cellulose, as indicated by alpha-cellulose content and copper number, the acidity, and the rosin content. The more stable papers under the heat test were characterized by a good condition of the cellulose as shown by a high alpha-cellulose content and a low copper number, by low acidity, and by low rosin content, although the last apparently was of minor importance. It was found that the papers could be grouped satisfactorily with respect to the degree of stability required for different record purposes by means of these physical and chemical data, and classifications of record papers based on such data have been proposed [2].

[1] Numbers in brackets indicate the literature references at the end of the paper.

To obtain further information, 33 of the papers mentioned were stored at the Bureau for testing at various periods of time to compare the effects of normal aging with the effects of aging accelerated by heating. The storage conditions are those of the average good business office practice, that is, the papers are not exposed to any abnormal conditions of temperature, humidity, or air pollution. The first retests of the papers were made after they had been stored for 4 years. The papers were tested for strength, alpha-cellulose, copper number, and acidity, and despite the short period of aging, the grading of the papers for stability was very similar to that foretold by the accelerated aging [3]. The following is an account of retests of the stored papers after 8 years of aging.

II. TEST METHODS

As in the first retest of the papers, they were tested again for folding endurance, acidity (Kohler-Hall), alpha-cellulose, and copper number. These tests were made by the present methods of the Technical Association of the Pulp and Paper Industry,[2] which yield values comparable with those originally obtained for the papers. (In considering the results of the folding endurance tests, papers having very low values should not be regarded as being actually brittle, as the test strips are folded under a tension of 1 kg, therefore, such papers may still be in a serviceable condition.) In addition, tests were made for acidity in terms of pH, beta-cellulose, and gamma-cellulose. Suitable methods for these tests were not available when the papers were previously tested. With development of satisfactory technique and equipment for the determination of pH, this has now become the preferred way of expressing the acidity of paper. The procedure employing hot extraction of paper with water, which is specified in the present method of the Technical Association of the Pulp and Paper Industry, and a cold-extraction method developed by H. F. Launer [4] were used. The latter method appears to be preferable, and its adoption is being considered by the Technical Association. The cellulose fractions were determined by a modified volumetric procedure, also developed by Launer, in which oxidation by dichromate is used [5]. Satisfactory determination of the beta and gamma fractions cannot always be made by gravimetric procedures, and the volumetric method has several other advantages.

III. TEST DATA

Descriptions of the papers and the test data are given in table 1. For additional information on the papers, see reference [1]. There are no data given herein for samples 104, 113, 122, 115, 148 (corresponding to Nos. 1, 2, 20, 24 and 32 in fig. 1) included in the previous work, as the supply of these had become exhausted. Sample 782, a paper made in the Bureau mill from purified wood fibers, was added to include a high-grade paper of this kind. The figure of 55-percent retention of folding endurance on heating previously reported for sample 118 appears to be in error on consideration of the general good quality of this paper, and a retest made at this time yielded a figure of 76 percent. Therefore, this latter value is given in this report.

[2] Copies can be obtained from the Association at 122 East 42d Street, New York, N. Y.

TABLE 1.—*Test data on paper*

Numbers in this column refer to the numbers in figures 1 and 2	Sample number	Kind of fiber			Original tests											After heating sample at 100° C for 72 hours				Tests after 8 years of normal aging					
		Rag	Chemical wood		Before heat treatment											Folding endurance in percentage of initial	Increase in acidity Kohler-Hall	Decrease in alpha-cellulose in percentage of initial	Increase in copper number	Folding endurance in percentage of initial	Increase in acidity Kohler-Hall	Decrease in alpha-cellulose in percentage of initial	Increase in copper number		
			Coniferous	Deciduous	Folding endurance		Ash	Rosin	Glue	Acidity ª Kohler-Hall	Alpha-cellulose ª	Copper number													
					Machine direction	Cross direction																			
					Double folds	*Double folds*																			
		%	%	%			%	%	%	%	%														
3	114	100	0	0	1,700	440	0.10	1.4	.....	0.034	99.0	0.30	79	0.000	1.0	0.08	91	−0.004	0.0	0.10	5.7	6.1	99.0	0.5	0.5
4	118	100	0	0	4,700	6,200	.60	1.6	4.7	.169	95.1	.88	76	.016	.6	.04	84	.021	−1.89	.62	4.1	4.6	96.9	1.5	1.6
5	119	100	0	0	2,600	1,700	.54	2.4	.....	.086	92.9	1.28	22	.043	6.0	.46	62	.054	0.43	.32	4.4	5.0	92.5	4.5	3.0
6	120	100	0	0	3,600	2,800	.73	1.4	2.2	.090	94.4	1.11	82	.042	1.4	.26	84	.050	.64	.19	4.3	4.8	93.8	3.6	2.6
7	127	100	0	0	3,300	1,200	.75	2.2	.....	.138	91.1	.93	70	.045	3.4	.78	80	.012	−.55	.27	4.2	5.0	91.6	4.2	4.2
8	126	100	0	0	3,000	1,900	.80	2.3	4.6	.235	94.4	1.23	77	.046	2.2	.39	84	.035	−.53	.77	4.3	4.8	93.9	1.6	4.5
9	129	100	0	0	3,100	2,600	.71	2.4	3.5	.218	94.3	1.12	69	.039	2.6	.16	95	.040	−.54	.17	4.2	4.9	92.7	3.1	4.2
10	128	100	0	0	3,500	2,600	.77	2.5	.....	.275	83.9	2.26	63	.056	5.7	.52	81	.045	3.93	.18	4.0	4.7	94.8	1.4	3.8
11	131	100	0	0	9	9	.82	1.7	3.4	.075	86.6	2.48	53	.048	2.6	.23	71	.036	2.77	.12	4.6	5.1	84.2	13.4	2.4
12	130	100	0	0	22	20	.72	1.5	.....	.084	86.6	.....	.....	.....	.....	.....	.....	.....	.....	.....	.....	.....	.....	.....	.....
		ALL-RAG PAPERS																							
13	111	60	40	0	102	71	0.48	2.7	.....	0.076	82.0	3.24	24	0.051	7.8	0.57	39	0.044	5.61	0.06	4.4	4.9	77.4	16.6	6.0
14	112	60	40	0	210	110	.52	2.5	1.1	.119	81.8	3.39	16	.043	6.3	.42	28	.021	4.52	−.09	4.3	4.7	78.1	15.8	6.1
15	133	65	35	0	340	190	.39	1.6	.....	.055	79.0	2.31	15	.049	5.7	1.80	34	.035	5.95	1.09	4.5	5.1	74.3	19.3	6.4
16	132	65	35	0	340	220	.43	1.5	1.1	.079	80.2	3.38	17	.047	4.7	.53	23	.021	8.59	.12	4.5	5.2	74.3	20.0	5.7
		PART-RAG PAPERS																							

ª Acid calculated as percentage of SO_3.

ª Based on total cellulose.

TABLE 1.—*Test data on paper*—Continued

Numbers in this column refer to the numbers in figures 1 and 2	Sample number	Kind of fiber: Rag	Kind of fiber: Chemical wood: Coniferous	Kind of fiber: Chemical wood: Deciduous	Original tests: Before heat treatment: Folding endurance: Machine direction	Original tests: Before heat treatment: Folding endurance: Cross direction	Original tests: Before heat treatment: Ash	Original tests: Before heat treatment: Rosin	Original tests: Before heat treatment: Glue	Original tests: Before heat treatment: Acidity Kohler-Hall	Original tests: Before heat treatment: Alpha-cellulose	Original tests: Before heat treatment: Copper number	Original tests: After heating sample at 100° C for 72 hours: Folding endurance in percentage of initial	Original tests: After heating sample at 100° C for 72 hours: Increase in acidity Kohler-Hall	Original tests: After heating sample at 100° C for 72 hours: Decrease in alpha-cellulose in percentage of initial	Original tests: After heating sample at 100° C for 72 hours: Increase in copper number	Tests after 8 years of normal aging: Folding endurance in percentage of initial	Tests after 8 years of normal aging: Increase in acidity Kohler-Hall	Tests after 8 years of normal aging: Decrease in alpha-cellulose in percentage of initial	Tests after 8 years of normal aging: Increase in copper number	Tests after 8 years of normal aging: pH (hot extraction)	Tests after 8 years of normal aging: pH (cold extraction)	Tests after 8 years of normal aging: Alpha-cellulose	Tests after 8 years of normal aging: Beta-cellulose	Tests after 8 years of normal aging: Gamma-cellulose
PURIFIED WOOD FIBER PAPERS *																									
		%	%	%	*Double folds*	*Double folds*	%	%	%	%	%												%	%	%
17	105	0	100	0	1,400	800	0.34	1.4	2.7	0.092	90.5	1.40	54	0.050	1.1	0.32	40	0.038	0.55	0.10	4.1	4.5	90.0	2.5	7.5
18	106	0	100	0	2,500	1,600	.51	1.5	2.4	.063	88.8	1.37	71	.031	1.9	.35	52	.047	2.27	.43	4.5	5.1	86.8	4.5	8.7
19	107	0	100	0	1,900	1,200	.39	1.2	2.2	.114	88.3	1.78	56	.028	1.9	.20	63	.036	1.36	.12	4.2	5.1	87.1	5.3	7.6
84	782	0	100	0	4,400	5,500	.42	1.8	-----	.016	90.5	.67	96	-----	.4	.14	91	.004	2.43	.10	5.2	6.1	88.3	4.9	6.8
SULFITE WOOD FIBER PAPERS																									
21	108	0	100	0	15	17	7.12	2.2	-----	0.108	77.8	4.89	10	0.056	5.7	0.46	16	0.092	7.58	0.41	4.2	4.9	71.9	17.1	11.0
22	109	0	100	0	49	22	1.06	2.4	-----	.084	77.2	4.78	9	.071	4.1	.49	14	.136	5.96	.12	4.3	4.8	72.6	16.7	10.7
23	110	0	100	0	530	250	.60	2.8	-----	.113	81.6	3.77	1	.014	5.9	.55	14	.077	3.06	.03	4.4	4.7	79.1	9.0	11.9
25	116	0	100	0	500	360	.51	1.9	-----	.119	76.4	4.27	3	.075	7.9	.51	8	.041	3.14	.23	4.4	4.9	74.0	12.6	13.4
26	117	0	100	0	150	160	2.92	1.4	-----	.033	80.6	2.98	12	.023	4.3	.59	29	.067	1.61	.18	5.3	5.4	79.3	7.2	13.5
27	134	0	100	0	510	190	.48	1.7	-----	.082	79.9	3.75	1	.058	4.1	.36	16	.068	3.75	.15	4.3	5.0	76.9	10.5	12.6
28	135	0	100	0	110	72	6.12	2.0	-----	.066	79.2	3.29	6	.031	4.1	.80	21	.034	2.02	.31	4.7	5.0	77.6	10.1	12.3
SODA-SULFITE WOOD FIBER PAPERS																									
29	123	0	65	35	5	4	19.11	0.6	-----	0.085	74.0	3.72	35	0.072	6.8	0.40	46	0.065	14.43	0.68	4.3	5.0	63.1	27.5	9.4
30	124	0	50	50	2	2	19.99	.8	-----	.095	63.8	5.19	48	.067	8.4	.19	50	.095	8.46	.41	4.4	5.1	58.4	31.5	10.1
31	147	0	35	65	16	6	17.25	.6	-----	.038	77.9	2.29	64	.010	.2	.06	68	.012	1.28	.41	6.1	6.5	76.9	18.6	4.5
33	152	0	25	75	9	7	15.55	1.1	-----	.031	78.8	2.55	69	.011	.4	.10	75	.009	1.27	.05	5.9	6.5	77.8	16.7	5.5

* Fibers produced by special cooking and bleaching treatments to obtain improved quality.

Bursting strength, tensile strength, and tearing strength tests were made but the data are not included because, as found in the previous work, they appear to have no consistent relation to the weakening of paper on aging. The results of folding-endurance tests, however, agree very well with the degree of stability of paper indicated by its chemical characteristics.

IV. DISCUSSION

In considering the relation of these test data to the stability of the papers, only fairly large differences in the values should be regarded as having much significance. One reason for this is that the papers are complex materials; they contain several components that may have a deteriorative effect and the interreaction of such components during the aging of the papers must be complicated. It is because of this that one cannot expect any one component to indicate closely how stable a paper will be. Another variable is introduced by the nonhomogeneous structure of paper. This affects the folding endurance particularly. It has been found that duplicate determinations of the folding endurance of a sample of paper may yield values differing as much as 25 percent or so, if the two sets of test strips are taken from separated areas of the sample [6]. The strips were so taken in this case because it was felt that a better indication of the condition of the sample as a whole would be thus obtained than if contiguous strips were taken. Surface sizing presents another complication. In a Bureau study of the manufacture of writing paper from rags, it was found that increased folding endurance imparted to paper by glue or starch surface sizing was generally largely lost in the heat test [7]. In the present report, the glue content reported is from surface sizing. However, despite these adverse influences on the accuracy of the indicated relative stability of these papers, very good agreement on the whole was obtained between the results from accelerated aging and those from normal aging, between the chemical condition of the papers and their stability, and between the retests made after the two periods of natural aging.

In figure 1 is shown the relation between the effects on folding endurance of heating the papers and of normal aging for 4 years and for 8 years. It will be noted that there is good agreement in the grouping of the papers according to their relative stability, as found by their retention of folding endurance after heating and after the two aging periods. As was to be expected, there was better agreement in this respect after the 8 years of natural aging than after the shorter period of 4 years, but the agreement, in general, between the results of the two aging periods is very good. On the whole, papers previously found to have a high retention of folding endurance showed little further loss of folding endurance during the additional 4 years of aging, but the opposite is true of the less stable papers. The comparison of the effects of normal aging for 8 years and of accelerated aging is shown in another way in figure 2 in order to bring out more effectively the good correlation between them.

Also, as was found in the previous retest, and as has been consistently found in the many other Bureau studies relating to the stability of papers, there is good correlation between certain chemical properties of the papers and their degree of stability. As has been

mentioned before, a straight-line relationship between any one component of paper and its stability cannot be expected. Considering the papers as a whole, those having cellulose of good quality, as indicated by high alpha-cellulose and low copper number, and having a low or moderate degree of acidity proved to be the more stable papers. Of these two considerations, the condition of the cellulose appears to be of primary importance because generally the papers which contain very poor cellulose deteriorated rapidly, irrespective of the initial

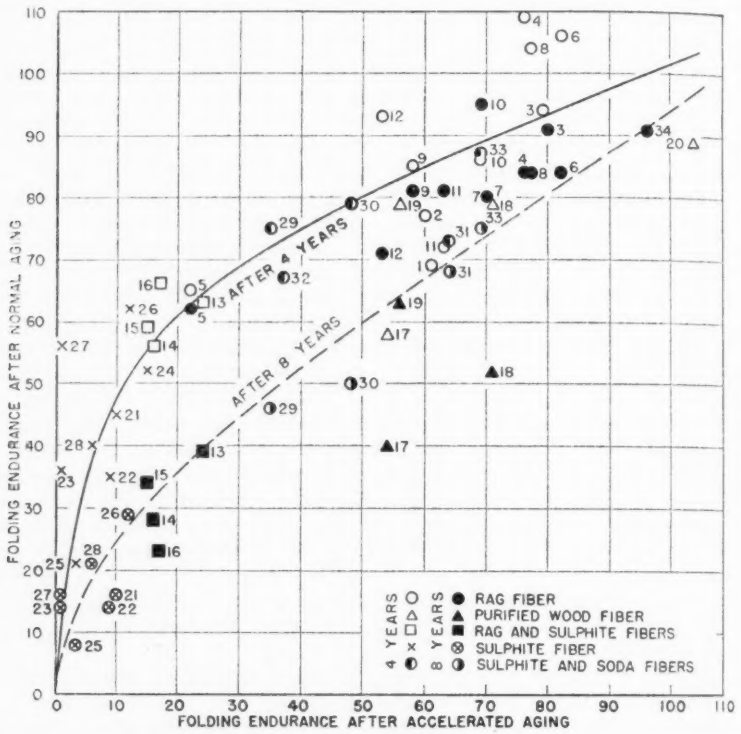

FIGURE 1.—*Comparison of retention of folding endurance of papers after normal and accelerated aging, in percentage of initial.*

The values for accelerated aging were obtained at the time the papers were stored, therefore, the figures for the 4-year and 8-year normal-aging periods bear a vertical straight-line relationship. No values are given for the 8-year period for samples 1, 2, 20, 24, and 32 as these had become exhausted. No value is given for the 4-year period for sample 34 as it was not tested at that time. The curves have no significance except to indicate the grouping of the papers. The accelerated aging consisted in heating for 72 hours at 100° C.

acidity. As pointed out in the previous report, the papers made from soda and sulfite pulps have a better degree of stability than would be expected from consideration of the condition of the cellulose. This has been found to be true, in general, for papers containing soda pulp fibers. Such fibers are characterized by a high content of pentosans, which change very little under the heat test, and this may have some bearing on the stability of the fibers [8]. The rosin content of the papers is apparently of minor importance, as has been found in other studies.

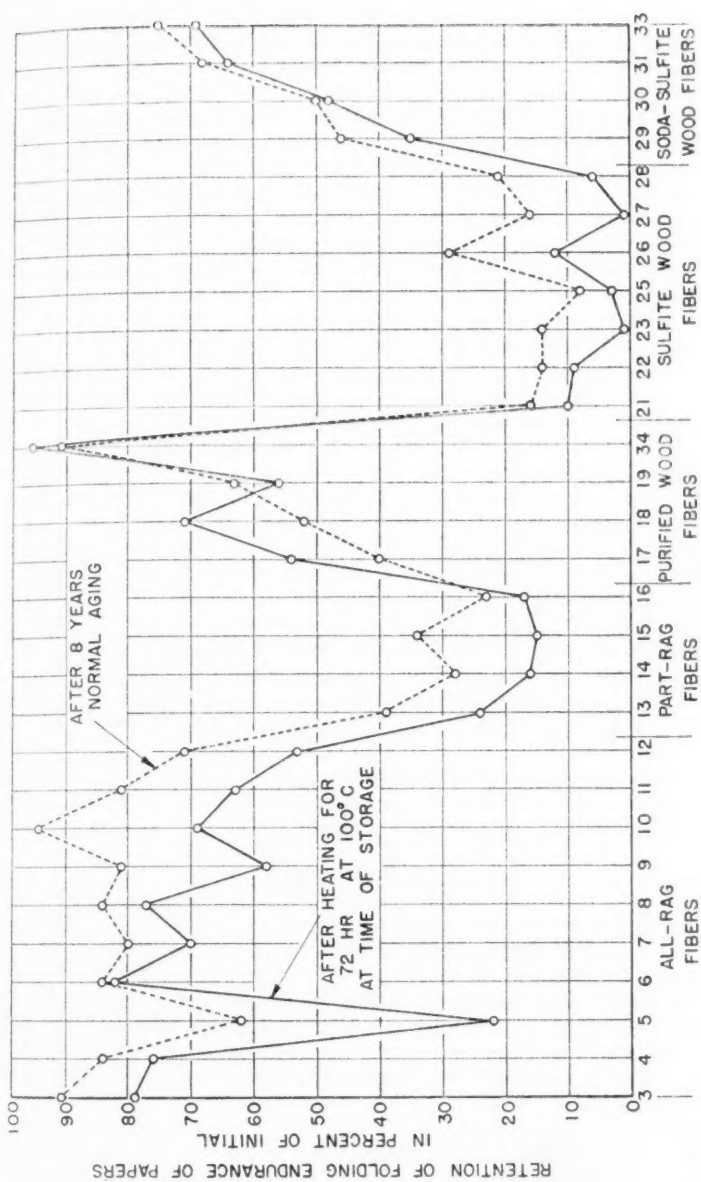

FIGURE 2.—*Further comparison of retention of folding endurance of papers after normal and accelerated aging.*

Contrary to the findings at the end of the 4-year natural-aging period, at the end of the 8-year period the papers in many cases showed significant changes in alpha-cellulose, copper number, and acidity. These same kinds of changes took place under the accelerated aging. Many of the more unstable papers showed an appreciable decrease in alpha-cellulose, and it is interesting to note that such papers generally had a high content of the beta-cellulose fraction after aging. Other work at the Bureau has shown that the decrease in alpha-cellulose of papers on accelerated aging is largely reflected in an increase in beta-cellulose with little change in the gamma portion [9]. Also in this connection, the results of tests of some papers from books that were from 150 to 200 years old are of interest. Although the papers were apparently composed largely of linen fibers, which are very stable under good conditions, several of the papers were very brittle; they cracked apart when creased only a few times between the fingers. Apparently the deterioration of the papers had been caused by storage in a damp place, as there was evidence of mold, which is known to damage paper. These papers showed the same condition of cellulose found in the papers under discussion which had deteriorated considerably on heating and on natural aging for 8 years, that is, a low content of alpha-cellulose and a high content of beta-cellulose, typical values being alpha-cellulose, 51.0 percent; beta-cellulose, 44.5 percent; gamma-cellulose, 4.5 percent. A sample of new linen-fiber paper had the following values: Alpha-cellulose, 90.1 percent; beta-cellulose, 6.6 percent; gamma-cellulose, 3.3 percent. Increases in acidity and copper number occurred in most cases during the 8-year storage, but showed little relation to the initial quality of the papers.

As mentioned in the previous reports, these papers are not representative of the average quality of such papers of current manufacture. With the better knowledge developed during the past several years of the factors which affect the strength and stability of papers, and of technique for controlling these factors in the manufacturing processes, considerable improvement in the quality of all grades of record papers has been effected.

V. SUMMARY

The results of retests of various grades of commercial record papers after a normal aging period of 8 years confirm the results of a retest of them made 4 years ago, in that:

1. The papers were grouped in the same relative order of stability by their retention of folding endurance during the natural-aging period and under accelerated aging by heating them for 72 hours at 100° C. The agreement was better for the 8-year period than for the 4-year period.

2. Generally, the papers which showed high retention of folding endurance during the 4-year natural-aging period lost little folding endurance during the following 4 years, but the opposite is true of the less stable papers.

3. There was good correlation between the chemical properties of the papers and their stability. As found in many other Bureau studies, the more stable papers were characterized by a good condition of the cellulose, as indicated by a high alpha-cellulose content and a

low copper number, and by a low or moderate degree of acidity. The rosin content proved to be of less importance.

At the end of the 8-year normal-aging period a further correlation with the accelerated aging test was found, in that appreciable decreases in alpha-cellulose and increases in copper number and acidity took place in the papers of low stability. This did not happen during the 4 years of normal aging. A further additional finding at the end of the 8-year period is that the cellulose of the more unstable papers has a high content of beta-cellulose. Other Bureau studies have shown that when the alpha-cellulose fraction decreases on accelerated aging of paper by heating there is a proportionate increase in beta-cellulose, very little change generally occurring in the gamma portion.

The recent tests of the papers were made by R. W. Carr and W. K. Wilson and this assistance is acknowledged by the author.

VI. REFERENCES

[1] R. H. Rasch, *A study of purified wood fibers as a papermaking material.* BS J. Research **3,** 469 (1929) RP107.

[2] B. W. Scribner, *Permanence standards for printing and writing papers.* Transactions of Am. Soc. Mech. Engrs. **52,** No. 19 (August 1930).
J. O. Burton, *Permanence studies of current commercial book papers.* BS J. Research **7,** 429 (1931) RP349.

[3] R. H. Rasch and B. W. Scribner, *Comparison of natural aging of paper with accelerated aging by heating.* BS J. Research **11,** 727 (1933) RP620.

[4] H. F. Launer, *Determination of the* pH *values of papers.* J. Research NBS **22,** 553 (1939) RP1205.

[5] H. F. Launer, *Simplified volumetric determination of alpha, beta, and gamma cellulose in pulps and papers.* J. Research NBS **18,** 333 (1937) RP979.
H. F. Launer, *Volumetric determination of alpha-, beta- and gamma-cellulose in pulps and in papers containing sizing, filler, and other materials.* J. Research NBS **20,** 87 (1938) RP1068.

[6] R. H. Rasch and G. O. Stone, *Estimating stability of paper by heating.* Paper Trade J. **95,** No. 4, 28 (July 28, 1932).

[7] M. B. Shaw, G. W. Bicking, and M. J. O'Leary, *A study of the relation of some properties of cotton rags to the strength and stability of experimental papers made from them.* J. Research NBS **14,** 649 (1935) RP794.

[8] M. B. Shaw and M. J. O'Leary, *Study of the effect of fiber components on the stability of book papers.* J. Research NBS **17,** 859 (1936) RP949. See also reference [1].

[9] M. B. Shaw and M. J. O'Leary, *Effect of filling and sizing materials on stability of book papers.* J. Research NBS **21,** 671 (1938) RP1149.

WASHINGTON, July 11, 1939.

U. S. DEPARTMENT OF COMMERCE NATIONAL BUREAU OF STANDARDS

RESEARCH PAPER RP1242

Part of Journal of Research of the National Bureau of Standards, Volume 23, September 1939

AN APPARATUS FOR MAGNETIC TESTING AT MAGNETIZING FORCES UP TO 5,000 OERSTEDS

By Raymond L. Sanford and Evert G. Bennett

ABSTRACT

An apparatus is described for general magnetic testing in the range of values of magnetizing force from 100 to 5,000 oersteds. Specimens of rectangular cross section up to 3.8 cm (1½ in.) wide and 1.9 cm (¾ in.) thick can be tested. It is estimated that under favorable conditions values of induction or magnetizing force accurate within 0.5 percent can be obtained and that under ordinary conditions of routine testing the accuracy is within 1 percent. The apparatus is convenient and simple to operate and does not heat the specimen.

CONTENTS

	Page
I. Introduction	415
II. Description of apparatus	416
III. Experimental investigation	418
IV. Accuracy of test data	423
V. Summary	425

I. INTRODUCTION

Previous to 1920, when Honda and Saito announced their KS magnet steel,[1] a maximum magnetizing force of 300 oersteds was adequate for the testing of permanent-magnet steels. However, cobalt magnet steels of the KS type, and others which were developed soon after, required a maximum magnetizing force of 1,000 oersteds, and consequently new permeameters were needed. The need was fairly well met by the Babbitt permeameter,[2] the Full-Range permeameter,[3] and an apparatus developed by the present authors.[4]

In 1932 Mishima [5] announced an entirely new type of permanent-magnet alloy containing aluminum and nickel as the essential alloying elements. Following this, several alloys of similar characteristics, including the alloy known as Alnico,[6] have been produced, which are magnetically harder than the earlier permanent magnet materials and consequently require higher magnetizing forces for testing. The authors were able to extend the range of their apparatus to 2,000 oersteds by the addition of auxiliary magnetizing coils, but a further

[1] Honda and Saito, *On KS magnet steel*, Phys. Rev. **16**, pt. 2, 495 (1920).
[2] H. J. Babbitt, *An improved permeameter for testing magnet steel*, J. Opt. Soc. Rev. Sci. Instr. **17**, 47 (1928).
[3] R. M. Smith, *A new full-range permeameter*, Gen. Elec. Rev. **38**, 520 (1935).
[4] Sanford and Bennett, *An apparatus for magnetic testing at high magnetizing forces*, BS J. Research **10**, 667 (1933) RP548.
[5] T. Mishima, *Magnetic properties of iron-nickel-aluminum alloys*, Ohm (July 1932); Iron Age (abstract) **130**, 346 (1932).
[6] J. Q. Adams, *Alnico—its properties and possibilities*, Gen. Elec. Rev. **41**, 518 (1938).

increase was impracticable because the magnetic circuit had too small a cross section.

In view of the increasing use of the new materials and the possibility that magnetizing forces higher than 2,000 oersteds might be needed before long, the development of a new permeameter was undertaken. It was hoped that an instrument could be produced which would be capable of applying magnetizing forces up to 5,000 oersteds and of giving a better accuracy than the previous instrument.

The final result was the "High-H permeameter" shown in figure 2. This apparatus is capable of testing specimens up to 3.8 cm (1½ in.) wide and 1.9 cm (¾ in.) thick. At magnetizing forces from 100 to 5,000 oersteds, values of either magnetizing force or of induction can be measured with an error not greater than 1 percent. Measurements have been made at magnetizing forces as high as 9,000 oersteds without appreciable heating, but the accuracy at these higher forces has not been determined.

II. DESCRIPTION OF APPARATUS

In designing the present apparatus, essentially the same principles were followed as in the case of the earlier one. The principal modifications were made for the purpose of increasing the range and improving the accuracy of the measurements. Certain features were also added in order to provide flexibility and convenience in operation.

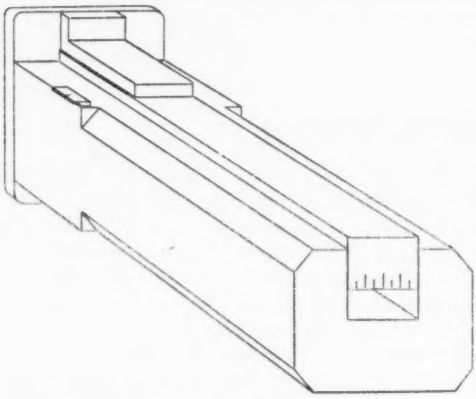

FIGURE 1.—*Pole-piece*

To prevent undue heating of the specimen, a magnetic circuit of the isthmus type was adopted, as the necessary high magnetizing forces can thus be applied using only a moderate amount of power. This type of circuit, involving only a relatively short length of specimen, has the added advantage that specimens of ordinary length can easily be examined for uniformity—an important point if specimens are to be used for the intercomparison of permeameters. Furthermore, it has been found possible to obtain satisfactory results on a specimen only 2.5 cm (1 in.) long, which is too short to be tested in other existing permeameters.

Saturation effects have been reduced by substantially increasing the cross sections of the yokes and pole pieces, which form a symmetrical magnetic circuit.

If values of magnetizing force are obtained by means of a stationary H-coil, the errors in the determination of points on a hysteresis loop may be large, because it is necessary to calculate the values as the difference between two relatively large quantities. This difficulty has been overcome by the use of a rotating H-coil (flip-coil), by means of which the value of magnetizing force is obtained directly.

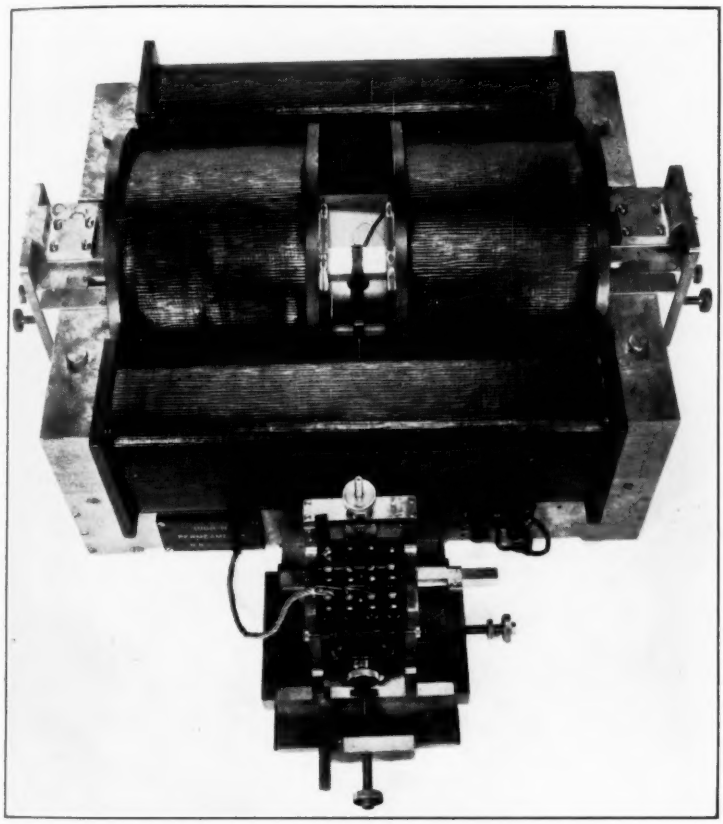

FIGURE 2.—*The High-H permeameter.*

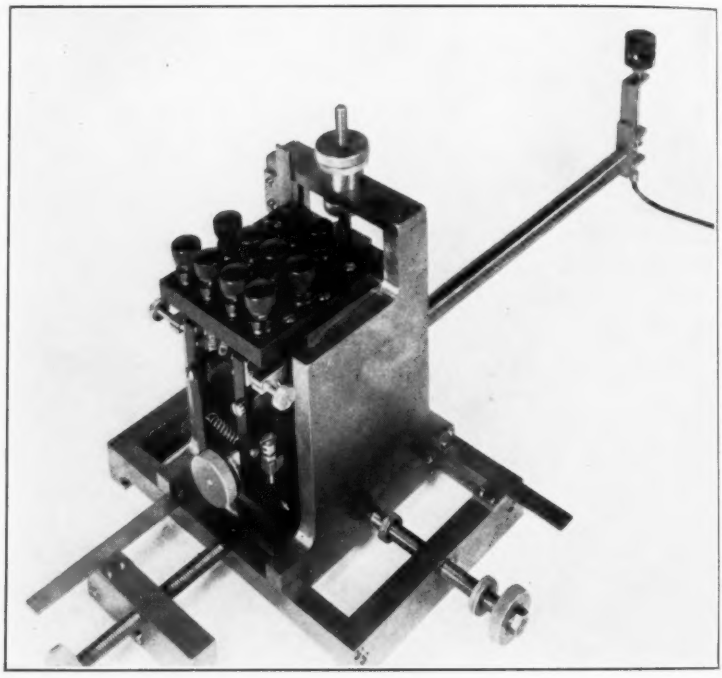

FIGURE 3.—*Rotating H-coil and accessory apparatus.*

The magnetic circuit is shown in figure 2. The specimen is held in pole pieces extending between two U-shaped yokes. The construction of the pole pieces is indicated in the sketch of figure 1. They have longitudinal channels into which are fitted filler pieces as shown. The specimen is located in the space between the bottom of the channel and the filler. The magnetic circuit is constructed of laminations of No. 16 gage armature-grade silicon steel. The distance between the pole pieces, or gap length, is adjustable; and scales are provided to indicate the gap length up to 10 cm, which is the maximum generally used. Scales are also located on the inner ends of the filler pieces to aid in centering the specimen. The filler pieces are fastened at their outer ends to heavy brass plates which are clamped to the ends of the pole pieces so as to keep the fillers parallel with the bottom of the channels.

The main magnetizing coils are on the pole pieces, and auxiliary windings are located on the yokes. The design of the magnetic circuit and magnetizing windings was greatly facilitated by preliminary experiments with a small model, by means of which the probable distribution of flux in the magnetic circuit was approximately determined. The principal dimensions and constants of the apparatus are given in table 1.

TABLE 1.—*Constants of the apparatus*

Magnetic circuit	
Over-all length	50 cm.
Over-all width	40 cm.
Cross section of yokes	5×8 cm.
Length of pole pieces	25 cm.
Cross section of pole pieces	8×10 cm.
Width of channels	4 cm.
Depth of channels	4 cm.
Thickness of filler pieces	3 cm.
Magnetizing coils	
No. 14 AWG silk-enamel throughout	
Length, main coils	15 cm.
Inside diameter, main coils	11.4 cm.
Number of layers, main coils	30.
Number of turns, main coils	2,690 each.
Length, yoke coils	38 cm.
Number of layers, yoke coils	7.
Number of turns, yoke coils	1,600 each.
Total number of turns	8,580.
***H*-coils**	
Length	7 mm.
Over-all width	11 mm.
Over-all thickness	2.5 mm.
Cross section, coil forms	0.5×9 mm.
Turns, No. 44 AWG, enamel	1,200.
Approximate area-turns	140 $cm.^2$

In view of the high induced voltage resulting from the reversal of the magnetizing current, care was taken to provide ample insulation and spacing of the conductors to avoid breakdown of the insulation. The coil forms and flanges are of bakelite. As a precaution against undue arcing at the switch contacts, the apparatus is shunted with a 500-ohm resistor.

The general arrangement of the *H*-coil system is shown in figure 3. There are two similar coils mounted one above the other at the top of a hollow vertical shaft so that their axes are parallel to that of the specimen. This vertical shaft can be rotated by a horizontal shaft through small beveled gears. The horizontal shaft is 32 cm long and is driven through spur gears by a small series-wound motor. The motor is enclosed in a soft-iron box. Adjustable stops limit the rotation of the coils to 180°. By means of a cam-operated switch, resistance is inserted in the motor circuit at the proper time to prevent excessive jar. The resistance is adjusted so that when it is in the circuit the motor still exerts enough torque to bring the coils back to their proper position if rebound from the stops occurs. The operating switch opens automatically so as to prevent overheating of the motor.

The carriage which supports the flip-coil assembly is mounted on ways so that its position can be adjusted in three directions by means of screws. The position of the test coils in the gap is indicated by scales graduated in millimeters. This arrangement has been found very convenient for determining field distribution in the gap. The constants of the test coils are given in table 1 under the heading *H*-coils. The coils are connected to the leads through small brass blocks held in place by screws and so located as to avoid extra loops in the test-coil circuit. This facilitates removal of the coils from the mounting for replacement or calibration.

In order to keep the air correction small, individual *B*-coils are wound on thin brass forms to fit specimens of various sizes. The coils are 5 mm long and have 25 turns.

The ballistic galvanometer has a period on open circuit of 45 seconds and an external resistance for critical damping of about 40,000 ohms. As the external resistance rarely exceeds 200 ohms, the behavior of the galvanometer approximates that of a fluxmeter. The galvanometer is connected by means of a selector switch to the desired test coil through any one of a number of resistors. The sensitivity is adjusted in the usual way, using a standard mutual inductor, the calibrating current being measured by a Brooks deflection potentiometer and standard shunts.

III. EXPERIMENTAL INVESTIGATION

In order to obtain accurate results, it is important that the induction in the specimen shall be uniform throughout the length covered by the *B*-coil and that it be possible to determine accurately the axial component of the field adjacent to the surface of the specimen over the same length. It is also desirable to know how the distribution of induction and field is affected when the gap length is varied. Accordingly, a large number of measurements were made to determine these distributions.

Most of the measurements of distribution were made using a bar of Alnico prepared by the General Electric Co. A hole approximately 8 mm in diameter extended longitudinally along its axis. Thus it was possible to determine the value of the field within the specimen at any point along its length by means of a test coil inserted in the hole.

The principal data obtained were longitudinal distribution of induction in the specimen, longitudinal distribution of the axial com-

ponent of the field within the specimen, longitudinal distribution of the axial component of the field outside the specimen, and radial distribution of the axial component of the field. By radial distribution is meant the variation of the axial component of the field with the vertical distance from the bottom surface of the specimen midway between the faces of the pole pieces. The test coil used for measurements of the field outside the specimen was 5 mm long, 5 mm wide,

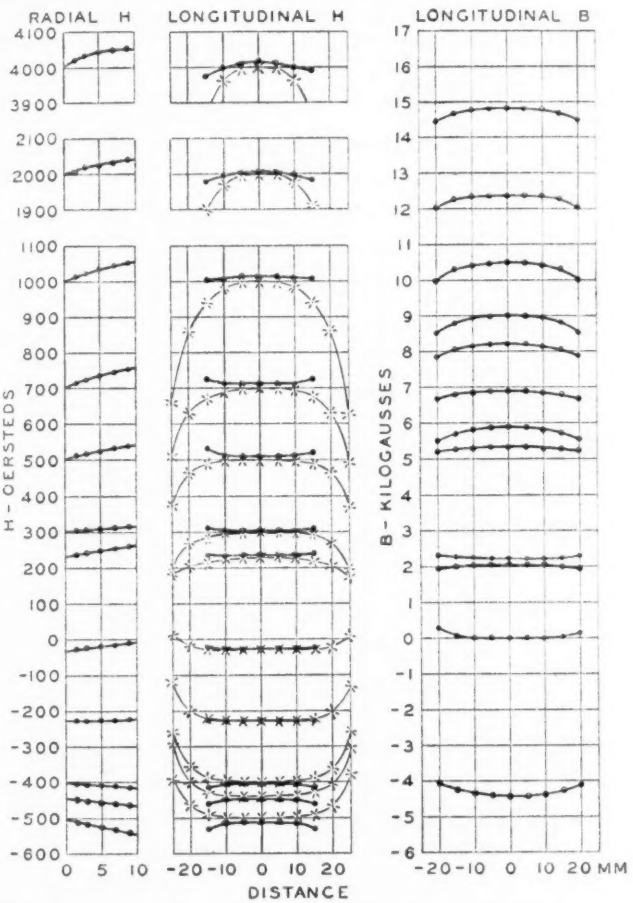

FIGURE 4.—*Typical distribution data taken with a 5-cm gap.*

and 3.2 mm thick. Longitudinal distribution of the field outside the specimen was obtained with the axis of the coil 1.6 mm below the surface. In addition to the distribution data, the influence of variations in experimental conditions, such as length of the specimen, contact reluctance at the pole pieces, straightness of the specimen, etc., was determined.

The curves shown in figure 4 are typical of the distribution data obtained and represent the results for a 5-cm gap. The curves of

radial H show that for this length of gap the field increases with distance from the surface of the specimen. Under these conditions, a test coil of any practical dimensions calibrated in a uniform field would indicate too high values of magnetizing force. The curves of longitudinal H, indicated by crosses, are for the field inside the bar. This field has its highest value at the middle of the gap and decreases toward the pole pieces. Observations showed that the field is very nearly zero at points only about 2.5 cm inside the pole pieces. The field outside the bar has its lowest value at the middle of the gap and increases toward the pole pieces. The curves of longitudinal B have their highest value at the middle of the gap. The induction is very nearly constant over the middle centimeter.

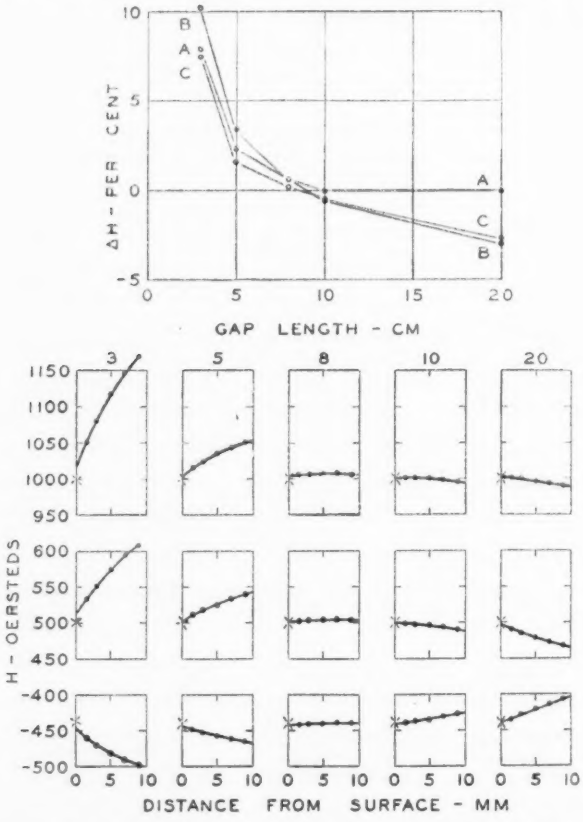

FIGURE 5.—*Influence of gap length on radial distribution.*

Δ H shown in upper part is the difference between the true value of H and the value at a distance of 3 mm from the surface of the specimen. Crosses in lower part indicate the values inside the specimen.

Figure 5 shows how the radial distribution varies with the gap length. The lower part of the figure shows the radial distributions corresponding to fields of 1,000, 500, and −450 oersteds, respectively, measured inside the bar at the middle. The value −450 corresponds to a point on the hysteresis loop determined from a maximum magnetizing force of 1,000 oersteds. The crosses indicate the values

obtained inside the specimen. It will be noted that the extrapolated values for the 3-cm gap are higher than the values obtained inside the specimen. This indicates that the distribution of induction is not uniform across the section for this short gap. The variation of H with distance from the surface becomes less as the gap length is increased. For a gap of 8 cm the field is practically uniform over a distance of 1 cm. For longer gaps the field decreases with distance from the surface.

In the upper part of figure 5 are plotted the percentage differences between the value of H at a distance of 3 mm from the surface and

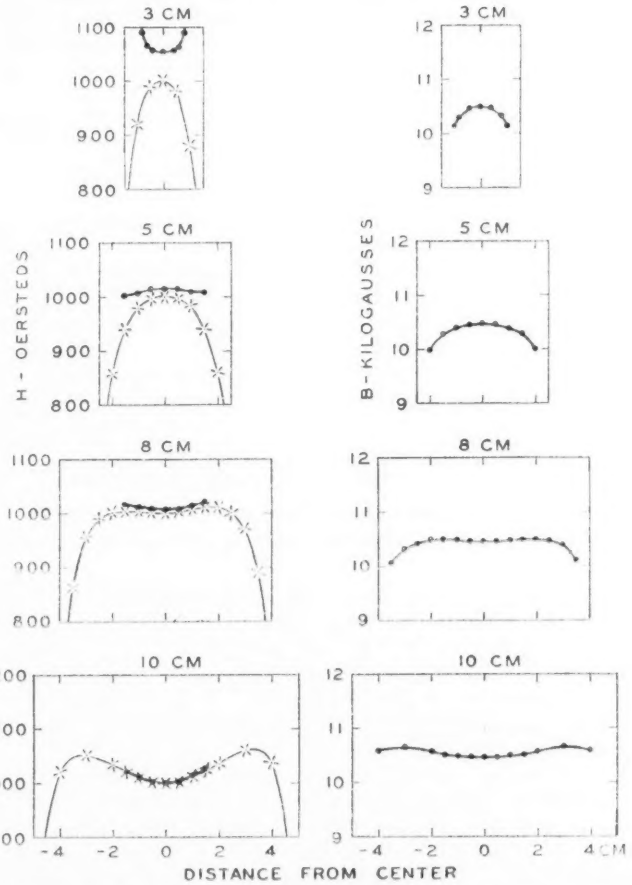

FIGURE 6.—*Influence of gap length on longitudinal distribution of H and B.*
Crosses indicate values of H inside the specimen. The gap lengths are 3, 5, 8, and 10 cm, respectively.

the value inside the specimen as a function of the length of gap. Curves A, B, and C represent the values for 1,000, 500 and −450 oersteds, respectively. The minimum difference for all values of H appears to come at a gap length of about 8 cm. Figure 6 shows the variations in the longitudinal distributions of H and B with the length of gap.

The principal thing to be observed is that for a distance of about 1 cm at the middle of the specimen the distribution is satisfactory except for the 3-cm gap.

The distribution data were used as a guide for the design of the final *H*-coil system. The two *H*-coils are mounted with their axes parallel and 2.5 mm apart. The height of the system is set so that the axis of the upper coil is 2.5 mm away from the lower surface of the specimen. In order to determine the value of *H* at the surface, readings are taken first with the upper coil and then with the two coils connected in series-opposition. The second reading is then

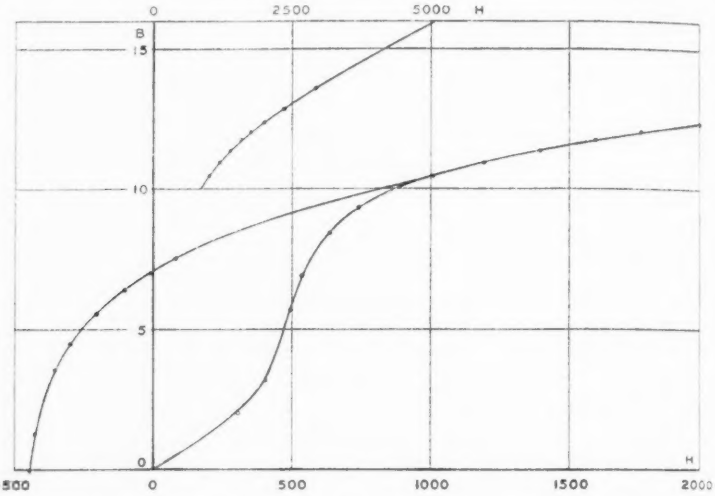

FIGURE 7.—*Normal induction and hysteresis curves for hollow specimen.*

Values of *H* for the curves were obtained inside the specimen. Points refer to values taken outside the specimen. Gap length, 8 cm.

added algebraically to the first. Since the distribution is very nearly linear and the distance between coils is equal to that between the upper coil and the surface of the specimen, this gives directly the value at the surface. The differential reading may be zero, positive or negative according to the gap length. It is probable that the cross section and properties of the test specimen also influence the radial distribution to a certain degree.

As a final check on the results using the double *H*-coil system, measurements of normal induction and hysteresis were made on the hollow bar and the results were compared with those obtained by measuring *H* on the inside of the bar. A typical set of results is shown in figure 7. The full lines represent the values obtained with the internal *H*-coil, and the points were obtained with the external coils. The data obtained from measurements of the field outside the bar agree with those obtained from measurements inside the bar within the experimental error for either a 5-cm or an 8-cm gap. Results obtained with a 3-cm gap did not agree so well, but the discrepancies did not exceed about 2 percent.

Measurements on several solid bars having different dimensions showed good agreement between data obtained with a 5-cm gap and those for an 8-cm gap.

Experiments to determine the influence of variations in experimental conditions led to the following conclusions:

1. Ordinary variations in contact reluctance at the pole pieces do not appreciably affect the accuracy of the results.

2. The accuracy of the results does not depend upon the thickness of the specimen. The same values were obtained on a specimen having a cross section approximately 0.6 by 1.3 cm tested in the ordinary position and with its narrow side toward the *H*-coil.

3. Satisfactory results can be obtained with relatively short specimens. For specimens 5 cm or less in length, it is better to butt the ends against the pole pieces rather than to attempt to insert them in the regular way. Results agreeing within the observational error were obtained on the same section of a specimen originally 25 cm long after it had been cut to lengths of 10, 5, and 2.5 cm, respectively.

4. Moderate deviations from straightness do not affect the accuracy of the results. If a bar is not straight, it is somewhat better to insert it in the apparatus with the concave side down.

5. Unless the radial gradient is practically zero, an error in the observed value of induction may result from the use of a *B*-coil of too great area. It is best to use a *B*-coil having an area not more than 50 percent greater than that of the specimen.

The value of area-turns of the *H*-coil is too small to give satisfactory sensitivity at magnetizing forces below about 100 oersteds. For this reason no attempt has been made to determine the accuracy for lower magnetizing forces. If at some future time it should appear desirable to use the apparatus for measurements with magnetizing forces below 100 oersteds, the feasibility of using larger *H*-coils would have to be investigated.

IV. ACCURACY OF TEST DATA

In order to estimate the accuracy of test data obtained with the apparatus, it is necessary to consider not only sources of error peculiar to the individual apparatus but also those inherent in ballistic methods in general. The principal points common to all ballistic methods include: value of the mutual inductor; area-turns of the test coils; adjustment of galvanometer sensitivity; characteristics of the galvanometer; temperature effects; uniformity of the specimen; magnetic viscosity; and observational errors. Points peculiar to the individual apparatus include: dimensions of the test coils; and method of measuring *H* for points on the hysteresis loop.

The values of mutual inductors such as are used in connection with permeameters are generally determined to an accuracy of about ± 0.1 percent. However, we have compared [7] the inductors used with the present apparatus with a mutual inductor constructed for use in the determination of electrical resistance in absolute units under the direction of F. Wenner with an estimated accuracy of ± 0.05 percent.

The area-turns of the test coils were determined by measuring the mutual inductance between the coils and a standard solenoid within

[7] The method used is described in Cir. NBS C415, p. 20 (1937).

which the coils were placed. This solenoid is wound on a threaded form and its constant, H/I, is known to about 0.05 percent. The distribution of field along the axis of this coil has been explored experimentally and varies by less than 0.05 percent from the calculated values. It is important in determining area-turns that the axes of the test coil and solenoid be in alinement. This was checked experimentally. It is estimated that the area-turns of the H-coils are known within ± 0.2 percent. The areas of the B-coils were determined in the same manner and to the same accuracy.

In calibrating the galvanometer for a test, the sensitivity can be adjusted to about 0.1 percent. Unless considerable care is taken, however, the error may be as great as 0.2 percent.

There is some difference of opinion with regard to the influence of galvanometer characteristics on the accuracy obtained. It is the authors' opinion, however, that a heavily overdamped galvanometer gives better results than a critically damped instrument, for this type of work.

It is important to avoid heating the specimen, especially if a high accuracy is desired. Since the present apparatus requires less than 600 watts to give 5,000 oersteds and has considerable radiating surface and heat capacity, there is practically no trouble from heating. Even after a rather long-continued test the temperature of the specimen does not rise more than about 2° C.

The magnetic uniformity of the specimen is of particular importance if the results obtained with different permeameters which include different lengths of the specimen in the test are to be compared. With the present apparatus it is possible to investigate the uniformity of a specimen and thus determine whether or not it is suitable for use in intercomparisons.

One source of uncertainty, not heretofore considered to be characteristic of magnetically hard materials, is the phenomenon known as magnetic viscosity. This effect is noticeable in the range of magnetization represented by the steep parts of the normal induction and hysteresis curves. It was observed in Alnico and cobalt magnet steel and shown to be associated with the test specimens themselves and not to be brought about primarily by the rest of the magnetic circuit. It is proposed to study this effect further, as it may be the cause of some of the differences between the results obtained on the same specimens in different laboratories.

The observational error of a single reading may be as great as 0.2 or 0.3 percent. If a sufficient number of readings of the same quantity are taken, however, the average is probably good within 0.1 percent.

The uniformity of the field determines the limits of length and thickness of test coils which can be used in a given apparatus. The dimensions chosen for the coils in the present apparatus are such that errors due to nonuniform distribution do not exceed 0.2 percent.

The determination of values of magnetizing force corresponding to points on a hysteresis loop by means of a fixed H-coil involves taking the difference between two relatively large quantities. This may lead to large errors. By using a flip-coil, it is possible to determine directly the required value of magnetizing force and thus reduce materially the experimental error. The use of the flip-coil cuts down the amount of switching necessary and also makes it possible to check for initial polarization of the specimen by noting whether

or not equal values of H_m are obtained for the same value of magnetizing current flowing in either direction.

Taking into consideration all of the sources of error noted above, it is estimated that by the exercise of care in taking the readings and averaging several readings for each point, values of either induction or magnetizing force can be obtained which will be accurate within about 0.5 percent. For routine tests made without extreme precaution, values accurate within 1 percent should be obtained without difficulty.

V. SUMMARY

In order to meet the demand occasioned by the recent development of permanent-magnet alloys requiring the application of very high magnetizing forces for magnetizing and testing, a new permeameter has been constructed which has been called the NBS High-*H* permeameter. In its design the aim has been to provide an instrument whose accuracy is sufficient to meet the requirements of present-day magnetic testing and which is simple and convenient to operate.

The fundamental principle is that of the well-known isthmus method, in which the magnetizing force is taken as the value of magnetic field at the surface of the specimen. By including only a relatively short length of specimen in the test, it is possible to apply the necessary high magnetizing forces without appreciable heating. Also, a symmetrical magnetic circuit promotes a uniform distribution of flux across the section of the specimen and a symmetrical distribution of field within the gap.

The requisite degree of accuracy is obtained by the use of test coils whose dimensions were chosen with reference to the observed distribution of flux and field in the magnetic circuit. Furthermore, by the use of a double *H*-coil it is possible to determine the value of the field at the surface of the specimen more accurately than can be done with a single coil. By using a rotating *H*-coil, it is possible in determining points on a hysteresis loop to avoid the errors which may arise from calculating the magnetizing force as the difference of two relatively large quantities.

It is estimated that for magnetizing forces from 100 to 5,000 oersteds it is possible under favorable conditions to obtain values of either induction or magnetizing force which will be accurate within 0.5 percent. Under ordinary conditions of routine testing the errors probably do not exceed 1 percent.

Washington, June 16, 1939.

U. S. DEPARTMENT OF COMMERCE NATIONAL BUREAU OF STANDARDS

RESEARCH PAPER RP1243

Part of Journal of Research of the National Bureau of Standards, Volume 23, September 1939

LENGTH CHANGES AND ENDOTHERMIC AND EXOTHERMIC EFFECTS DURING HEATING OF FLINT AND ALUMINOUS CLAYS

By Raymond A. Heindl and Lewis E. Mong

ABSTRACT

Changes in length on heating from room temperature to 1,000° C and the temperatures at which endothermic and exothermic effects occurred were determined on flint clays from Kentucky, Missouri, Ohio, Pennsylvania, and Washington; on a plastic clay from Pennsylvania; on a hard kaolin and a bauxitic clay from Georgia; and on a Zettlitz kaolin and a diaspore from Missouri. Changes in the length of granular pieces and of pulverized materials were measured both in air and in an atmosphere of the products of gas combustion. The two ranges of temperature (approximately 500° to 600° C and 925° to 980° C) in which very rapid contraction took place during heating were the same as those in which endothermic and exothermic reactions, respectively, occurred. The ranges of temperature in which rapid contraction took place were slightly lower for the pulverized than for the granular pieces of the clays, except for the Missouri clay, in which there was no difference.

CONTENTS

	Page
I. Introduction	427
II. Materials	428
1. Pyrometric cone equivalent	428
2. Microscopic analyses	429
III. Methods of test	429
1. Length changes	429
(a) Preparation of test specimens	429
(b) Procedure	429
(1) Atmospheric conditions	429
2. Endothermic and exothermic effects	430
IV. Results and discussion	430
1. Missouri flint	430
2. Kentucky flint	432
3. Ohio flint	434
4. Pennsylvania flint	435
5. Washington flint	437
6. Tyrone plastic clay	438
7. Georgia kaolins	439
8. Diaspore	440
9. Zettlitz kaolin	440
10. Reproducibility of results	441
V. Summary	441

I. INTRODUCTION

The properties of fire-clay refractories are obviously dependent, at least in part, upon the changes which occur in the individual raw

clays as they are heated.[1] Plans have been made to study finished refractory bodies prepared primarily from raw flint clays obtained from the various producing districts in this country. The present report contains the results of a study of the irreversible expansion and contraction characteristics of each of these raw flint clays when heated in air and when heated in an atmosphere of the products of gas combustion. Also, endothermic and exothermic effects were studied in most cases to determine whether there was any relation between these irreversible heat effects[2] and the changes in length of the clays. In addition, several miscellaneous refractory materials were tested for comparison with the flint clays.

II. MATERIALS

One sample of flint clay was obtained from Kentucky, one from Missouri, and one from each of two deposits in Ohio, Pennsylvania, and Washington. Miscellaneous materials included one sample each of a refractory plastic clay from Pennsylvania, a hard kaolin from Georgia, a bauxitic clay from Georgia, a diaspore from Missouri, and a Zettlitz[3] kaolin. The materials and their sources are listed in table 1.

TABLE 1.—*Types of clay, sources, and pyrometric cone equivalents*

Material	Source	Pyrometric cone equivalents
Flint clay	Missouri	35
Do	Kentucky	34–35
Flint clay,[a] grayish tan	do	34
Flint clay,[a] bluish	do	35
Flint clay, light	Ohio	34–35
Flint clay, dark	do	32
Flint clay	Pennsylvania	32–33
Flint clay, Dean	do	34–35
Flint clay, Farrow	Washington	34
Flint clay, Dark Kummer [a]	do	35
Flint clay, Light Kummer [a]	do	37
Plastic clay, Tyrone	Pennsylvania	32–33
Kaolin, hard	Georgia	34–35
Kaolin, bauxitic	do	37
Diaspore	Missouri	
Kaolin	Zettlitz	35

[a] Tests were made of specimens of differently colored clay selected from the same sample.

1. PYROMETRIC CONE EQUIVALENT

The pyrometric cone equivalents (pce, or softening points) were determined according to the American Society for Testing Materials standard method, serial designation C24–35.[4] The values, given in table 1, range from cone 32 to cone 37 for the materials tested.

2. MICROSCOPIC ANALYSES[5]

The petrographic microscope was used in making examinations of thin sections of Kentucky, Missouri, and Pennsylvania (Dean) flint clays to determine whether any differences in structure or composi-

[1] R. A. Heindl, *Progress report on investigation of sagger clays*, J. Am. Ceram. Soc. **9**, 131 (1926).
R. A. Heindl, *A study of sagger clays and sagger bodies*, J. Research NBS **15**, 255 (1935) RP827.
[2] Herbert Insley and Raymond H. Ewell, *Thermal behavior of the kaolin minerals*, J. Research NBS 14, 615 (1935) RP792.
[3] For other tests, see the paper referred to in footnote 2.
[4] Am. Soc. Testing Materials, Standards, pt. 2, Non-Metals, p. 299 (1936).
[5] Made by H. Insley.

tion could be detected. In each case the ground mass appeared to be largely amorphous under a high magnification. This ground mass had a mean index of refraction of about 1.55. Vermicular aggregates with a low to medium double refraction and a mean index of about 1.56 were fairly abundant and occurred as inclusions in the ground mass. These aggregates may have been kaolinite or halloysite. Clouds of minute particles (1 micron or less) with high double refraction and high index of refraction also occurred as inclusions in the ground mass. These particles were possibly rutile. The petrographic examination failed to show any significant differences between the three clays, with the possible exception that the material identified in the Pennsylvania flint as probably being rutile was present in larger aggregates than in the others.

III. METHODS OF TEST

1. LENGTH CHANGES

(a) PREPARATION OF TEST SPECIMENS

In order to obtain data on the flint clay in its unaltered structure, comparable to the larger particles used in batches from which refractory shapes and bricks are made, pieces for test were cut from large lumps. These pieces were finished by grinding them to cubes approximately 0.2 in. on a side. Furthermore, for making tests under different atmospheric conditions specimens were cut from the same lump of clay as the cubes to reduce possible variation.

Specimens representing the fine portion of the brick batch were prepared by pulverizing an average sample of flint clay to pass a No. 200 United States Standard Sieve. Cylinders 0.25 in. in diameter and 0.15 in. long were pressed from the slightly dampened material. Such specimens represented a uniform and intimately mixed sample of the clay. This was in contrast to the cubical specimens in which nonuniformity was indicated by differences in color of the clay.

In both cases specimens were dried overnight at approximately 105° C.

(b) PROCEDURE

The interferometer [6] was used for making measurements, during heating, of the expansion or contraction of the raw clays. Measurements were made over the range from room temperature to 1,000° C. A heating rate of 2.5° C/min was used.

The linear shrinkage after heating and cooling the clays was measured with a micrometer.

(1) *Atmospheric conditions.*—Length changes of the clays were measured under ordinary atmospheric conditions such as obtained in the muffle of an electrically heated furnace. They were measured also in an atmosphere of the products of gas combustion obtained by burning a small gas flame in the lower end of the furnace muffle. This atmosphere should partially simulate that present in many commercial kilns.

[6] George E. Merritt, *The interference method of measuring thermal expansion*, BS J. Research **10**, 59 (1933), RP515.

2. ENDOTHERMIC AND EXOTHERMIC EFFECTS

The study of the thermal effects was limited to the determination of the relative magnitude of the endothermic and exothermic reactions and the temperature ranges over which they occurred.

For these tests, clays ground to pass a No. 200 sieve were used. The heat effects were measured by the modified differential-thermocouple method [7] which has been made use of by many ceramic investigators in studies of clay materials. However, in place of the divided platinum cylinder usually used for the sample and reference material, a refractory thermocouple insulator, 1 by ½ by ⅜ in. with two holes slightly less than ¼ in. in diameter, was used. This was cemented in a vertical position to two legs, ¾ in. long.

The reference material was a clay calcined at 1,000° C, and of the same fineness as the test specimens. It was considered suitable because it was inert and approached in composition the clays being tested. The reference material and the test material were packed tightly in the respective halves of the container around the junctions of the thermocouples. The rate of heating was 2.5° C/min. Readings of the temperature of the test sample and of the galvanometer deflection due to temperature difference between the materials in the two sides of the cylinder were taken at 1- to 5-min. intervals, depending on the rate of change of the differential temperature.

IV. RESULTS AND DISCUSSION

1. MISSOURI FLINT

A series of specimens of Missouri flint clay, taken from different lumps of the 1,000-lb. lot received, was tested for change of length during heating. From visual examination the lumps selected appeared different in color and texture. Tests were made only on small cubes or pieces. The results of five such tests, all of which were made under ordinary atmospheric conditions, are shown in figure 1. The results show considerable differences in total length changes at 1,000° C, the range extending from 3.9 to 4.9 percent. The average linear shrinkages of the specimens after completing the heating and cooling cycle ranged from 4.4 to 5.3 percent. The fact that each specimen was shorter after cooling than at 1,000° C was to be expected, since the contraction on heating was due to irreversible reactions, whereas that on cooling was ordinary reversible thermal contraction.

The curves show that the clays expanded uniformly and rather slowly from room temperature to within the range 470° to 500° C. This expansion amounted to approximately 0.3 percent. Contraction commenced thereafter and proceeded relatively slowly for approximately 60° C, then very rapidly for approximately 50° C. The contraction for this interval of approximately 110° C ranged for the different specimens from 1.0 to 1.8 percent. For the next interval of approximately 320° (600° to 920° C) the contraction proceeded again at a somewhat slower pace, resulting in 1.5 to 2.3 percent additional shortening. For the next 50° C interval (approximately 930° to 980° C) the contraction was very rapid again, ranging from 1.0 to 1.4 percent. After passing this range and up to 1,000° C, con-

[7] Burgess and Le Chatelier, Measurements of high temperatures, 3d ed., p. 383 (J. Wiley & Sons, New York, N. Y., 1912).

traction proceeded again at a slower rate. The curves, therefore, show two comparatively short ranges of temperature in which the contraction of the clays proceeded at a very rapid rate.

Additional tests of Missouri flint clay were made to determine whether the rate and extent of the contraction of the granules and that of the fines were different and also whether the contraction was affected by a change of atmosphere. Figure 2 (left) shows that when pieces were heated in an atmosphere of the products of gas combustion, the type of curve obtained was not greatly different from that already discussed. There are, however, two noteworthy features, namely: (a) The beginning of the first period (about 500° C) of rapid contraction of the clay in air precedes that of the clay in an atmosphere of the products of gas combustion by at least 15° C; however, in the beginning of the second period of rapid contraction (about 900° C), it follows that of the clay tested in the spent gases by about 30° C. (b) The total contraction at 1,000° C was the same in the two tests.

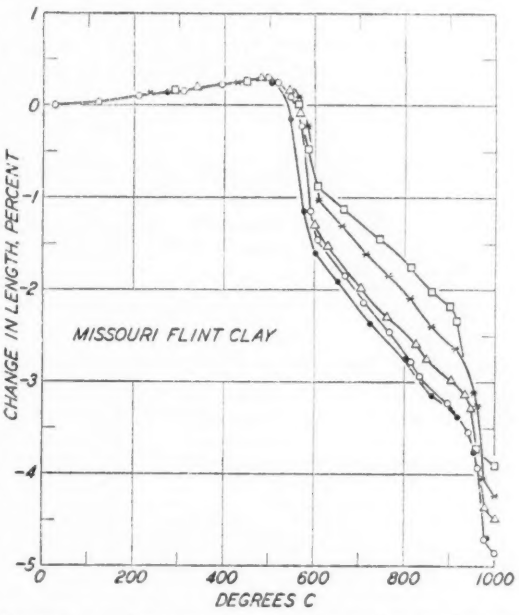

FIGURE 1.—*Length changes during heating of five different pieces of clay selected from a sample of flint clay from Missouri.*

Selection was based primarily on color.

Figure 2 (right) shows the results obtained in two atmospheres when tests were made on specimens prepared from a composite sample of the fines. The trend of the expansion and contraction in this case was similar to that obtained on the coarse or granular particles. The rapid contraction which occurred between 500° and 600° C was approximately 0.75 percent less and that between 800° and 900° C was approximately 0.50 percent greater than that of the unpulverized clay.

Figure 3 compares contraction curves obtained from tests in air of coarse pieces of Missouri flint clay and of specimens prepared from the fines taken adjacent to the coarse pieces. Very little difference in results was obtained. This indicated that the differences shown in figure 2 between the pieces and the fines may be attributed to sampling.

In these tests the first period of rapid contraction occurred at about 500° C, where according to J. W. Mellor,[8] among others, the clay

[8] *Chemical constitution of the clay molecule. Review of later theories,* Trans. Ceram. Soc. 37, 118–125 (1938).

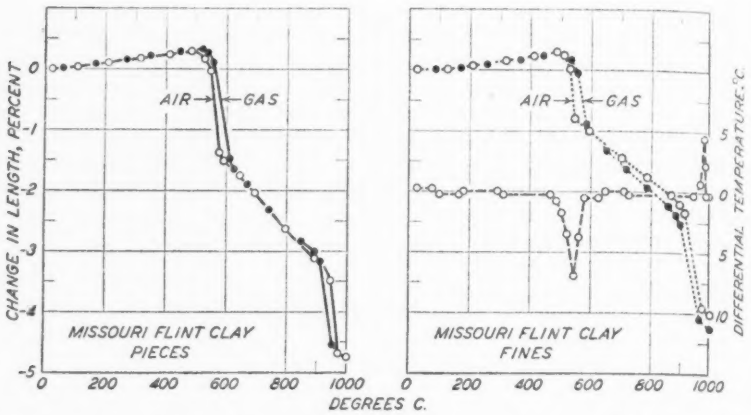

FIGURE 2.—*Comparing changes in length of an average sample of Missouri flint-clay fines (right) and granular pieces (left) when heated in air and in the products of gas combustion.*

The difference between the pieces and the fines is not attributed to difference in grind but to variation in the material. The curve showing the endothermic and exothermic effects in the fines heated in air is given also in the graph on the right.

molecule is completely disrupted to form water, free silica, and free alumina. The second period of rapid contraction occurred at about 900° C, where gamma alumina (see footnote 8) is formed.

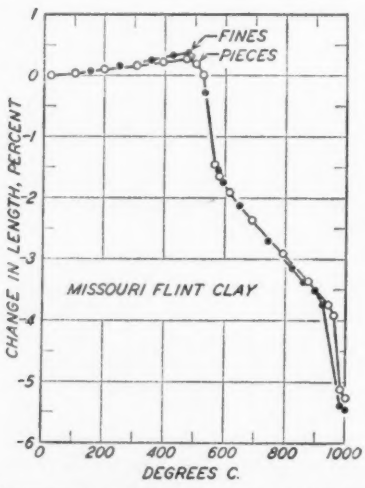

FIGURE 3.—*No significant differences in changes in length between pieces and fines of Missouri flint clay were noted when specimens were prepared from adjacent material and heated in air.*

The heating curve for the Missouri flint clay as given on the right in figure 2 shows two effects. An endothermic effect took place between approximately 470° and 580° C and reached its maximum at about 550° C. This corresponds closely to the first period of rapid contraction. An exothermic effect took place between about 940° and 990° C and reached its maximum at about 985° C. This corresponds fairly closely to the second period of rapid contraction.

2. KENTUCKY FLINT

Figure 4 shows the results of tests of granular pieces and also of fines of Kentucky flint clay. Considering either the pieces or the fines alone, only a slight difference was noted in the contraction characteristics when each was tested in air or in an atmosphere of the products of gas combustion. There was however, a considerable difference between the results obtained in tests of the granular pieces of clay and of specimens prepared from the fines. The maximum expansion of

the pieces was 0.4 percent and that of the fines 0.2 percent. Furthermore, the specimens made from the fines and tested in an atmosphere of burned gases reached their maximum expansion at a temperature 50° C higher than when tested in air. The shrinkage taking place during the first period of rapid contraction ranged from 1.75 to 2.0 percent and for the second period from 1.6 to 2.15 percent. The higher values were recorded with the fines, which is the reverse order from that obtained with the Missouri flint clay. The total contraction at 1,000° C ranged from 5.0 percent for the granular pieces to 6.0 percent for the fines.

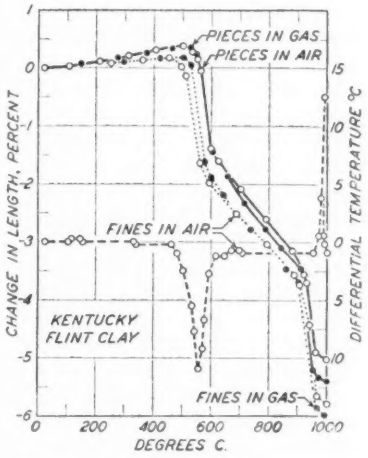

FIGURE 4.—*Comparing changes in length during heating of granular pieces and fines of Kentucky flint clay determined in air and in an atmosphere of the products of gas combustion*

The endothermic and exothermic effects in the fines heated in air are shown also

To determine whether there was any difference in change of length with heating between pieces and fines of Kentucky flint clay, specimens were prepared from adjacent material to represent these two conditions. The results of the tests are shown on the left in figure 5. In contrast with the Missouri clay, where there were no significant differences between the results obtained with the pieces and fines, the Kentucky clay showed a pronounced difference. The fines showed slightly less expansion up to 500° C and considerably greater con-

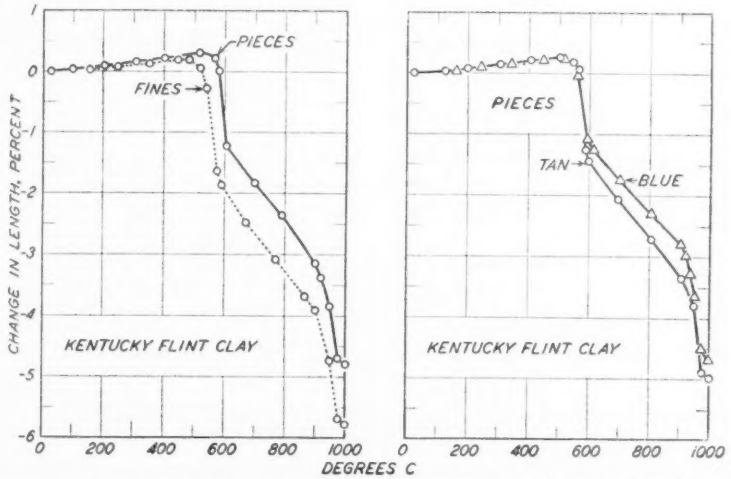

FIGURE 5.—*Left, significant differences in measurements of change in length between pieces and fines of Kentucky flint clay were obtained when specimens were prepared from adjacent material and heated in air.*

Right, changes in length of specimens from the same lump of clay but of two different colors which blended into one another.

traction between approximately 500° and 600° C. Also the total contraction up to 1,000° C was approximately 1.0 percent greater for the fines.

A separation was made of a light-bluish clay which appeared as streaks in lumps of Kentucky flint clay. As given in table 1, this material had a pyrometric cone equivalent of 35; the grayish-tan portion was 34. The index of refraction of the bluish material was slightly higher than that of the tan, and the latter contained clouds of low-index material. X-ray photographs indicated both materials to be kaolinites. The length changes obtained on heating of pieces taken adjacent to each other are shown on the right in figure 5. The bluish portion showed about 0.4 percent less contraction between 500° and 600° C and about 0.25 percent less up to 1,000° C than the tan portion. There was little difference between the two materials in the magnitude of the rapid contraction between 900° and 1,000° C.

The heating curve for the Kentucky flint is given in figure 4. A rather pronounced endothermic change occurred between 460° and 610° C, which reached its maximum at 550° C. Also, a pronounced exothermic change took place between 960° and 1,000° C, which reached its maximum at approximately 990° C. These effects corresponded relatively well with the intervals of rapid contraction shown in the change of length curves.

3. OHIO FLINT

There are two flint clays from Ohio listed in table 1. Figure 6 (left) shows the results of tests of the contraction of the light-colored flint

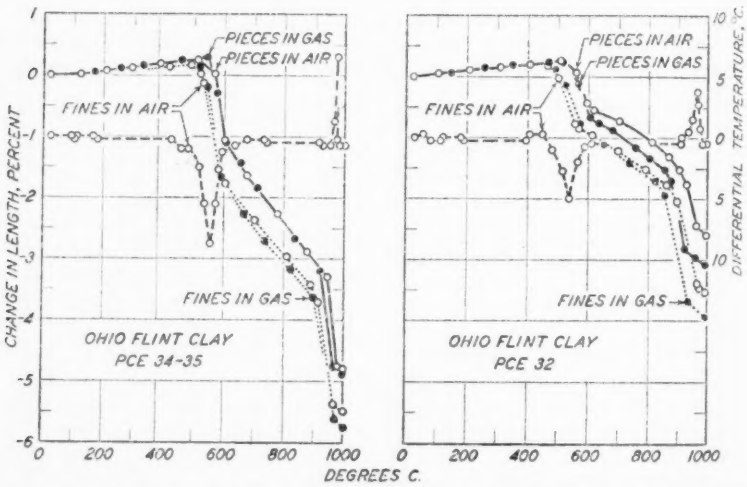

FIGURE 6.—*Changes in length and endothermic and exothermic effects during heating of two different flint clays from Ohio.*

clay (pce 34–35). There were only minor differences between this clay and the Kentucky flint clay. The expansion which occurred below 550° C, the rapid contraction which occurred between approximately 500° and 600° C, and the total contraction up to 1,000° C were all slightly lower in the Ohio clay.

Figure 6 (right) shows the results of tests of the second Ohio flint clay (pce 32). The fines, when tested in air, commenced to contract at a temperature about 40° C lower than that at which the pieces did. The shrinkage beginning at the end of the expansion period and ending at about 600° C in this case was only about one-half, and the total contraction up to 1,000° C was approximately two-thirds of that in the first Ohio clay. Both clays showed greater contraction when pulverized than when not pulverized.

The heating curves for the two Ohio flint clays are shown in the respective sections of figure 6. No significant differences were noted between the heat effects of the two clays.

4. PENNSYLVANIA FLINT

There are two flint clays from Pennsylvania listed in table 1. Figure 7 shows the results of tests made on the clay which had a pyrometric cone equivalent of 32–33. Among the several notable differences between this clay and the others which have been discussed is that the expansion of the pieces was greater in the case of this clay and occurred over a longer temperature range. The fines showed an expansion of about the same magnitude as the fines of the other clays. Also, the Pennsylvania flint in the first period of contraction showed less change for both the fines and the pieces, but in the second period of rapid contraction this held true for the pieces only. Both the total contraction up to 1,000° C and the total shrinkage on cooling were low compared with the clays already discussed.

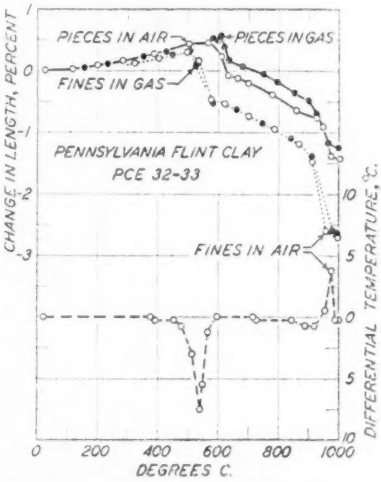

FIGURE 7.—*Changes in length and endothermic and exothermic effects during heating of a flint clay from Pennsylvania.*

The expansion of the clay occurred over a greater temperature range and the total length change was much less than obtained with flint clays from other sources.

The results of tests of the Dean flint clay from Pennsylvania are given in figure 8. The lumps of clay as received were a mixture of very dark- to light-gray material. Results obtained with the pieces and the fines of the clay of an intermediate color, which formed the greater portion of the sample, are shown in the left section of figure 8. The results on clay representing the extremes of the dark- and light-colored pieces are compared in the section on the right.

In the pieces the behavior of the clay was quite different from that of all other clays. The expansion proceeded slowly and uniformly, as noted in other clays, but extended over a slightly greater temperature range. Then with almost explosive violence the particular pieces of clay tested (fig. 8) expanded about three times as much within 50° C as they had within the preceding 500° C. Immediately thereafter, for approximately 70° C, fairly rapid contraction took place, which, however, was small in extent and slow when compared

to that obtained with clays from the other States. The same diminution of extent and rapidity applied to the contraction which occurred between 900° and 1,000° C. Because of the high expansion and relatively lower contraction occurring below 650° C, the length of the specimen at 1,000° C in one case was greater and in the other cases very little less than the original length.

Figure 8 also shows the results of tests of the pulverized clay. The appearance of the curves is very similar to that shown for specimens made from the fines of other flint clays. It is apparent that pulverizing the clays eliminated the causes of the rapid expansion between 500° and 600° C. This may possibly be accounted for by the destruction of lamination planes as discussed by J. O. Everhart.[9] Also, since this clay was much harder than the other flint clays, pulverizing could facilitate the escape of the water or steam. In the granular pieces the steam might build up considerable pressure before

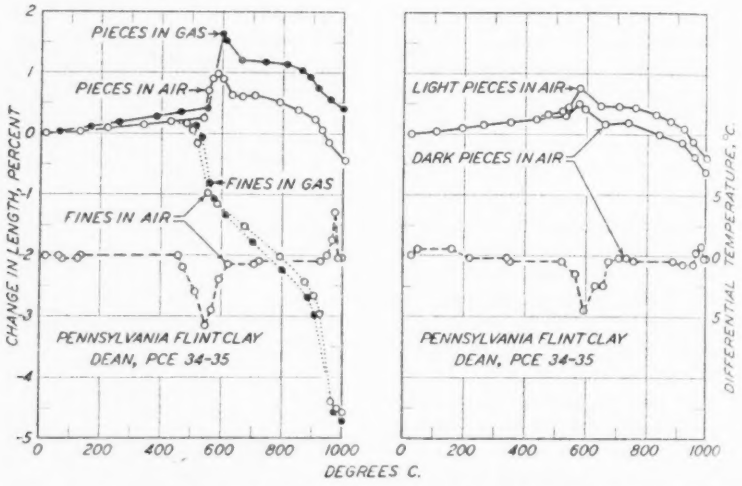

FIGURE 8.—*Changes in length and endothermic and exothermic effects during heating of a second flint (Dean) clay from Pennsylvania.*

In the graph on the left the decided difference between the expansion and contraction of the granular pieces and the fines is shown. In the graph on the right are compared changes in length of pieces of clay taken from the same sample but different in color.

it was released. Changes in length of the fines were not significantly affected by the atmosphere. (See fig. 8.)

The curves showing the thermal changes which took place in this clay with heating to 1,000° C are given in figure 8. Both the endothermic and exothermic peaks[10] occurred at a higher temperature in the pieces than in the fines.

---

[9] *Secondary expansion in refractory clays*, J. Am. Ceram. Soc. **20**, 353 (1937).

[10] Some data were obtained on the effect of atmosphere, size of particle, and rate of heating on the endothermic and exothermic effects of several of the clays. The data are limited in quantity and the values are, therefore, not reported. However, it was indicated that the exothermic peak in an atmosphere of the products of gas combustion (three tests) was reached at a slightly lower temperature than when tested in air. The endothermic peak was not significantly affected. Both the endothermic and exothermic peaks occurred at a higher temperature with unpulverized clay (two tests) than with the fines. (See fig. 8.) In the single test made, a heating rate of 5° C/min caused the endothermic effect to occur at an appreciably higher temperature than when a rate of 2.5° C was used.

5. WASHINGTON FLINT

Two flint clays, known as Kummer and Farrow, respectively, were obtained from the State of Washington. The Farrow flint clay was

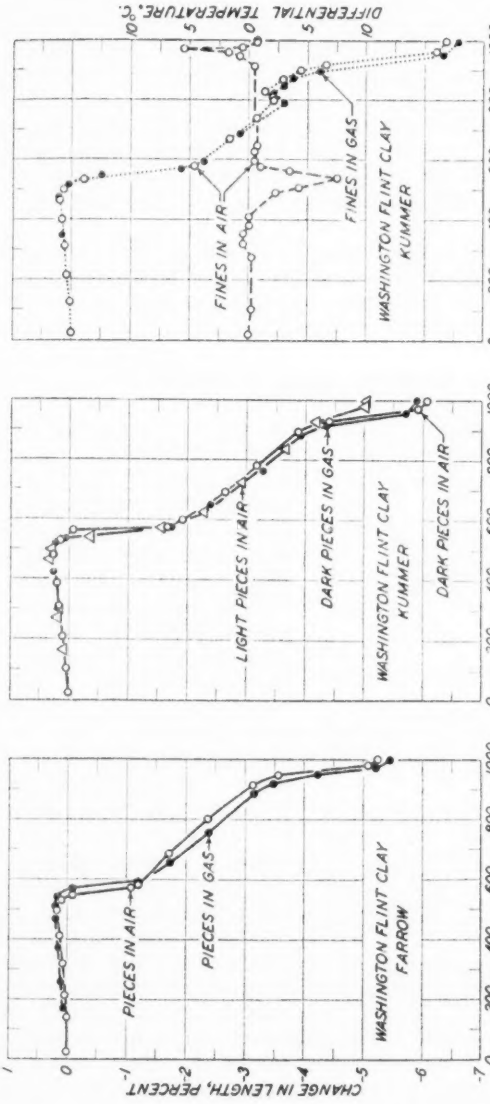

FIGURE 9.—*Changes in length and endothermic and exothermic effects during heating of two flint clays from Washington.*

The graph in the center shows that the light-colored inclusions contracted approximately 1 percent less to 1,000° C than the dark flint clay. The graph on the right shows that the Kummer flint, when pulverized, was different from the other clays in that it had a slight expansion at about 800° C and showed a greater total contraction.

tested in the two atmospheres but in the unpulverized form only. The curves (fig. 9, left) are, in general, similar to those for Missouri, Kentucky, and Ohio clays. No data were obtained on thermal changes.

The Kummer flint clay was streaked with small quantities of a very light-colored material. This, when separated, gave a pyrometric cone equivalent of 37 as against 35 for the dark material. The curve for the light-colored material shows this clay to be significantly different from the darker clay (center graph, fig. 9), in that its maximum contraction up to 1,000° C was considerably less (5.0 versus 6.05 percent). The dark clay showed greater contraction than any other flint clay during the two periods of rapid contraction (between 500° and 600° C and 850° and 950° C) and also a greater total contraction up to 1,000° C. The pulverized dark clay, whether tested in air or in the atmosphere of burned gases, showed an expansion of 0.2 percent between 790° and 820° C (fig. 9, right). Tests were not made of the fines of the light portion of this clay, but none of the other flint clays showed a similar expansion.

The curve illustrating the thermal changes of the fines of the dark Kummer clay is shown in the section on the right in figure 9. No effect corresponding to the slight expansion noted at about 800° C in the change-of-length curve occurred in the thermal-change curve.

6. TYRONE PLASTIC CLAY

Figure 10 shows the data obtained on a plastic clay. There is a striking similarity between these curves and those shown in figure 7 for one of the Pennsylvania flint clays, in spite of the fact that the plastic clay contains an appreciable amount of free silica and the flint clay contains practically none. The curves giving the changes in length for the pieces tested in air or in the atmosphere of burned gases are characterized by a slight but rapid expansion between 600° and 620° C. This expansion occurred after a slight contraction which followed the slow expansion between 20° and 450° C. It was accompanied by a minor explosion which cracked the specimens. The rapid contraction between approximately 500° and 600° C, generally pronounced in the flint clays, was very slight in this plastic clay, and hence the total shrinkage up to 1,000° C was small. The expansion at approximately 600° C was eliminated by pulverizing the material. Both the pieces and fines showed slightly greater contraction when tested in burned gases than when tested in air.

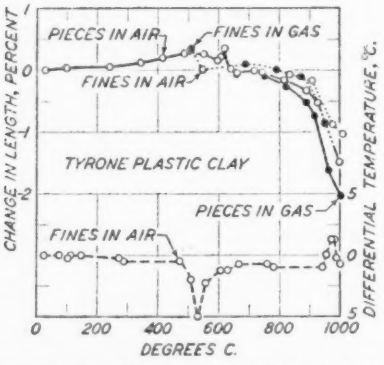

FIGURE 10.—*Changes in length and endothermic and exothermic effects during heating of Tyrone plastic clay from Pennsylvania.*

The curves showing changes of length for the pieces of this clay show a marked similarity with those for the pieces of the Pennsylvania flint clay (fig. 7).

7. GEORGIA KAOLINS

The results of tests of a Georgia hard kaolin [11] tested in air are shown in figure 11 (left). The curves are very similar to those obtained for the Kentucky, Missouri, and Ohio flint clays. The effect of pulverizing was to increase slightly the magnitude of the rapid contraction which occurred between 500° and 600° C as well as the total contraction up to 1,000° C.

The heating curve for this kaolin is given in the same section of figure 11. It is similar to heating curves obtained on some of the flint clays.

A bauxitic Georgia kaolin was pulverized to obtain a composite sample, and the results of the tests are given in figure 11 (right).

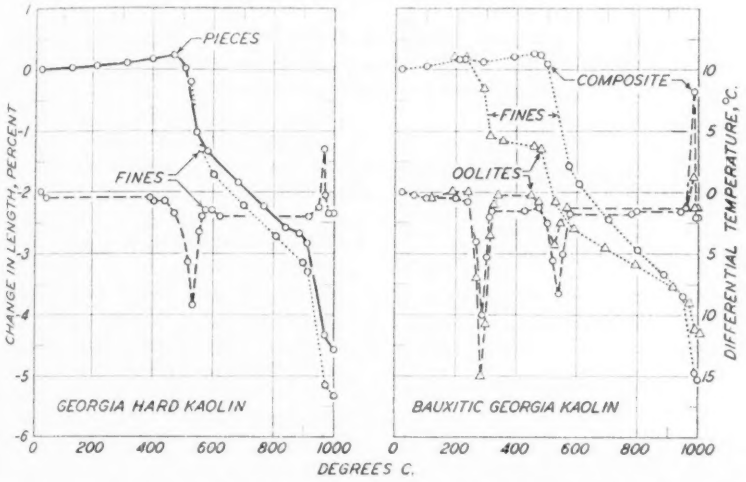

FIGURE 11.—*Changes in length and endothermic and exothermic effects during heating in air of pulverized and unpulverized Georgia hard kaolin (left) and pulverized bauxitic Georgia kaolin and oolites taken from the latter (right).*

The bauxitic kaolin and the oolites showed two endothermic effects and one exothermic. Only the oolites reflected the first thermal change by a large contraction between 200° and 300° C.

The curve is similar to those obtained for the flint clays, except for a slight contraction evident between about 230° and 290° C.

Specimens were made from oolites removed from the lumps of kaolin and pulverized to pass a No. 200 sieve. The manner in which the contraction of these specimens proceeded is shown also on the right in figure 11. The first period of rapid contraction occurred between 230° and 315° C, the second between about 485° and 580° C, and the third between 970° and 990° C.

[11] The dehydration studies of the kaolin minerals by Ross and Kerr, The kaolin minerals, U. S. Geological Survey, Professional Paper 165–E (1930), Halloysite and allophane, U. S. Geological Survey, Paper 185–G (1934–35), show that these minerals lose water very slowly from room temperature to just below 400° C and very rapidly between 400° and 500°C. The period of rapid dehydration for both kaolinite and halloysite had in most cases been completed before 500° C had been reached. The data on change of length obtained in the present study indicated that a slow expansion occurred during most of that interval. Also, the temperature range of the first period of greatest contraction, which took place in the Georgia kaolin (also that of the flint clays, except the Dean), occurred between 500° and 600° C. The higher temperature range (500° to 600° C) at which dehydration of the kaolin occurred in the present study could be accounted for by the fact that a continuously rising temperature was used in making the tests, whereas the range (400° to 500° C) of rapid dehydration reported by Ross and Kerr was based on losses obtained at constant temperatures.

The heating curves for the bauxitic Georgia kaolin and for the oolitic material appear in figure 11 (right). In each case a large endothermic effect took place between about 240° and 320° C, which reached its maximum at about 290° C. This effect was probably due to the presence of gibbsite.[12] Although the oolitic material showed such a pronounced change in the contraction curve in that temperature range, the bauxitic kaolin showed only a slight irregularity in its curve though the endothermic change was large in both instances. Both materials showed an endothermic change in the temperature range within which the clay molecule breaks down. In the case of the oolitic material this indicated the presence of kaolin, as also did the slight exothermic change between 960° and 990° C.

8. DIASPORE

The results of tests of pieces and fines of diaspore are given in figure 12. This figure shows that a slightly greater expansion occurred in the pieces between room temperature and 450° C than was the case with the flint clays. The contraction which occurred between 450° and 510° C was, however, low (0.5 percent) compared to that shown by the flint clays. A gradual expansion was shown between 510° and 1,000° C, which was the reverse of the trend shown by the flint clays. Also, no period of rapid contraction was shown between 900° and 1,000° C such as occurred in the flint clays. Pulverizing the material had little effect on its expansion up to 460° C. The entire contraction (less than 0.1 percent) between 460° and 490° C caused scarcely more than a ripple in the curve, and from there to 850° C very little change took place. However, between 850° and 1,000° C a rather large contraction occurred (1.5 percent).

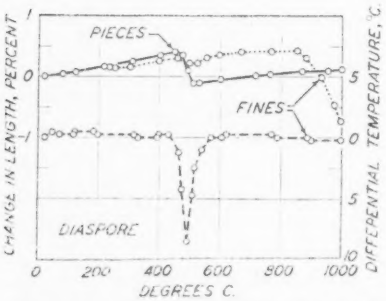

FIGURE 12.—*Length changes and endothermic effect during heating in air of diaspor from Missouri.*

The heating curve showed but one break and that was due to an endothermic change which occurred between 400° and 600° C and reached its maximum at 500° C. The endothermic change was rather large, but only a slight change in length occurred in this temperature range.

9. ZETTLITZ KAOLIN

The results of two tests of Zettlitz kaolin are shown in figure 13. Tests by W. Steger [13] failed to show the rapid contraction between 500° and 600° C. It was for that reason that a sample of Zettlitz kaolin was tested. The same heating rate (2.5° C/min) was used with this kaolin as was used in all other tests; and, in addition, a heating rate of 6° C, as used by Steger, was tried. Both curves (fig. 13) show the period of rapid contraction between about 540°

[12] Unpublished data, H. Insley.
[13] Ber. deut. keram. Ges. **19**, 2 (1938).

and 600° C, though the higher heating rate caused the contraction to take place over a slightly greater temperature range. The total contraction at 1,000° C was about 3.25 percent, which is considerably greater than the 1.75 percent shown by Steger. The large difference would indicate that the two kaolins may have been of different purity.

J. F. Hyslop and A. McMurdo [14] reported on changes in length of an English china clay and of a Missouri halloysite, but in neither case did they show a period of rapid contraction between 500° and 600° C.

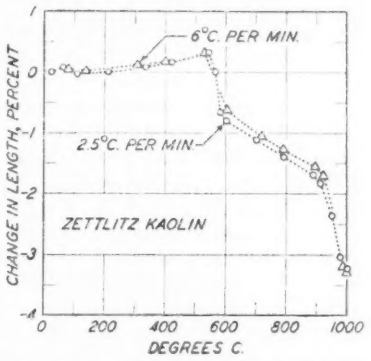

FIGURE 13.—*Changing the rate of heating from 2.5°C to 6°C per minute does not greatly affect the results in measurements of change of length during heating in air of Zettlitz kaolin.*

10. REPRODUCIBILITY OF RESULTS

Tests were made on each of two sets of specimens prepared from the same small batch of fines of the Missouri and Kentucky clays to determine the reproducibility of the data on change of length. In each case, the difference in results between the first and second tests was less than 1 percent of the total length change.

The peaks of the endothermic and exothermic changes made on duplicate samples of Missouri clay in air and in burned gases, and also of Kentucky clay in air only, did not vary more than 2° C between the first and second tests.

V. SUMMARY

A study was made of the changes in length and endothermic and exothermic effects between room temperature and 1,000° C in nine flint clays, three kaolins, and one each of a diaspore and a plastic clay. Also, their pyrometric cone equivalents were determined and some microscopic examinations were made.

The following results were noted:

All the flint clays (except one mined in Pennsylvania), as well as the Georgia and Zettlitz kaolins, showed a slight expansion between room temperature and approximately 500° C, a rapid contraction of considerable proportions between approximately 500° and 600° C, a gradual contraction between about 600° and 925° C, a rapid contraction between approximately 925° and 980° C, and a slower contraction again from there to 1,000° C. The Pennsylvania (Dean) flint, which was one of the exceptions in the unpulverized condition, showed a sharp expansion between about 540° and 590° C, but when pulverized through a No. 200 sieve acted similarly to the other flint clays.

In general, the pulverized clays showed greater total shrinkage up to 1,000° C than the unpulverized.

Also, the ranges in temperature in which rapid contraction took place were slightly lower for the fines than for the coarse material. The Missouri flint clay showed no differences in these ranges when the two types of specimens were prepared from adjacent material.

[14] Trans. Ceram. Soc. **37**, 180 (1938).

Much variation in the magnitude of the rapid contraction during heating occurred in specimens prepared from different lumps of a sample of flint clay as well as from the same lump. The nonuniformity of the clays could readily be determined by visual examination.

The one plastic refractory clay tested showed very little contraction in the 500° to 900° C range, but between 900° and 1,000° C showed approximately the same as that shown by some of the flint clays.

Most of the clays showed slightly greater contraction in an atmosphere of the products of gas combustion than in air.

Endothermic reactions took place between approximately 475° and 575° C and exothermic reactions between about 940° and 990° C in all the flint clays, the plastic clay, and the Georgia kaolin. The temperature ranges during which these reactions occurred corresponded fairly closely to those in which rapid contraction took place.

The bauxitic Georgia kaolin contracted rapidly during two ranges of temperature, namely, approximately 480° to 540° C and 970° to 990° C. A slight inflection or temporary reversal in trend from expansion to contraction to expansion was also indicated between 250° and 310° C. A pronounced endothermic effect was observed at the lower range of temperature and a moderately large one within the intermediate range. An exothermic effect was observed within the highest range.

The oolites from the bauxitic Georgia kaolin showed fairly pronounced contraction during three ranges of temperature, namely, approximately 250° to 310° C, 480° to 560° C, and 970° to 990° C. An unusually large endothermic effect was observed at the lower range and a rather small one at the intermediate range. The exothermic effect, which reached its maximum at 980° C, was small.

Diaspore showed contraction during one stage only, namely between 450° and 510° C, and but one heat effect, namely, an endothermic one between 450° and 510° C.

WASHINGTON, March 1, 1939.

U. S. DEPARTMENT OF COMMERCE NATIONAL BUREAU OF STANDARDS

RESEARCH PAPER RP1244

Part of Journal of Research of the National Bureau of Standards, Volume 23, September 1939

SECOND SPECTRUM OF CHLORINE AND ITS STRUCTURE

By C. C. Kiess and T. L. deBruin

ABSTRACT

New wave lengths of Cl II, extending from 9483 A, in the infrared, to 2100 A in the ultraviolet, have been derived at the National Bureau of Standards from observations employing Geissler-tube and electrodeless discharges as light sources. These, together with unpublished observations of the Schumann region made by others, have been used to extend the analysis of the term system of Cl II. New terms have been added to the partially known quintet and triplet systems, and the singlet system has been established. All three systems are linked together with intersystem combinations. Series of ^5S and ^3S terms, with ^4S of Cl III as their limit, and of ^3D terms, with ^2D of Cl III as their limit, are in excellent agreement in fixing the value of the deepest term at 192,000 cm^{-1}, whence an ionization potential of 23.70 volts is derived for Cl^+.

CONTENTS

	Page
I. Introduction	443
II. Experimental procedure	444
III. Results	445
1. Wave lengths and intensities	445
2. Term structure	461
3. Series and ionization potential	468
4. Comparison with similar spectra	469

I. INTRODUCTION

The description and analysis of the second spectrum of chlorine presented in this paper are an outgrowth of the investigation, made 10 years ago at the National Bureau of Standards,[1] of the spectrum emitted by neutral chlorine atoms. The observations on which that earlier work was based yielded a list of additional wave lengths that were recognized as characteristic of the spectrum emitted by singly ionized chlorine atoms. At that time a beginning had already been made on the analysis of Cl II—the spectral regularities first detected by Paulson [2] among the visible and ultraviolet lines had been extended and interpreted by Paschen; [3] and the triplet groups first observed by Hopfield [4] in the Schumann region had been subsequently verified and extended by Bowen.[5] To the lines classified by Paschen a new group had been added by the Blochs.[6] The multiplets that we worked out from our new wave-length data were found to link together with those already known from the work of the earlier investigators; therefore, we decided to carry on the analysis to the extent warranted by the obtainable observational data.

[1] C. C. Kiess and T. L. deBruin, BS J. Research **2**, 1117 (1929) RP73.
[2] E. Paulson, Astrophys. J. **40**, 299 (1914).
[3] F. Paschen, Ann. Physik **71**, 559 (1923).
[4] J. J. Hopfield, Phys. Rev. **26**, 282 (1925).
[5] I. S. Bowen, Phys. Rev. **31**, 34 (1928).
[6] L. and E. Bloch, Ann. physique [10] **8**, 402 (1927).

As the analysis progressed with the aid of our own and published wave lengths, notably those of the Blochs, we realized that the spectrum had not been sufficiently well observed to permit the theoretical term structure of Cl II to be worked out fully. Accordingly, a new series of observations was planned to cover those regions of the spectrum that hitherto had been inadequately observed.

While this work was in progress, Murakawa began the publication of the results of his observations and analysis of Cl II. His findings have been presented in a series of six papers.[7] As Murakawa's analysis was, for the greater part, in harmony with our own, we felt that any additional publication on the subject should represent an analysis that was approximately complete. This status was nearly reached in 1932, at which time a description of our results was presented to the American Optical Society at its annual meeting.[8] To aid in approaching this goal, we have had at our disposal the unpublished lists of observations of the extreme ultraviolet made by Bowen, by Weinberg,[9] and by Boyce.

II. EXPERIMENTAL PROCEDURE

Both Geissler tubes and the electrodeless discharge were used to obtain the spectra emitted by ionized Cl atoms. The Geissler tubes and their behavior under different conditions of excitation have already been described in our paper on the arc spectrum. Although they emitted the visible portions of the spectrum with considerable intensity, they proved to be relatively weak in the violet and shorter regions owing, in part, to the scaly deposit that formed within the capillary of the tube. Furthermore, many of the lines excited by the highly condensed discharge were broad and fuzzy, the fainter ones being particularly difficult to measure.

To obtain a source emitting sharp lines, and intense in the ultraviolet, we adopted the electrodeless discharge, which has been employed so effectively by L. and E. Bloch, and others, in studying the spectra of the halogens and other elements. The tube was a Pyrex cylinder 12 cm long and 6 cm in diameter. To one end of it a fused-quartz window was cemented and to the other end was sealed the connection for the vacuum line. The chlorine was supplied by the decomposition of specially purified and dried NaCl, about a gram of which was introduced within the tube shortly before the observations began. During operation, the tube was continuously open to the vacuum line, which was maintained by a Hickman [10] diffusion pump supported by a forepump. The exciting field was maintained by the discharge of five condensers rated at 0.002 μf each, and connected in parallel through a coil surrounding the tube and in series with a 2-cm spark gap. The coil consisted of 11 turns of No. 8 bare copper wire, each turn being 8 cm in diameter. The condensers were charged from a 40,000-volt

[7] K. Murakawa, Sci. Papers Inst. Phys. Chem. Research (Tokyo), **15**, 41 (1930); **15**, 105 (1938); **20**, 265 (1933). Z. Physik **69**, 507 (1931); **96**, 117 (1935); **109**, 173 (1938).
[8] C. C. Kiess and T. L. deBruin, J. Opt. Soc. Am. **23**, 121 (1933).
[9] F. Weinberg, University of California Master's Dissertation (1925).
[10] K. C. D. Hickman and C. R. Sanford, Rev. Sci. Instr. **1**, 140 (1930).

transformer, the primary of which was connected to mains supplying current of 15 to 20 amp at 110 v.

The spectra were photographed with the grating and quartz-prism spectrographs of the National Bureau of Standards. These instruments have been adequately described in previous publications.[11] The 21-foot concave gratings ruled with 7,500, 15,000, and 20,000 lines per inch were used in recording the spectra between 2200 A in the ultraviolet and 9483 A in the infrared. The quartz-prism spectrographs were used to record the ultraviolet portion of the spectrum between 2000 and 3500 A. Exposure times ranging from a few minutes up to 4 hours were required for the electrodeless discharge; but for the Geissler tubes longer exposure times, up to 20 hours, were needed. All of the spectrograms were also exposed to the iron arc to obtain the standard wave lengths [12] needed in the reductions.

When the 21-foot concave grating, ruled by Wood [13] with 30,000 lines per inch, became available, some additional observations were made in order to resolve certain lines known to be complex from the results of the analysis. The source used for this final set of observations was a condensed discharge through a Pyrex Geissler tube.

The observations from which we obtained our first results for Cl II were made prior to the advent of the new types of Eastman photographic plates. For these earlier observations we used ordinary plates sensitized by bathing in dye solutions in order to record the regions of longer wave length. The new types of plates [14] used for the observations of the electrodeless discharge and subsequent Geissler tube observations gave us an improved description of the long-wave portion of the spectrum that has furnished the clues for tying together the singlets and quintets with the more extensive triplet system.

III. RESULTS

1. WAVE LENGTHS AND INTENSITIES

The wave lengths that are characteristic of the spectrum emitted by singly ionized chlorine atoms are listed in the first column of tables 1 and 2. All of those extending from 9483 to 2100 A were derived from measurements of the spectrograms obtained at the National Bureau of Standards. They represent the means of from 2 to 10 or more measurements of the grating and prism observations. A few lines, measured on only one plate, have been corrected by amounts necessary to reduce the plate to the mean of the others. The intensities assigned to the lines are the usual visual estimates and are not comparable between widely separated regions of the spectrum. The letter *b* following an intensity indicates that the line is diffuse in the electrodeless discharge; *d* indicates that the line is double.

[11] W. F. Meggers and K. Burns, BS Sci. Pap. **18**, 191 (1922) S441.
[12] Trans. Int. Astron. Union **3**, 77 (1928).
[13] R. W. Wood, Nature **140**, 723 (1937).
[14] C. E. K. Mees, J. Opt. Soc. Am. **23**, 229 (1933).

TABLE 1.—*Wave lengths in the second spectrum of chlorine*

λ_{air}A	Intensity	ν_{vac}cm^{-1}	Term combination
9483. 00	2	10542. 30	$(^2D)3d\ ^3D^0_3-(^2P)4p\ ^3P_2$
8820. 70	5	11333. 86	
8391. 96	3	11912. 90	$(^4S)3d\ ^3D^0_1-(^4S)4p\ ^3P_1$
8382. 76	5	11925. 97	$(^4S)3d\ ^3D^0_1-(^4S)4p\ ^3P_0$
8361. 81	8	11955. 85	$(^4S)3d\ ^3D^0_2-(^4S)4p\ ^3P_1$
8360. 63	15	11957. 54	$(^4S)3d\ ^3D^0_3-(^4S)4p\ ^3P_2$
8353. 00	2	11968. 46	$(^4S)3d\ ^3D^0_2-(^4S)4p\ ^3P_2$
8272. 38	3	12085. 10	
8184. 78	2	12214. 45	
7644. 80	4	13077. 19	$(^2D)3d\ ^3D^0_1-x'$ $(^2P)4p\ ^1D_2-(^2D)4d\ ^3F^0_2$
7620. 51	4	13118. 88	$(^2D)3d\ ^3D^0_3-x'$
7578. 07	10	13192. 35	$(^2D)3d\ ^3D^0_2-x'$
7565. 53	18	13214. 21	
7389. 28	7	13529. 40	$(^2D)3d\ ^3P^0_2-x'$
7147. 80	3	13986. 47	$(^2P)3d\ ^3P^0_2-4s'\ ^3P_1$
7074. 98	4	14130. 42	$(^2P)3d\ ^3P^0_2-4s'\ ^3P_2$
6993. 27	2	14295. 53	$(^2D)3d\ ^3G^0_4-(^2D)4p\ ^3D_3$
6952. 13	25	14380. 12	$(^2P)3d\ ^3F^0_2-(^2P)4p\ ^3D_1$
6930. 45	4	14425. 10	$(^2P)3d\ ^3F^0_2-(^2P)4p\ ^3D_2$
6850. 21	40	14594. 07	$(^2P)3d\ ^3F^0_3-(^2P)4p\ ^3D_2$
6841. 86	10	14611. 88	$(^2P)3d\ ^3F^0_3-(^2P)4p\ ^3D_3$
6831. 62	30	14633. 79	$(^2P)4s\ ^1P^0_1-(^2D)4p\ ^1D_2$
6759. 42	35	14790. 09	$(^2P)3d\ ^3F^0_4-(^2P)4p\ ^3D_3$
6713. 43	40	14891. 41	$(^2D)3d\ ^3G^0_5-(^2D)4p\ ^3F_4$
6686. 04	45	14952. 42	$(^2D)3d\ ^3G^0_4-(^2D)4p\ ^3F_3$
6681. 03	15	14963. 63	$(^2D)3d\ ^3G^0_3-(^2D)4p\ ^3F_3$
6661. 68	75	15007. 09	$(^2D)3d\ ^3G^0_3-(^2D)4p\ ^3F_4$
6653. 75	25	15024. 98	$(^2D)3d\ ^3G^0_4-(^2D)4p\ ^3F_4$
6556. 35	1	15248. 08	$(^2P)4p\ ^1D_2-(^2D)4d\ ^3D^0_2$
6522. 38	10	15327. 60	$(^2D)4p\ ^3D_3-(^4S)4d\ ^3D^0_3$
6478. 07	2	15432. 44	$(^2D)3d\ ^3G^0_4-(^2D)4p\ ^1F_3$
6475. 38	2	15438. 85	$(^2D)4p\ ^3D_3-(^4S)\ 4d\ ^3D^0_2$
6465. 32	3	15462. 87	$(^2D)4p\ ^3D_2-(^4S)4d\ ^3D^0_3$
6419. 25	8	15573. 85	$(^2D)4p\ ^3D_2-(^4S)4d\ ^3D^0_2$
6417. 59	2	15577. 88	$(^2D)4p\ ^3D_1-(^4S)4d\ ^3D^0_2$
6399. 41	10	15622. 13	$(^2P)3d\ ^3P^0_2-(^2P)4p\ ^3P_2$
6391. 30	3	15641. 95	$(^2P)3d\ ^3P^0_2-(^2P)4p\ ^3P_1$
6385. 51	2	15656. 14	$(^2D)4p\ ^3D_2-(^4S)4d\ ^3D^0_1$
6384. 13	5	15659. 52	$(^2D)4p\ ^3D_1-(^4S)4d\ ^3D^0_1$
6366. 72	3*b*	15702. 34	
6365. 95	3*b*	15704. 24	
6364. 89	3*b*	15706. 86	
6243. 00	2	16013. 52	$(^4S)4s\ ^3S^0_1-(^4S)4p\ ^5P_1$
6227. 18	6	16054. 20	$(^4S)4s\ ^3S^0_1-(^4S)4p\ ^5P_2$
6094. 65	100	16403. 30	$(^2D)4s\ ^1D^0_2-(^2D)4p\ ^1P_1$
5922. 33	7	16880. 58	
5790. 50	25	17264. 89	$(^2D)4s\ ^1D^0_2-(^2D)4p\ ^3D_1$
5763. 70	2	17345. 17	
5744. 26	1	17403. 87	$(^2D)4s\ ^1D^0_2-(^2D)4p\ ^3D_2$
5634. 84	18	17741. 82	$(^2D)3d\ ^1P^0_1-(^2D)4p\ ^1P_1$

TABLE 1.—*Wave lengths in the second spectrum of chlorine*—Continued

λ_{air} A	Intensity	ν_{vac} cm^{-1}	Term combination
5568. 81	15	17952. 18	$(^2D)4p\ ^1D_2 - (^2D)5s\ ^1D_2^\circ$
5535. 39	5	18060. 57	$(^2D)4s\ ^1D_2^\circ - (^2D)4p\ ^3F_3$
5457. 47	30	18318. 43	$(^4S)3d\ ^5D_0^\circ - (^4S)4p\ ^5P_1$
5457. 02	75	18319. 94	$(^4S)3d\ ^5D_1^\circ - (^4S)4p\ ^5P_1$
5456. 27	50	18322. 46	$(^4S)3d\ ^5D_2^\circ - (^4S)4p\ ^5P_1$
5444. 99	10	18360. 42	$(^4S)3d\ ^5D_1^\circ - (^4S)4p\ ^5P_2$
5444. 25	60	18362. 92	$(^4S)3d\ ^5D_2^\circ - (^4S)4p\ ^5P_2$
5443. 42	100	18365. 71	$(^4S)3d\ ^5D_3^\circ - (^4S)4p\ ^5P_2$
5424. 36	25	18430. 24	$(^4S)3d\ ^5D_2^\circ - (^4S)4p\ ^5P_3$
5423. 52	100	18433. 10	$(^4S)3d\ ^5D_3^\circ - (^4S)4p\ ^5P_3$
5423. 25	150	18434. 02	$(^4S)3d\ ^5D_4^\circ - (^4S)4p\ ^5P_3$
5414. 20	2	18464. 83	$(^2P)3d\ ^1D_2^\circ - (^2P)4p\ ^3D_1$
5398. 32	1	18519. 15	$(^2P)4p\ ^1P_1 - (^2D)4d\ ^1P_1^\circ$
5392. 12	100	18540. 44	$(^2D)4s\ ^1D_2^\circ - (^2D)4p\ ^1F_3$
5356. 14	10	18664. 98	
5338. 92	5	18725. 18	$(^2D)4s\ ^3D_2^\circ - (^2D)4p\ ^1P_1$
5333. 70	15	18743. 51	$(^2D)4s\ ^3D_1^\circ - (^2D)4p\ ^1P_1$
5285. 48	30	18914. 51	$(^4S)4p\ ^3P_2 - (^2D)3d\ ^3P_2^\circ$
5249. 22	3	19045. 16	$(^4S)4p\ ^3P_2 - (^2D)3d\ ^3P_1^\circ$
5245. 69	4	19057. 98	$(^4S)4p\ ^3P_1 - (^2D)3d\ ^3P_1^\circ$
5221. 34	75	19146. 85	$(^4S)4s\ ^3S_1^\circ - (^4S)4p\ ^3P_1$
5217. 93	150	19159. 37	$(^4S)4s\ ^3S_1^\circ - (^4S)4p\ ^3P_2$ $(^4S)4s\ ^3S_1^\circ - (^4S)4p\ ^3P_0$
5193. 03	10	19251. 23	$(^4S)4p\ ^3P_2 - (^2D)3d\ ^3D_2^\circ$
5189. 70	25	19263. 59	$(^4S)4p\ ^3P_1 - (^2D)3d\ ^3D_2^\circ$
5175. 85	20	19315. 13	$(^2P)3d\ ^1D_2^\circ - (^2P)4p\ ^1D_2$ $(^2D)4p\ ^1D_2 - (^2D)4d\ ^3F_2^\circ$
5173. 15	25	19325. 21	$(^4S)4p\ ^3P_2 - (^2D)3d\ ^3D_3^\circ$
5162. 34	10	19365. 68	$(^4S)4p\ ^3P_0 - (^2D)3d\ ^3D_1^\circ$
5160. 75	3	19371. 64	
5158. 79	8	19379. 01	$(^4S)4p\ ^3P_1 - (^2D)3d\ ^3D_1^\circ$
5140. 43	1	19448. 22	$(^2D)4p\ ^3P_2 - (^4S)6s\ ^3S_1^\circ$
5113. 36	40	19551. 18	$(^2D)4s\ ^3D_3^\circ - (^2D)4p\ ^3D_2$
5104. 08	25	19586. 34	$(^2D)4s\ ^3D_2^\circ - (^2D)4p\ ^3D_1$
5103. 04	125	19590. 68	$(^2D)4s\ ^3D_2^\circ - (^2D)4p\ ^3D_2$
5099. 30	100	19605. 09	$(^2D)4s\ ^3D_1^\circ - (^2D)4p\ ^3D_1$
5098. 34	20	19608. 78	$(^2D)4s\ ^3D_1^\circ - (^2D)4p\ ^3D_2$
5078. 25	150	19686. 35	$(^2D)4s\ ^3D_3^\circ - (^2D)4p\ ^3D_3$
5068. 10	10	19725. 78	$(^2D)4s\ ^3D_2^\circ - (^2D)4p\ ^3D_3$
4995. 52	60	20012. 37	$(^2D)3d\ ^3F_4^\circ - (^2D)4p\ ^3D_3$
4970. 12	50	20114. 64	$(^2D)3d\ ^3F_3^\circ - (^2D)4p\ ^3D_2$
4943. 24	15	20224. 02	$(^2P)3d\ ^1P_1^\circ - (^2P)4p\ ^1D_2$
4936. 99	25	20249. 62	$(^2D)3d\ ^3F_3^\circ - (^2D)4p\ ^3D_2$
4931. 76	2b	20271. 10	$(^2D)4s\ ^3D_3^\circ - (^2D)4p\ ^3F_2$
4928. 26	1	20285. 49	$(^2P)3d\ ^3D_3^\circ - (^2P)4p\ ^3P_2$
4925. 17	15	20298. 22	$(^2D)3d\ ^3F_2^\circ - (^2D)4p\ ^3D_1$
4924. 83	10	20299. 62	$(^2P)4s\ ^3P_2^\circ - (^2P)4p\ ^3S_1$
4924. 28	18	20301. 88	$(^2D)3d\ ^3F_2^\circ - (^2D)4p\ ^2D_2$
4922. 14	20	20310. 71	$(^2D)4s\ ^3D_2^\circ - (^2D)4p\ ^3F_2$
4917. 72	125	20328. 97	$(^2D)4s\ ^3D_1^\circ - (^2D)4p\ ^3F_2$
4914. 32	12	20343. 03	$(^2D)4s\ ^3D_3^\circ - (^2D)4p\ ^3F_3$
4907. 17	15	20372. 67	$(^2P)4s\ ^3P_1^\circ - (^2P)4p\ ^3S_1$

TABLE 1.—*Wave lengths in the second spectrum of chlorine*—Continued

λ_{air}A	Intensity	ν_{vac}cm^{-1}	Term combination
4904. 76	135	20382. 68	$(^2D)4s\ ^3D_2^3-(^2D)4p\ ^3F_3$
4898. 94	7	20406. 90	$(^2P)4s\ ^3P_2^0-(^2P)4p\ ^3S_1$
4896. 77	200	20415. 94	$(^2D)4s\ ^3D_3^3-(^2D)4p\ ^3F_4$
4891. 62	4	20437. 43	$(^2D)3d\ ^3F_2^3-(^2D)4p\ ^3D_3$
4877. 70	5	20495. 76	$(^2D)4p\ ^3P_0-(^2D)5s\ ^3D_1^1$
4874. 94	2	20507. 36	
4857. 04	10	20582. 94	$(^2D)4p\ ^3P_1-(^2D)5s\ ^3D_2^2$
4847. 07	4	20625. 28	$(^2P)3d\ ^3D_2^2-(^2P)4p\ ^3P_2$
4842. 44	8	20645. 00	$(^2P)3d\ ^3D_2^2-(^2P)4p\ ^3P_1$
4836. 79	20	20669. 11	$(^2D)3d\ ^3F_4^4-(^2D)4p\ ^3F_3$
4833. 50	2	20683. 18	$(^2P)4p\ ^3P_1-(^2P)5s\ ^3P_0^0$
4829. 23	3	20701. 47	$(^2P)4p\ ^3P_0-(^2P)5s\ ^3P_1^1$
4821. 87	2	20733. 07	$(^2D)4s\ ^1D_2^2-(^2D)4p\ ^3P_2$
4820. 95	4	20737. 02	$(^2D)4p\ ^3P_3-(^2D)5s\ ^3D_3^3$ $(^2P)4p\ ^3P_2-(^2P)5s\ ^3P_1^1$
4819. 79	25	20742. 01	$(^2D)3d\ ^3F_4^4-(^2D)4p\ ^3F_4$
4819. 46	200	20743. 43	$(^4S)4s\ \ ^5S_2^2-(^4S)4p\ ^5P_1$
4811. 57	12	20777. 45	$(^2D)4p\ ^3P_2-(^2D)5s\ ^3D_2^2$
4810. 06	225	20783. 97	$(^4S)4s\ \ ^5S_2^2-(^4S)4p\ ^5P_2$
4809. 05	9	20788. 34	$(^2D)4p\ ^1D_2-(^2D)4d\ ^1F_3^3$
4807. 68	5	20794. 26	$(^2P)4p\ \ ^3P_1-(^2P)5s\ ^3P_2^2$
4803. 16	2	20813. 83	$(^2P)4p\ ^3P_2-(^2P)5s\ \ ^3P_2^2$
4798. 40	15	20834. 47	$(^2D)3d\ ^3F_3^3-(^2D)4p\ ^3F_2$
4794. 54	250	20851. 25	$(^4S)4s\ \ ^5S_2^2-(^4S)4p\ \ ^5P_3$
4792. 04	12	20862. 13	$(^2D)4s\ ^3D_2^3-(^2D)4p\ ^1F_3$
4785. 44	50	20890. 90	$(^2P)4s\ ^3P_2^2-(^2P)4p\ \ ^3D_2$
4784. 46	1	20895. 18	$(^2P)3d\ ^3D_1^1-(^2P)4p\ \ ^3P_2$
4781. 82	50	20906. 71	$(^2D)3d\ ^3F_2^3-(^2D)4p\ ^3F_3$
4781. 32	75	20908. 90	$(^2P)4s\ ^3P_2^2-(^2P)4p\ \ ^3D_3$
4780. 02	1	20914. 58	$(^2P)3d\ ^3D_1^1-(^2P)4p\ \ ^3P_1$
4778. 93	45	20919. 36	$(^2P)4s\ ^3P_1^1-(^2P)4p\ \ ^3D_1$
4776. 38	5	20930. 52	$(^2P)3d\ ^3D_1^1-(^2P)4p\ \ ^3P_0$
4771. 66	20	20951. 23	$(^2P)4s\ ^1P_1^1-(^2P)4p\ \ ^1D_2$
4771. 09	40	20953. 73	$(^2P)4s\ ^3P_0^0-(^2P)4p\ \ ^3D_1$
4768. 68	150	20964. 32	$(^2P)4s\ ^3P_1^1-(^2P)4p\ \ ^3D_2$
4765. 30	10	20979. 19	$(^2D)3d\ ^3F_3^3-(^2D)4p\ \ ^3F_4$
4755. 64	50	21021. 80	$(^2D)3d\ ^3F_2^3-(^2D)4p\ \ ^3F_2$
4753. 49	8	21031. 31	$(^2D)4p\ ^3P_0-(^4S)5d\ \ ^3D_1^1$
4748. 67	20	21052. 66	$(^2D)4p\ ^3P_1-(^4S)5d\ \ ^3D_2^2$
4740. 40	150	21089. 39	$(^2P)3d\ ^1D_2^2-(^2P)4p\ \ ^1P_1$
4739. 42	10	21093. 75	$(^2D)3d\ ^3F_3^3-(^2D)4p\ \ ^3F_3$
4738. 41	10	21098. 24	$(^2D)4p\ ^3P_1-(^4S)5d\ \ ^3D_1^1$
4721. 43	25	21174. 12	$(^2D)4p\ ^3P_2-(^4S)5d\ \ ^3D_2^2$
4714. 28	8	21206. 23	$(^2D)4p\ ^3P_2-(^4S)5d\ \ ^3D_2^2$
4713. 51	3	21209. 70	
4676. 73	8	21376. 50	$(^2P)4s\ ^1P_1^1-\quad 4s'\ ^3P_1$ $(^2P)3d\ ^1D_2^2-(^2P)4p\ ^3P_2$
4656. 16	1	21470. 93	$(^4S)3d\ ^5D_3^3-(^4S)4p\ ^3P_2$
4627. 68	2	21603. 07	
4624. 36	6	21618. 58	
4610. 59	1	21683. 15	
4607. 72	1	21696. 65	$(^2P)4s\ ^3P_2^2-(^2P)4p\ ^1D_2$

TABLE 1.—*Wave lengths in the second spectrum of chlorine*—Continued

λ_{air}A	Intensity	ν_{vac}cm^{-1}	Term combination
4592. 29	2	21769. 55	$(^2P)4s\ ^3P_1^\circ - (^2P)4p\ ^1D_2$
4585. 03	15	21804. 02	$(^4S)4p\ ^3P_2 - (^2D)3d\ ^3S_1^\circ$
4584. 28	20	21807. 59	
4582. 40	8	21816. 53	$(^4S)4p\ ^3P_1 - (^2D)3d\ ^3S_1^\circ$
4572. 13	100	21865. 54	$(^4S)4p\ ^3P_2 - (^4S)5s\ ^3S_1^\circ$ $(^4S)4p\ ^3P_0 - (^4S)5s\ ^3S_1^\circ$
4569. 42	50	21878. 50	$(^4S)4p\ ^3P_1 - (^4S)5s\ ^3S_1^\circ$
4544. 48	10	21998. 57	$(^2P)3d\ ^1P_1^\circ - (^2P)4p\ ^1P_1$
4540. 29	6	22018. 87	
4539. 25	6	22023. 92	
4536. 78	20	22035. 91	$(^2P)4s\ ^3P_1^\circ - 4s'\ ^3P_0$
4534. 34	5	22047. 76	
4519. 19	18	22121. 68	$(^2P)4s\ ^3P_2^\circ - 4s'\ ^3P_1$
4504. 27	20	22194. 95	$(^2P)4s\ ^3P_1^\circ - 4s'\ ^3P_1$
4497. 30	18	22229. 35	$4s'\ ^3P_2 - (^2P)5s\ ^3P_1^\circ$ $(^2P)4s\ ^3P_0^\circ - 4s'\ ^3P_1$
4490. 00	50	22265. 49	$(^2P)4s\ ^3P_2^\circ - 4s'\ ^3P_2$
4482. 02	10	22305. 13	$4s'\ ^3P_2 - (^2P)5s\ ^4P_2^\circ$
4475. 28	20	22338. 72	$(^2P)4s\ ^3P_1^\circ - 4s'\ ^3P_2$ $4s'\ ^3P_1 - (^2P)5s\ ^3P_0^\circ$
4468. 48	2	22372. 72	$4s'\ ^3P_1 - (^2P)5s\ ^3P_1^\circ$
4453. 32	3	22448. 88	$4s'\ ^3P_1 - (^2P)5s\ ^3P_2^\circ$
4436. 96	3	22531. 65	$4s'\ ^3P_0 - (^2P)5s\ ^3P_1^\circ$
4399. 14	15	22725. 35	$(^2P)4s\ ^1P_1^\circ - (^2P)4p\ ^1P_1$
4372. 91	80	22861. 66	$(^2P)3d\ ^3D_3^\circ - x'$
4359. 88	1	22929. 99	$(^2D)4p\ ^1F_3 - (^2D)5s\ ^3D_2^\circ$
4343. 62	100	23015. 82	$(^2D)4s\ ^3D_3^\circ - (^2D)4p\ ^3P_2$
4342. 80	1	23020. 17	$(^2P)4p\ ^3P_2 - (^2P)4d\ ^3F_3^\circ$
4336. 26	45	23054. 89	$(^2D)4s\ ^3D_2^\circ - (^2D)4p\ ^3P_2$
4332. 80	9	23073. 30	$(^2D)4s\ ^3D_1^\circ - (^2D)4p\ ^3P_2$
4315. 82	1	23164. 07	$(^2D)3d\ ^3D_3^\circ - x''$
4309. 06	50	23200. 41	$(^2P)3d\ ^3D_2^\circ - x'$
4307. 42	75	23209. 25	$(^2D)4s\ ^3D_2^\circ - (^2D)4p\ ^3P_1$
4304. 07	40	23227. 31	$(^2D)4s\ ^3D_1^\circ - (^2D)4p\ ^3P_1$
4302. 10	1	23237. 95	$(^2D)3d\ ^3D_2^\circ - x''$
4291. 76	50	23293. 93	$(^2D)4s\ ^3D_1^\circ - (^2D)4p\ ^3P_0$
4290. 87	1	23298. 77	
4276. 51	30	23377. 00	$(^2D)4p\ ^3F_4 - (^2D)5s\ ^3D_3^\circ$
4270. 61	25	23409. 29	$(^2D)4p\ ^3F_3 - (^2D)5s\ ^3D_2^\circ$
4263. 25	1	23449. 70	$(^2D)4p\ ^3F_3 - (^2D)5s\ ^3D_3^\circ$
4261. 22	20	23460. 88	$(^2D)4p\ ^3F_2 - (^2D)5s\ ^3D_1^\circ$
4259. 52	35	23470. 24	$(^2P)3d\ ^3D_1^\circ - x'$ $(^2P)4s\ ^3P_2^\circ - (^3P)4p\ ^1P_1$
4257. 54	4	23481. 16	$(^2D)4p\ ^3F_2 - (^2D)5s\ ^3D_2^\circ$
4253. 51	75	23503. 40	$(^4S)4p\ ^5P_3 - (^4S)5s\ ^5S_2^\circ$
4241. 38	60	23570. 62	$(^4S)4p\ ^5P_2 - (^4S)5s\ ^5S_2^\circ$
4240. 52	1	23575. 40	$(^2D)3d\ ^3P_2^\circ - x''$
4235. 49	25	23603. 39	$(^2P)4p\ ^3D_2 - (^2P)5s\ ^3P_1^\circ$ $(^2D)4p\ ^1F_3 - (^2D)5s\ ^1D_2^\circ$
4234. 09	50	23611. 20	$(^4S)4p\ ^5P_1 - (^4S)5s\ ^5S_2^\circ$

TABLE 1.—*Wave lengths in the second spectrum of chlorine*—Continued

λ_{air}A	Intensity	ν_{vac}cm^{-1}	Term combination
4233. 60	4	23613. 93	$(^2P)4p\ ^3D_1 - (^2P)5s\ ^3P^o_0$
4227. 37	4	23648. 73	$(^2P)4p\ ^3D_1 - (^2P)5s\ ^3P^o_1$
4224. 92	15	23662. 45	$(^2P)4p\ ^3D_3 - (^2P)5s\ ^3P^o_2$
4221. 80	3	23679. 93	$(^2P)4p\ ^3D_2 - (^2P)5s\ ^3P^o_2$
4218. 76	4	23697. 00	
4208. 03	30	23757. 42	$(^2P)4s\ ^3P^o_2 - (^2P)4p\ ^3P_2$
4205. 07	10	23774. 14	$(^2D)4p\ ^3F_4 - (^4S)5d\ ^3D^o_3$
4204. 54	18	23777. 14	$(^2P)4s\ ^3P^o_2 - (^2P)4p\ ^3P_1$
4195. 11	18	23830. 59	$(^2P)4s\ ^3P^o_1 - (^2P)4p\ ^3P_2$
4192. 24	6	23846. 90	$(^2D)4p\ ^3F_3 - (^4S)5d\ ^3D^o_2$
4191. 59	15	23850. 60	$(^2P)4s\ ^3P^o_1 - (^2P)4p\ ^3P_1$
4188. 82	15	23866. 37	$(^2P)4s\ ^3P^o_1 - (^2P)4p\ ^3P_0$
4187. 06	2	23876. 40	$(^4S)4s\ ^5S^o_2 - (^4S)4p\ ^3P_1$
4186. 63	5	23878. 85	$(^2D)4p\ ^3F_3 - (^4S)5d\ ^3D^o_2$
4185. 61	20	23884. 67	$(^2P)4s\ ^3P^o_0 - (^2P)4p\ ^3P_1$
4184. 89	7	23888. 78	$(^4S)4s\ ^5S^o_2 - (^4S)4p\ ^3P_2$
4181. 05	4	23910. 72	
4179. 61	2	23918. 96	$(^2D)4p\ ^3F_2 - (^4S)5d\ ^3D^o_3$
4170. 66	8	23970. 29	$(^2D)3d\ ^1D^o_2 - (^2D)4p\ ^1P_1$
4166. 10	4	23996. 52	$(^2D)4p\ ^3F_2 - (^4S)5d\ ^3D^o_1$
4157. 98	5	24043. 39	
4157. 82	25	24044. 31	
4156. 15	7	24053. 97	
4153. 98	2	24066. 54	$(^2D)4p\ ^3D_2 - (^2D)5s\ ^3D^o_2$
4151. 12	1	24083. 12	$(^2D)4p\ ^3F_3 - (^4D5)s\ ^1D^o_2$
4147. 09	30	24106. 52	$(^2D)4p\ ^3D_3 - (^2D)5s\ ^3D^o_3$
4146. 47	1	24110. 12	$(^2P)4p\ ^3P_1 - (^2P)4d\ ^3P^o_2$
4143. 04	5	24130. 09	$(^2P)4p\ ^3P_2 - (^2P)4d\ ^3P^o_2$
4134. 31	4	24181. 04	$(^2D)4p\ ^3D_2 - (^2D)5s\ ^3D^o_1$
4133. 66	20	24184. 84	$(^2D)4p\ ^3D_1 - (^2D)5s\ ^3D^o_1$
4132. 48	200	24191. 74	$(^2D)4s\ ^1D^o_2 - (^2D)4p\ ^1D_2$
4131. 80	1	24195. 73	$(^2P)4p\ ^3S_1 - (^2P)5s\ ^3P^o_1$
4130. 86	25	24201. 23	$(^2D)4p\ ^3D_2 - (^2D)5s\ ^3D^o_2$
4130. 22	8	24204. 98	$(^2D)4p\ ^3D_1 - (^2D)5s\ ^3D^o_2$
4125. 96	3	24229. 97	$(^2P)4p\ ^3P_2 - (^2P)4d\ ^3D^o_3$
4125. 17	1	24234. 61	$(^2P)4p\ ^3P_0 - (^2P)4d\ ^3P^o_1$
4124. 00	12	24241. 49	$(^2D)4p\ ^3D_2 - (^2D)5s\ ^3D^o_3$
4122. 38	0	24251. 01	$(^2P)4p\ ^3P_1 - (^2P)4d\ ^3P^o_1$
4118. 84	4	24271. 86	$(^2P)4p\ ^3S_1 - (^2P)5s\ ^3P^o_2$
4079. 88	15	24503. 63	$(^2D)4p\ ^3D_3 - (^4S)5d\ ^3D^o_3$
4077. 93	4	24515. 35	$4s'\ ^3P_2 - (^2P)4d\ ^3F^o_3$
4074. 51	6	24535. 93	$(^2D)4p\ ^3D_3 - (^4S)5d\ ^3D^o_2$
4062. 53	3	24608. 28	
4057. 52	6	24638. 66	$(^2D)4p\ ^3D_2 - (^4S)5d\ ^3D^o_3$
4055. 46	4	24651. 18	
4054. 18	9	24658. 97	$4s'\ ^3P_1 - (^2P)4d\ ^3F^o_2$
4052. 22	12	24670. 89	$(^2D)4p\ ^3D_2 - (^4S)5d\ ^3D^o_2$
4051. 58	4	24674. 78	$(^2D)4p\ ^3D_1 - (^4S)5d\ ^3D^o_2$
4049. 08	2	24690. 02	
4044. 65	4	24717. 06	$(^2D)4p\ ^3D_2 - (^4S)5d\ ^3D^o_1$

TABLE 1.—*Wave lengths in the second spectrum of chlorine*—Continued

λ_{air}A	Intensity	ν_{vac}cm^{-1}	Term combination
4044. 09	9	24720. 48	$(^2D)4p\ ^3D_1 - (^4S)5d\ ^3D^\circ_1$
4040. 64	9	24741. 59	$(^2D)4p\ ^3D_3 - (^2D)5s\ ^1D^\circ_2$
4036. 53	10	24766. 78	$(^2D)4p\ ^3P_0 - (^2D)4d\ ^3D^\circ_1$
4025. 68	7	24833. 53	$(^2D)4p\ ^3P_1 - (^2D)4d\ ^3D^\circ_1$
4020. 06	15	24868. 25	$(^2D)4p\ ^3P_1 - (^2D)4d\ ^3D^\circ_2$
4018. 24	3	24879. 51	$(^2D)4p\ ^3D_1 - (^2D)5s\ ^1D^\circ_2$
3995. 24	6	25022. 67	$(^2D)4p\ ^3P_2 - (^2D)4d\ ^3D^\circ_2$
3994. 64	2	25026. 49	
3990. 19	20	25054. 40	$(^2D)4p\ ^3P_2 - (^2D)4d\ ^3D^\circ_3$
3988. 17	4	25067. 09	$(^2D)4p\ ^1P_1 - (^2D)5s\ ^1D^\circ_2$
3984. 60	2	25089. 55	
3981. 94	15	25106. 31	
3972. 45	3	25166. 29	
3971. 18	7	25174. 34	
3968. 00	1	25194. 52	
3956. 35	3	25268. 70	
3954. 21	20	25282. 37	$(^2D)4p\ ^1D_2 - (^2D)4d\ ^1D^\circ_2$
3949. 96	10	25309. 57	$(^4S)4p\ ^3P_2 - 4p'\ ^3P^\circ_2$
3948. 06	1	25321. 76	$(^4S)4p\ ^3P_1 - 4p'\ ^3P^\circ_2$
3928. 63	5	25446. 99	$(^2D)4p\ ^3F_3 - (^2D)4d\ ^3F^\circ_2$
3927. 88	6	25451. 84	$(^2D)4p\ ^3F_4 - (^2D)4d\ ^3F^\circ_3$
3921. 75	3	25491. 64	$(^2D)3d\ ^1F^\circ_3 - (^2D)4p\ ^3F_3$
3917. 57	18	25518. 83	$(^2D)4p\ ^3F_2 - (^2D)4d\ ^3F^\circ_2$
3916. 70	20	25524. 50	$(^2D)4p\ ^3F_3 - (^2D)4d\ ^3F^\circ_3$
3915. 82	3	25530. 23	$(^2D)3d\ ^1P^\circ_1 - (^2D)4p\ ^1D_2$
3913. 92	30	25542. 62	$(^2D)4p\ ^3F_4 - (^2D)4d\ ^3F^\circ_4$
3910. 60	2	25564. 31	$(^2D)3d\ ^1F^\circ_3 - (^2D)4p\ ^3F_4$
3905. 80	4	25595. 73	$(^2D)4p\ ^3F_3 - (^2D)4d\ ^3F^\circ_3$
3902. 84	9	25615. 14	$(^2D)4p\ ^3F_2 - (^2D)4d\ ^3F^\circ_2$
3901. 89	5	25621. 37	$4s'\ ^3P_2 - (^2P)4d\ ^3P^\circ_2$
3901. 12	4	25626. 43	$(^4S)3d\ ^3D^\circ_1 - (^2D)4p\ ^1P_1$
3899. 27	4	25638. 59	$(^2D)4p\ ^1F_3 - (^2D)4d\ ^3G^\circ_4$
3898. 43	3	25644. 12	
3894. 55	2	25669. 66	$(^4S)3d\ ^3D^\circ_2 - (^2D)4p\ ^1P_1$
3886. 63	4	25721. 97	$4s'\ ^3P_1 - (^2P)4d\ ^3D^\circ_2$
3883. 80	12	25740. 71	$(^2D)4p\ ^1P_1 - (^2D)5s\ ^1D^\circ_2$
3874. 85	3	25800. 16	
3868. 62	40	25841. 71	$(^2P)4p\ ^3D_3 - (^2P)4d\ ^3F^\circ_4$
3864. 60	15	25868. 59	$(^2P)4p\ ^3D_3 - (^2P)4d\ ^3F^\circ_3$
3861. 95	20	25886. 34	$(^2P)4p\ ^3D_2 - (^2P)4d\ ^3F^\circ_2$
3861. 40	50	25890. 03	$(^4S)4p\ ^5P_2 - (^4S)4d\ ^5D^\circ_2$
3860. 98	100	25892. 84	$(^4S)4p\ ^5P_3 - (^4S)4d\ ^5D^\circ_3$
3860. 80	150	25894. 05	$(^4S)4p\ ^5P_2 - (^4S)4d\ ^5D^\circ_1$
3860. 05	2	25899. 08	$(^4S)4p\ ^3P_2 - 4p'\ ^3P^\circ_1$ $(^4S)4p\ ^3P_0 - 4p'\ ^3P^\circ_1$
3859. 17	7	25905. 00	$4s'\ ^3P_1 - (^2P)4d\ ^3P^\circ_1$
3854. 75	15	25934. 69	$(^2P)4p\ ^3D_1 - (^2P)4d\ ^3F^\circ_2$
3851. 69	30	25955. 29	$(^4S)4p\ ^5P_2 - (^4S)4d\ ^5D^\circ_1$
3851. 38	75	25957. 38	$(^4S)4p\ ^5P_2 - (^4S)4d\ ^5D^\circ_2$
3850. 97	100	25960. 15	$(^4S)4p\ ^5P_2 - (^4S)4d\ ^5D^\circ_3$
3849. 33	3	25971. 21	$(^2D)3d\ ^1F^\circ_3 - (^2D)4p\ ^1F_3$

TABLE 1.—*Wave lengths in the second spectrum of chlorine*—Continued

λ_{air}A	Intensity	ν_{vac}cm^{-1}	Term combination
3845. 84	30	25994. 77	$(^4S)4p\ ^5P_1-(^4S)4d\ ^5D_0^0$
3845. 69	75	25995. 79	$(^4S)4p\ ^5P_1-(^4S)4d\ ^5D_1^0$
3845. 42	50	25997. 61	$(^4S)4p\ ^5P_1-(^4S)4d\ ^5D_2^0$
3843. 26	100	26012. 22	$(^3P)3d\ ^1P_1^0-(^2P)4p\ ^1S_0$
3838. 37	20	26045. 36	$(^2D)4p\ ^3F_4-(^2D)4d\ ^3G_4^0$
3833. 40	200	26079. 13	$(^2D)4p\ ^3F_4-(^2D)4d\ ^3G_5^0$
3830. 80	15	26096. 83	$(^2D)4p\ ^3F_3-(^2D)4d\ ^3G_4^0$
3829. 27	15	26107. 26	$(^2D)3d\ ^1D_2^0-(^2D)4p\ ^1F_3$
3827. 62	150	26118. 51	$(^2D)4p\ ^3F_3-(^2D)4d\ ^3G_3^0$
3820. 25	100	26168. 90	$(^2D)4p\ ^3F_3-(^2D)4d\ ^3G_3^0$
3818. 40	30	26181. 58	$(^2D)4p\ ^3D_3-(^2D)4d\ ^3F_3^0$
3815. 43	1	26201. 96	$(^4S)4p\ ^3P_1-\quad 4p'\ ^3P_0^0$
3810. 10	30	26238. 61	$(^2D)4p\ ^3D_1-(^2D)4d\ ^3F_2^0$
3809. 51	40	26242. 67	$(^2D)4p\ ^3D_1-(^2D)4d\ ^3F_1^0$
3805. 24	75	26272. 13	$(^2D)4p\ ^3D_3-(^2D)4d\ ^3F_4^0$
3798. 80	50	26316. 66	$(^2D)4p\ ^3D_3-(^2D)4d\ ^3F_3^0$
3793. 75	25	26351. 69	
3781. 23	30	26438. 94	$(^2D)4p\ ^1F_3-(^2D)4d\ ^1F_3^0$
3776. 20	4	26474. 16	$(^2D)4s\ ^3D_2^0-(^2D)4p\ ^1D_2$
3774. 25	25	26487. 83	$(^4S)3d\ ^3D_1^0-(^2D)4p\ ^3D_1$
3773. 68	20	26491. 84	$(^4S)3d\ ^3D_1^0-(^2D)4p\ ^3D_2$
3770. 69	1	26512. 84	$(^2D)4s\ ^3D_2^0-(^2D)4p\ ^1D_2$
3769. 13	20	26523. 81	$(^4S)3d\ ^3D_2^0-(^2D)4p\ ^3D_2$
3768. 13	18	26530. 85	$(^4S)3d\ ^3D_2^0-(^2D)4p\ ^3D_1$
3767. 57	30	26534. 80	$(^4S)3d\ ^3D_2^0-(^2D)4p\ ^3D_2$
3756. 92	2	26610. 01	$(^2D)4p\ ^1D_2-(^2D)4d\ ^1P_1^0$
3750. 00	30	26659. 12	$(^4S)3d\ ^3D_3^0-(^2D)4p\ ^3D_3$
3748. 46	15	26670. 07	$(^4S)3d\ ^3D_3^0-(^2D)4p\ ^3D_3$
3738. 76	4	26739. 26	$(^2P)4s\ ^1P_1^0-(^2P)4p\ ^1S_0$
3733. 73	10	26775. 28	$(^2D)4p\ ^3D_3-(^2D)4d\ ^3G_4^0$
3717. 94	15	26888. 99	$(^2D)4p\ ^3D_2-(^2D)4d\ ^3G_3^0$
3705. 54	2	26978. 97	$(^2P)4p\ ^3D_1-(^2P)4d\ ^3P_2^0$
3691. 88	5*b*	27078. 80	$(^2P)4p\ ^3D_3-(^2P)4d\ ^3D_3^0$
3688. 44	15	27104. 05	$(^2D)4p\ ^1P_1-(^2D)4d\ ^3F_2^0$
3673. 83	18	27211. 83	$(^4S)3d\ ^3D_1^0-(^2D)4p\ ^3F_2$
3669. 46	2	27244. 24	$(^4S)3d\ ^3D_2^0-(^2D)4p\ ^3F_2$
3669. 14	1	27246. 61	$(^2D)4p\ ^1F_3-(^2D)4d\ ^3D_3^0$
3668. 03	20	27254. 85	$(^4S)3d\ ^3D_2^0-(^2D)4p\ ^3F_2$
3659. 84	18	27315. 85	$(^4S)3d\ ^3D_2^0-(^2D)4p\ ^3F_1$
3658. 38	20	27326. 75	$(^4S)3d\ ^3D_3^0-(^2D)4p\ ^3F_3$
3650. 13	30	27388. 51	$(^4S)3d\ ^3D_3^0-(^2D)4p\ ^3F_4$
3648. 07	10	27403. 97	$(^2D)4p\ ^3P_0-(^2D)4d\ ^3S_1^0$
3639. 19	18	27470. 84	$(^2D)4p\ ^3P_1-(^2D)4d\ ^3S_1^0$
3623. 79	9	27587. 58	$(^2P)4p\ ^3S_1-(^2P)4d\ ^3P_2^0$
3618. 88	15	27625. 00	$(^2D)4p\ ^3P_2-(^2D)4d\ ^3S_1^0$
3615. 09	10	27653. 97	$(^2D)4p\ ^3F_4-(^2D)4d\ ^3D_3^0$
3610. 07	12	27692. 42	
3609. 75	4	27694. 88	$(^2D)4p\ ^3F_3-(^2D)4d\ ^3D_2^0$
3605. 61	7	27726. 28	$(^2D)4p\ ^3F_3-(^2D)4d\ ^3D_3^0$
3605. 39	5	27728. 37	$(^2P)4p\ ^3S_1-(^2P)4d\ ^3P_1^0$

TABLE 1.—*Wave lengths in the second spectrum of chlorine*—Continued

λ_{air}A	Intensity	ν_{vac}cm^{-1}	Term combination
3604. 92	3	27731. 98	$(^2D)4p\ ^3F_2 - (^2D)4d\ ^3D_1^\circ$
3604. 51	15	27735. 14	$(^2D)4p\ ^3P_0 - (^2D)4d\ ^3P_1^\circ$
3603. 72	10	27741. 22	$(^2D)4p\ ^3P_1 - (^2D)4d\ ^3P_0^\circ$
3600. 42	5	27766. 64	$(^2D)4p\ ^3F_2 - (^2D)4d\ ^3D_2^\circ$
3595. 82	8	27802. 16	$(^2D)4p\ ^3P_1 - (^2D)4d\ ^3P_1^\circ$
3587. 78	12	27864. 49	$(^2D)4p\ ^3P_1 - (^2D)4d\ ^3P_2^\circ$
3576. 00	15	27956. 25	$(^2D)4p\ ^3P_2 - (^2D)4d\ ^3P_1^\circ$
3568. 04	20	28018. 62	$(^2D)4p\ ^3P_2 - (^2D)4d\ ^3P_2^\circ$
3526. 13	30	28351. 63	$(^2D)4p\ ^3D_3 - (^2D)4d\ ^3D_2^\circ$
3522. 14	40	28383. 74	$(^2D)4p\ ^3D_3 - (^2D)4d\ ^3D_3^\circ$
3518. 28	1	28414. 88	$(^4S)4p\ ^5P_2 - 4p'\ ^3P_2^\circ$
3513. 69	12	28452. 00	$(^2D)4p\ ^3D_2 - (^2D)4d\ ^3D_1^\circ$
3513. 22	35	28455. 81	$(^2D)4p\ ^3D_1 - (^2D)4d\ ^3D_1^\circ$
3509. 39	40	28486. 86	$(^2D)4p\ ^3D_2 - (^2D)4d\ ^3D_2^\circ$
3508. 94	12	28490. 51	$(^2D)4p\ ^3D_1 - (^2D)4d\ ^3D_2^\circ$
3505. 44	12	28518. 96	$(^2D)4p\ ^3D_2 - (^2D)4d\ ^3D_3^\circ$
3479. 82	30	28728. 93	
3470. 40	3	28806. 90	
3448. 14	4	28992. 86	
3420. 36	3	29228. 33	
3415. 57	2	29269. 32	
3409. 92	5	29317. 82	$(^2D)4p\ ^1P_1 - (^2D)4d\ ^3D_1^\circ$
3405. 89	3	29352. 51	$(^2D)4p\ ^1P_1 - (^2D)4d\ ^3D_2^\circ$
3353. 39	125	29812. 03	$3p'\ ^1P_1^\circ - (^2D)4p\ ^1P_1$
3350. 07	4	29841. 58	
3337. 20	3	29956. 66	$(^4S)3d\ ^3D_1^\circ - (^2D)4p\ ^3P_2$
3333. 64	40	29988. 65	$(^4S)3d\ ^3D_3^\circ - (^2D)4p\ ^3P_2$
3332. 42	15	29999. 63	$(^4S)3d\ ^3D_2^\circ - (^2D)4p\ ^3P_2$
3329. 12	150	30029. 36	$(^4S)4p\ ^3P_2 - (^4S)4d\ ^3D_3^\circ$
3324. 88	1	30067. 65	$(^2D)4p\ ^3P_2 - (^2D)4d\ ^1P_1^\circ$
3320. 14	30	30110. 58	$(^4S)3d\ ^3D_1^\circ - (^2D)4p\ ^3P_1$
3316. 86	50	30140. 35	$(^4S)4p\ ^3P_2 - (^4S)4d\ ^3D_2^\circ$
3315. 44	100	30153. 26	$(^4S)4p\ ^3P_1 - (^4S)4d\ ^3D_2^\circ$ and $(^4S)3d\ ^3D_2^\circ - (^2D)4p\ ^3P_1$
3312. 78	15	30177. 47	$(^4S)3d\ ^3D_1^\circ - (^2D)4p\ ^3P_0$
3307. 90	50	30221. 99	$(^4S)4p\ ^3P_0 - (^4S)4d\ ^3D_1^\circ$
3306. 45	40	30235. 24	$(^4S)4p\ ^3P_1 - (^4S)4d\ ^3D_1^\circ$
3276. 81	40	30508. 72	$(^2D)4s\ ^1D_2^\circ - (^2P)4p\ ^1D_2$
3231. 75	12	30934. 09	$(^2D)4p\ ^1F_3 - (^2D)4d\ ^1D_2^\circ$
3222. 55	7	31022. 41	
3203. 05	20	31211. 25	
3202. 12	6	31220. 32	
3189. 04	20	31348. 36	$(^2D)4p\ ^3D_3 - (^2D)4d\ ^3P_2^\circ$
3187. 42	5	31364. 30	$(^2D)4p\ ^3D_1 - (^2D)4d\ ^3P_0^\circ$
3181. 70	7	31420. 68	$(^2D)4p\ ^3D_2 - (^2D)4d\ ^3P_1^\circ$
3181. 26	5	31425. 03	$(^2D)4p\ ^3D_1 - (^2D)4d\ ^3P_1^\circ$
3180. 43	7	31433. 23	
3176. 95	5	31467. 66	
3175. 30	6	31484. 01	$(^2D)4p\ ^3D_2 - (^3D)4d\ ^3P_2^\circ$
3173. 66	20	31500. 28	
3172. 56	6	31511. 20	

TABLE 1.—*Wave lengths in the second spectrum of chlorine*—Continued

λ_{air}A	Intensity	ν_{vac}cm^{-1}	Term combination
3170. 23	15	31534. 36	
3169. 45	7	31542. 12	
3161. 44	20	31622. 03	$(^2D)3d\ ^1F_3^0-(^2D)4p\ ^1D_2$
3160. 52	10	31631. 24	
3147. 86	20	31758. 44	$(^2D)3d\ ^1D_2^0-(^2D)4p\ ^1D_2$
3125. 96	5	31980. 93	$(^2D)4s\ ^3D_2^0-(^2P)4p\ ^3D_1$
3125. 44	6	31986. 26	$(^2D)4s\ ^3D_3^0-(^2P)4p\ ^3D_2$
3124. 28	6	31998. 13	$(^2D)4s\ ^3D_1^0-(^2P)4p\ ^3D_1$
3123. 72	15	32003. 86	$(^2D)4s\ ^3D_3^0-(^2P)4p\ ^3D_3$
3121. 62	10	32025. 39	$(^2D)4s\ ^3D_2^0-(^2P)4p\ ^3D_2$
3119. 82	12	32043. 87	$(^2D)4s\ ^3D_2^0-(^2P)4p\ ^3D_3$ $(^2D)4s\ ^3D_1^0-(^2P)4p\ ^3D_2$
3096. 72	25	32282. 9	$(^2D)4s\ ^1D_2^0-(^2P)4p\ ^1P_1$
3092. 90	8	32322. 8	
3092. 22	50	32329. 9	$(^2D)3d\ ^3F_4^0-(^2P)4p\ ^3D_3$
3071. 35	40	32549. 5	$(^2D)3d\ ^3F_2^0-(^2P)4p\ ^3D_2$
3069. 66	5	32567. 4	$(^2D)3d\ ^3F_3^0-(^2P)4p\ ^3D_3$
3058. 00	40	32691. 6	$(^2D)3d\ ^3F_2^0-(^2P)4p\ ^3D_1$
3053. 74	10	32737. 2	$(^2D)3d\ ^3F_2^0-(^2P)4p\ ^3D_2$
3045. 00	10	32831. 2	$(^2D)4s\ ^3D_2^0-(^2P)4p\ ^1D_2$
3042. 29	2	32860. 4	
3037. 98	35	32907. 1	$(^2P)3d\ ^3D_3^0-x''$
3036. 40	3	32924. 2	
3022. 93	30	33070. 9	$(^2D)4p\ ^1P_1-(^2D)4d\ ^1D_2^0$
3018. 82	12	33115. 9	$(^2D)4s\ ^3D_1^0-4s'\ ^3P_0$
3006. 98	20	33246. 3	$(^2P)3d\ ^3D_2^0-x''$
3006. 05	20	33256. 6	$(^2D)4s\ ^3D_2^0-4s'\ ^3P_1$
3004. 39	10	33275. 0	$(^2D)4s\ ^3D_1^0-4s'\ ^3P_1$
2996. 63	40	33361. 1	$(^2D)4s\ ^3D_3^0-4s'\ ^3P_2$
2993. 09	8	33400. 6	$(^2D)4s\ ^3D_2^0-4s'\ ^3P_2$
2982. 78	18	33516. 0	$(^2P)3d\ ^3D_1^0-x''$
2980. 90	4	33537. 2	$(^2D)4p\ ^3D_1-(^2D)4d\ ^1P_1^0$
2980. 47	2	33542. 0	$(^2D)3d\ ^3F_2^0-(^2P)3p\ ^1D_2$
2978. 48	7	33564. 4	
2973. 46	2	33621. 1	$(^2D)3d\ ^1P_1^0-(^2P)4p\ ^1P_1$
2972. 63	5	33630. 4	
2964. 21	2	33726. 0	$(^4S)4s\ ^3S_1^0-(^2D)4p\ ^3D_2$
2950. 35	5	33884. 4	$(^2D)4p\ ^1D_2-(^2D)6s\ ^1D_2^0$
2945. 02	2	33945. 7	
2937. 14	2	34036. 8	
2934. 60	5	34066. 3	
2912. 06	15	34329. 9	
2906. 25	20	34398. 6	$(^2D)4p\ ^1P_1-(^2D)4d\ ^1P_1^0$
2902. 45	4	34443. 6	
2887. 41	4	34623. 0	$3p'\ ^3P_1^0-(^4S)4p\ ^5P_1$ $(^2D)4s\ ^3D_1^0-(^2P)4p\ ^1P_1$
2886. 63	3	34632. 3	
2884. 01	2	34663. 8	$3p'\ ^3P_1^0-(^4S)4p\ ^5P_2$
2879. 84	3	34714. 0	
2879. 50	2	34718. 1	
2876. 42	5	34755. 3	
2868. 41	10	34852. 3	$(^2D)4s\ ^3D_2^0-(^2P)4p\ ^3P_2$

TABLE 1.—*Wave lengths in the second spectrum of chlorine*—Continued

λ_{air}A	Intensity	ν_{vac}cm^{-1}	Term combination
2865. 21	4	34891. 2	$(^2D)4s\ ^3D_2^2-(^2P)4p\ ^3P_2$
2863. 55	7	34911. 5	$(^2D)4s\ ^3D_3^2-(^2P)4p\ ^3P_1$
2862. 06	5	34929. 6	$(^2D)4s\ ^3D_1^2-(^2P)4p\ ^3P_1$
2860. 71	5	34946. 1	$(^2D)4s\ ^3D_1^2-(^2P)4p\ ^3P_0$
2844. 28	4	35148. 0	
2839. 06	1	35212. 6	
2835. 59	3	35255. 7	$3p'\ ^3P_2^2-(^4S)4p\ ^5P_1$
2832. 33	4	35296. 3	$3p'\ ^3P_2^2-(^4S)4p\ ^5P_2$
2800. 27	4	35700. 3	
2799. 60	4	35708. 9	
2788. 63	3	35849. 4	
2771. 78	2	36067. 3	
2763. 88	10	36170. 4	
2758. 69	5	36238. 4	
2754. 10	25	36298. 8	
2751. 52	5	36332. 8	
2748. 09	1	36378. 2	$(^2P)4s\ ^3P_2^2-x''$
2747. 98	2	36379. 6	
2745. 75	3	36409. 2	
2744. 25	1	36429. 1	
2719. 85	1	36755. 9	$(^4S)3d\ ^5D_2^2-(^2D)4p\ ^3F_2$
2719. 61	4	36759. 1	$(^4S)3d\ ^5D_3^2-(^2D)4p\ ^3F_2$
2714. 38	8	36829. 9	$(^4S)3d\ ^5D_3^3-(^2D)4p\ ^3F_3$
2712. 77	4	36851. 8	
2709. 82	2	36891. 9	$(^2D)4p\ ^3P_1-(^2D)6s\ ^3D_1^2$
2709. 60	4	36894. 9	
2709. 03	10	36902. 7	$(^4S)3d\ ^5D_4^3-(^2D)4p\ ^3F_4$
2708. 60	1	36908. 5	$(^2D)4p\ ^3P_1-(^2D)6s\ ^3D_2^2$
2706. 76	4	36933. 6	
2698. 94	1	37040. 6	
2698. 56	2	37045. 8	$(^2D)4p\ ^3P_2-(^2D)6s\ ^3D_1^2$
2695. 02	3	37094. 5	
2694. 63	3	37099. 8	$(^2D)4p\ ^3P_2-(^2D)6s\ ^3D_2^2$
2693. 41	1	37116. 7	
2689. 39	6	37172. 1	
2688. 04	150	37190. 8	$(^4S)4s\ ^3S_1^2-(^2D)4p\ ^3P_2$
2679. 37	5	37311. 1	
2676. 95	100	37344. 9	$(^4S)4s\ ^3S_1^2-(^2D)4p\ ^3P_1$
2672. 19	50	37411. 4	$(^4S)4s\ ^3S_1^2-(^2D)4p\ ^3P_0$
2671. 43	6	37422. 0	$3p'\ ^3P_0^2-(^4S)4p\ ^3P_1$
2667. 36	40	37479. 1	$(^4S)4p\ ^3P_2-(^4S)6s\ ^3S_1^2$ $(^4S)4p\ ^3P_0-(^4S)6s\ ^3S_1^2$
2666. 46	20	37491. 8	$(^4S)4p\ ^3P_1-(^4S)6s\ ^3S_1^2$
2659. 67	3	37587. 5	
2658. 74	100	37600. 6	$3p'\ ^1P_1^2-(^2D)4p\ ^1D_2$
2648. 19	10	37750. 4	
2647. 79	5	37756. 1	$3p'\ ^3P_1^2-(^4S)4p\ ^3P_1$
2646. 88	25	37769. 1	$3p'\ ^3P_1^2-(^4S)4p\ ^3P_2$ $3p'\ ^3P_1^2-(^4S)4p\ ^3P_0$
2642. 28	4	37834. 8	
2635. 82	3	37927. 6	
2635. 44	3	37933. 0	

TABLE 1.—*Wave lengths in the second spectrum of chlorine*—Continued

λ_{air}A	Intensity	ν_{vac}cm^{-1}	Term combination
2634. 95	12	37940. 1	$(^2D)3d\ ^1F_3^3-(^2P)4p\ ^1D_2$
2634. 10	2	37952. 3	
2631. 33	2	37992. 3	$(^2D)3d\ ^3F_3^3-x'$
2630. 20	4	38008. 6	
2626. 91	3	38056. 2	
2621. 87	4	38129. 4	
2619. 80	4	38159. 5	$(^2D)4p\ ^3D_3-(^2P)4d\ ^3F_4^4$
2617. 91	1	38187. 0	$(^2D)4p\ ^3D_3-(^2P)4d\ ^3F_3^3$
2615. 13	10	38227. 6	
2614. 65	5	38234. 6	
2608. 72	2	38321. 5	$(^2D)4p\ ^3D_2-(^2P)4d\ ^3F_3^3$
2608. 24	2	38328. 6	$(^2D)4p\ ^3D_1-(^2P)4d\ ^3F_2^2$
2605. 67	5	38366. 4	
2604. 18	8	38388. 3	$3p'\ ^3P_2^2-(^4S)4p\ ^3P_1$
2603. 36	10	38400. 4	$3p'\ ^3P_2^2-(^4S)4p\ ^3P_2^2$
2582. 82	3	38705. 8	
2580. 40	4	38742. 1	
2571. 10	8	38882. 2	$(^4S)3d\ ^3D_1^1-(^2P)4p\ ^3D_1$
2568. 25	3	38925. 4	$(^4S)3d\ ^3D_2^2-(^2P)4p\ ^3D_1$
2568. 13	4	38927. 2	$(^4S)3d\ ^3D_1^1-(^2P)4p\ ^3D_2$
2566. 01	5	38959. 4	$(^4S)3d\ ^3D_3^3-(^2P)4p\ ^3D_2$
2565. 29	15	38970. 3	$(^4S)3d\ ^3D_2^2-(^2P)4p\ ^3D_2$
2564. 84	20	38977. 1	$(^4S)3d\ ^3D_3^3-(^2P)4p\ ^3D_3$
2564. 13	6	38987. 9	$(^4S)3d\ ^3D_2^2-(^2P)4p\ ^3D_3$
2549. 85	50	39206. 2	$(^4S)4p\ ^3P_2-(^4S)5d\ ^3D_3^3$
2547. 76	12	39238. 4	$(^4S)4p\ ^3P_2-(^4S)5d\ ^3D_2^2$
2546. 94	20	39251. 0	$(^4S)4p\ ^3P_1-(^4S)5d\ ^3D_2^2$
2544. 84	15	39283. 4	$(^4S)4p\ ^3P_0-(^4S)5d\ ^3D_1^1$
2543. 98	10	39296. 7	$(^4S)4p\ ^3P_1-(^4S)5d\ ^3D_1^1$
2520. 09	2	39669. 2	
2518. 15	4	39699. 8	$(^2D)4p\ ^3F_4-(^2D)6s\ ^3D_3^3$
2515. 92	3	39734. 9	$(^2D)4p\ ^3F_3-(^2D)6s\ ^3D_2^2$
2514. 01	3	39765. 1	$(^4S)3d\ ^3D_3^3-(^2P)4p\ ^1D_2$
2513. 34	1	39775. 7	$(^4S)3d\ ^3D_2^2-(^2P)4p\ ^1D_2$
2512. 41	2	39790. 4	$(^2D)4p\ ^3F_2-(^2D)6s\ ^3D_1^1$
2511. 33	3	39807. 6	$(^2D)4p\ ^3F_2-(^2D)6s\ ^3D_2^2$
2502. 75	40	39944. 0	$(^4S)4p\ ^5P_3-(^4S)6s\ ^5S_2^2$
2498. 53	30	40011. 5	$(^4S)4p\ ^5P_2-(^4S)6s\ ^5S_2^2$
2496. 04	20	40051. 4	$(^4S)4p\ ^5P_1-(^4S)6s\ ^5S_2^2$
2492. 84	3	40102. 8	
2492. 65	2	40105. 8	
2472. 69	3	40429. 6	$(^2D)4p\ ^3D_3-(^2D)6s\ ^3D_3^3$
2467. 50	1	40514. 6	$(^2D)4p\ ^3D_1-(^2D)6s\ ^3D_1^1$
2466. 72	2	40527. 4	$(^2D)4p\ ^3D_2-(^2D)6s\ ^3D_2^2$
2459. 86	10	40640. 4	
2452. 30	10	40765. 7	
2445. 34	20	40881. 7	
2444. 12	7	40902. 1	
2440. 98	3	40954. 7	
2440. 49	4	40963. 0	

TABLE 1.—*Wave lengths in the second spectrum of chlorine*—Continued

λ_{air}A	Intensity	ν_{vac}cm^{-1}	Term combination
2440. 33	5	40965. 6	
2434. 10	50	41070. 5	$(^4S)4p\ ^5P_3-(^4S)5d\ ^5D_4^?$
			$(^4S)4p\ ^5P_3-(^4S)5d\ ^5D_3^?$
2433. 26	3	41084. 7	
2430. 16	30	41137. 1	$(^4S)4p\ ^5P_2-(^4S)5d\ ^5D_3^?$
			$(^4S)4p\ ^5P_2-(^4S)5d\ ^5D_2^?$
2428. 02	10	41173. 3	
2427. 79	20	41177. 2	$(^4S)4p\ ^5P_1-(^4S)5d\ ^5D_2^?$
2424. 01	10	41241. 4	
2420. 30	2	41304. 6	
2419. 85	4	41312. 3	
2412. 48	10	41438. 5	
2407. 10	5	41531. 1	
2405. 86	2	41552. 5	
2405. 21	1	41563. 8	
2404. 59	5	41574. 5	
2404. 15	2	41582. 1	
2403. 87	3	41586. 9	
2401. 87	2	41621. 6	
2400. 62	1	41643. 2	
2399. 85	3	41656. 6	
2398. 91	2	41672. 9	$(^2D)4p\ ^1P_1-(^2D)6s\ ^1D_2^?$
2397. 81	1	41692. 0	
2380. 46	2	41995. 9	
2365. 80	2	42256. 1	
2340. 60	2	42711. 0	$(^2D)3d\ ^1D_2^?-x'$
2332. 90	2	42851. 9	
2327. 10	2	42958. 7	
2323. 02	4	43034. 2	
2322. 00	1	43053. 1	$(^4S)4p\ ^3P_2-(^2D)4d\ ^3D_2^?$
2321. 28	1	43066. 4	$(^4S)4p\ ^3P_1-(^2D)4d\ ^3D_2^?$
2320. 25	2	43085. 5	$(^4S)4p\ ^3P_2-(^2D)4d\ ^3D_3^?$
2308. 94	2	43296. 6	
2304. 59	1	43378. 3	
2295. 27	1	43554. 4	
2288. 17	7	43689. 5	
2276. 25	4	43918. 3	
2253. 16	30	44368. 3	$(^4S)3d\ ^3D_1^?-x'$
2251. 50	40	44401. 0	$(^4S)3d\ ^3D_2^?-x'$
2250. 96	20	44411. 7	$(^4S)3d\ ^3D_3^?-x'$
2109. 37	2	47392. 4	$(^4S)4s\ ^3S_1^?-4s'\ ^3P_1$
2102. 99	3	47536. 2	$(^4S)4s\ ^3S_1^?-4s'\ ^3P_2$

TABLE 2.—*Classified lines of* Cl II *in the Schumann region*

λ_{vac} A	Intensity and notes	ν_{vac} cm^{-1}	Term combination
1923. 35	4 (2)	51993	$3p'\ ^3P^o_0 - (^2D)4p\ ^3D_1$
1910. 76	0 (2, 3)	52335	$3p'\ ^3P^o_1 - (^2D)4p\ ^3D_2$
1887. 90	0 (2)	52969	$3p'\ ^3P^o_2 - (^2D)4p\ ^3D_3$
1883. 14	3 (2, 3)	53103	$3p'\ ^3P^o_2 - (^2D)4p\ ^3D_2$
1815. 61	0 (2)	55078	$(^4S)\ 4p\ ^3P_0 - (^2D)6s\ ^3D^o_1$
1815. 16	0 (2)	55092	$(^4S)\ 4p\ ^3P_1 - (^2D)6s\ ^3D^o_2$
1814. 43	0 (2)	55114	$(^4S)\ 4p\ ^3P_1 - (^2D)6s\ ^3D^o_1$
1813. 75	0 (2)	55134	$(^4S)\ 4p\ ^3P_2 - (^2D)6s\ ^3D^o_2$
1797. 91	0 (2)	55620	$3p'\ ^3P^o_0 - (^2D)4p\ ^3P_1$
1791. 91	4 (2)	55806	$3p'\ ^3P^o_1 - (^2D)4p\ ^3P_2$
1787. 10	3 (2)	55957	$3p'\ ^3P^o_1 - (^2D)4p\ ^3P_1$
1785. 06	1 (2)	56020	$3p'\ ^3P^o_1 - (^2D)4p\ ^3P_0$
1772. 01	3 (2, 3)	56433	$3p'\ ^3P^o_2 - (^2D)4p\ ^3P_2$
1767. 24	1 (2, 3)	56585	$3p'\ ^3P^o_2 - (^2D)4p\ ^3P_1$
1558. 05	1 (1, 2, 3)	64183	$3p'\ ^3P^o_1 - (^2P)4p\ ^3S_1$
1542. 94	0 (2, 3)	64811	$3p'\ ^3P^o_2 - (^2P)4p\ ^3S_1$
1528. 91	1 (2)	65406	$3p'\ ^3P^o_2 - (^2P)4p\ ^3D_2$
1484. 66	0 (2)	67356	$3p'\ ^3P^o_1 - (^2P)4p\ ^1P_1$
1471. 06	2 (2)	67978	$3p'\ ^3P^o_2 - (^2P)4p\ ^1P_1$
1401. 16	0 (2)	71369	$3p'\ ^3P^o_1 - (^2P)4p\ ^1S_0$
1223. 71	2 (2)	81719	$3p\ ^1D_2 - 3p'\ ^3P^o_2$
1079. 08	15 (1, 2, 4)	92672	$3p\ ^3P_1 - 3p'\ ^3P^o_2$
1075. 24	7 (1, 2, 4)	93002	$3p\ ^3P_0 - 3p'\ ^3P^o_1$
1071. 76	10 (1, 2, 4)	93304	$3p\ ^3P_1 - 3p'\ ^3P^o_1$
1071. 05	20 (1, 2, 4)	93366	$3p\ ^3P_2 - 3p'\ ^3P^o_2$
1067. 94	4 (1, 2, 4)	93638	$3p\ ^3P_1 - 3p'\ ^3P^o_0$
1063. 83	10 (1, 2, 4)	94000	$3p\ ^3P_2 - 3p'\ ^3P^o_1$
961. 49	10 (1, 2, 4)	104005	$3p\ ^1D_2 - 3p'\ ^1P^o_1$
926. 96	0 (1, 2)	107880	$3p\ ^3P_2 - (^4S)4s\ ^5S^o_2$
914. 90	2 (1, 2)	109302	$3p\ ^3P_0 - (^4S)3d\ ^5D^o_1$
912. 34	0 (2)	109608	$3p\ ^3P_1 - (^4S)3d\ ^5D^o_2$
910. 25	0 (1, 2)	109860	$3p\ ^1D_2 - (^2D)3d\ ^1D^o_2$
906. 60	0 (2)	110302	$3p\ ^3P_2 - (^4S)3d\ ^5D^o_3$
895. 95	3 (1, 2)	111613	$3p\ ^3P_2 - (^4S)4s\ ^3S^o_1$
893. 56	3 (1, 2, 4)	111912	$3p\ ^3P_1 - (^4S)4s\ ^3S^o_1$
888. 07	4 (1, 2, 4)	112604	$3p\ ^3P_2 - (^4S)4s\ ^3S^o_1$
872. 00	0 (2)	114679	$3p\ ^3P_0 - 3p'\ ^1P^o_1$
864. 67	5 (1, 2)	115651	$3p\ ^3P_2 - 3p'\ ^1P^o_1$
851. 70	7 (1, 2, 4)	117412	$3p\ ^1D_2 - (^2D)4s\ ^1D^o_2$
841. 41	4 (1, 2)	118848	$3p\ ^3P_0 - (^4S)3d\ ^3D^o_1$
839. 63	2 (1, 2, 4)	119100	$3p\ ^3P_1 - (^4S)3d\ ^3D^o_2$
839. 30	2 (1, 2)	119147	$3p\ ^3P_1 - (^4S)3d\ ^3D^o_1$
834. 67	10 (1, 2, 4)	119808	$3p\ ^3P_2 - (^4S)3d\ ^3D^o_3$
827. 85	1 (1, 2)	120795	$3p\ ^3P_1 - (^2D)3d\ ^1D^o_2$
797. 81	0 (2)	125343	$3p\ ^3P_1 - (^2D)3d\ ^3F^o_2$
795. 36	2 (1, 2)	125729	$3p\ ^3P_0 - (^2D)4s\ ^3D^o_1$
793. 47	3 (1, 2, 4)	126029	$3p\ ^3P_1 - (^2D)4s\ ^3D^o_1$
793. 34	3 (1, 2)	126049	$3p\ ^3P_1 - (^2D)4s\ ^3D^o_2$
792. 19	2 (1, 2)	126232	$3p\ ^1D_2 - (^2P)4s\ ^3P^o_2$
789. 01	7 (1, 2, 4)	126741	$3p\ ^3P_2 - (^2D)4s\ ^3D^o_2$

TABLE 2.—*Classified lines of* Cl II *in the Schumann region*—Continued

λ_{vac} A	Intensity and notes	ν_{vac} cm^{-1}	Term combination
788. 75	4 (1, 2, 4)	126783	$3p\ ^3P_2-(^2D)4s\ ^3D_3^3$
787. 62	3 (2)	126965	$3p\ ^1D_2-(^2P)4s\ ^1P_1^1$
787. 15	1 (1, 2)	127041	$3p\ ^3P_1-(^2D)3d\ ^1P_1^1$
777. 55	3 (1, 2)	128609	$3p\ ^1D_1-(^2P)3d\ ^1D_2^1$
774. 76	0 (1, 2)	129072	$3p\ ^1D_1-(^2P)3d\ ^3D_1^1$ $3p\ ^3P_1-(^2D)4s\ ^1D_1$
771. 00	0 (2)	129702	$3p\ ^1D_2-(^2P)3d\ ^3D_2^3$
754. 55	0 (2)	132529	$3p\ ^1D_2-(^2P)3d\ ^3F_3^3$
753. 66	0 (1, 2)	132686	$3p\ ^1D_2-(^2P)3d\ ^3F_2^3$
730. 92	3 (1, 2)	136814	$3p\ ^3P_0-(^2P)4s\ ^3P_1^1$
729. 52	2 (1)	137076	$3p\ ^3P_1-(^2P)4s\ ^3P_0^3$
729. 39	3*d* (2)	137101	$3p\ ^3P_1-(^2P)4s\ ^3P_1^3$
728. 94	3 (1, 2)	137186	$3p\ ^3P_1-(^2P)4s\ ^3P_2^3$
725. 64	2 (1, 2)	137809	$3p\ ^3P_2-(^2P)4s\ ^3P_1^3$
725. 27	3 (1, 2)	137880	$3p\ ^3P_2-(^2P)4s\ ^3P_2^3$
719. 26	1 (1, 2)	139032	$3p\ ^1D_2-(^2D)3d\ ^3P_2^3$
717. 15	2 (1, 2)	139441	$3p\ ^1D_2-(^2D)3d\ ^3D_3^3$
715. 58	3 (1, 2)	139747	$3p\ ^3P_0-(^2P)3d\ ^3D_1^3$
714. 03	2 (1, 2)	140050	$3p\ ^3P_1-(^2P)3d\ ^3D_1^3$
712. 66	3 (1, 2)	140319	$3p\ ^3P_1-(^2P)3d\ ^3D_2^3$
710. 53	0 (1, 2)	140740	$3p\ ^3P_2-(^2P)3d\ ^3D_1^3$
709. 16	2 (1, 2)	141012	$3p\ ^3P_2-(^2P)3d\ ^3D_3^3$
707. 43	4 (1, 2)	141357	$3p\ ^3P_2-(^2P)3d\ ^3D_2^3$
696. 11	0 (2)	143656	$3p\ ^3P_1-(^2P)3d\ ^3F_2^3$
693. 55	0 (2)	144186	$3p\ ^3P_2-(^2P)3d\ ^3F_3^3$
687. 55	1 (2)	145444	$3p\ ^1D_2-4p'\ ^3P_2^3$
684. 83	0 (2)	146022	$3p\ ^1D_2-4p'\ ^3P_1^3$
667. 49	1 (1)	149816	$3p\ ^3P_0-(^2D)3d\ ^3P_1^3$
666. 17	2 (1, 2)	150112	$3p\ ^3P_1-(^2D)3d\ ^3P_1^3$
666. 08	3 (1, 2)	150132	$3p\ ^3P_0-(^2D)3d\ ^3D_1^3$
665. 21	1 (1, 2)	150328	$3p\ ^3P_1-(^2D)3d\ ^3D_2^3$
664. 67	2 (1, 2)	150451	$3p\ ^3P_1-(^2D)3d\ ^3D_1^3$
663. 67	2 (1, 2)	150677	$3p\ ^3P_2-(^2D)3d\ ^3P_2^3$
663. 08	2 (1, 2)	150811	$3p\ ^3P_2-(^2D)3d\ ^3P_1^3$
662. 15	1 (1, 2)	151023	$3p\ ^3P_2-(^2D)3d\ ^3D_3^3$
661. 82	2 (1, 2)	151098	$3p\ ^3P_2-(^2D)3d\ ^3D_2^3$
661. 62	0 (2)	151144	$3p\ ^3P_2-(^2D)3d\ ^3D_1^3$
655. 09	1 (2)	152651	$3p\ ^3P_0-(^4S)5s\ ^3S_1^3$
653. 80	1 (2)	152952	$3p\ ^3P_1-(^4S)5s\ ^3S_1^3$
651. 13	1 (1, 2?)	153579	$3p\ ^3P_2-(^2D)3d\ ^3S_1^3$
650. 88	1 (1, 2)	153638	$3p\ ^3P_2-(^4S)5s\ ^3S_1^3$
639. 42	2 (1, 2)	156392	$3p\ ^3P_1-4p'\ ^3P_2^3$
638. 23	2 (1, 2)	156683	$3p\ ^3P_0-4p'\ ^3P_1^3$
637. 06	1 (1, 2)	156971	$3p\ ^3P_1-4p'\ ^3P_1^3$
636. 62	2 (1, 2)	157080	$3p\ ^3P_2-4p'\ ^3P_2^3$
635. 87	2 (1, 2)	157265	$3p\ ^3P_1-4p'\ ^3P_0^3$
634. 24	1 (1, 2)	157669	$3p\ ^3P_2-4p'\ ^3P_1^3$
626. 70	1 (1, 2)	159566	$3p\ ^1D_2-(^2D)5s\ ^1D_2^1$
621. 12	4*d* (1, 2)	161000	$3p\ ^3P_0-(^4S)4d\ ^3D_1^3$
620. 28	1 (1, 2)	161218	$3p\ ^3P_1-(^4S)4d\ ^3D_2^3$
619. 95	0 (2)	161303	$3p\ ^3P_1-(^4S)4d\ ^3D_1^3$

TABLE 2.—*Classified lines of* Cl II *in the Schumann region*—Continued

λ_{vac}A	Intensity and notes	ν_{vac}cm^{-1}	Term combination
618.02	2 (1, 2)	161807	$3p\ ^3P_2-(^4S)4d\ ^3D_3^\circ$
617.61	1 (1, 2)	161914	$3p\ ^3P_2-(^4S)4d\ ^3D_2^\circ$
617.27	0 (2)	162004	$3p\ ^3P_2-(^4S)4d\ ^3D_1^\circ$
612.73	0 (2)	163204	$3p\ ^1D_2-(^2D)4d\ ^3D_3^\circ$
599.19	0 (2)	166892	$3p\ ^1D_2-(^2D)4d\ ^1D_2^\circ$
594.49	0 (1, 2)	168211	$3p\ ^1D_2-(^2D)4d\ ^1P_1^\circ$
589.82	0 (2)	169543	$3p\ ^3P_0-(^2D)5s\ ^3D_1^\circ$
588.77	0 (2)	169846	$3p\ ^3P_1-(^2D)5s\ ^3D_2^\circ$
586.25	0 (2)	170576	$3p\ ^3P_2-(^2D)5s\ ^3D_3^\circ$
584.10	1 (2)	171204	$3p\ ^3P_2-(^2D)5s\ ^1D_2^\circ$
575.30	0 (2)	173822	$3p\ ^3P_0-(^2D)4d\ ^3D_1^\circ$
574.37	3 (1, 2)	174104	$3p\ ^3P_1-(^2D)4d\ ^3D_2^\circ$
571.95	1 (2)	174840	$3p\ ^3P_2-(^2D)4d\ ^3D_3^\circ$
566.77	0 (2)	176438	$3p\ ^3P_0-(^2D)4d\ ^3S_1^\circ$
565.75	0 (2)	176756	$3p\ ^3P_0-(^2D)4d\ ^3P_1^\circ$
563.58	0 (2)	177437	$3p\ ^3P_2-(^2D)4d\ ^3S_1^\circ$
562.54	0 (2)	177765	$3p\ ^3P_2-(^2D)4d\ ^3P_1^\circ$
562.28	3 (1, 2)	177847	$3p\ ^3P_2-(^2D)4d\ ^3P_2^\circ$
558.14	1 (1, 2)	179166	$3p\ ^3P_1-(^2D)4d\ ^1P_1^\circ$

The impurities that were encountered in the Geissler tube observations have been discussed in our paper on Cl I. In the observations with the electrodeless discharge impurity lines due to hydrogen, oxygen, water vapor, nitrogen, carbon, sulfur, and bromine were recognized. Hydrogen, oxygen, and water vapor were continuously present in the tube; the Balmer lines, the principal series of O I, and the lines of the 2811 and 3063 "water vapor" bands appearing strongly on the spectrograms. Whether or not some of the fainter unclassified lines of table 1 may be ascribed to the other water-vapor bands at 2608, 3428, 3472, and 3548 A, as described by Liveing and Dewar,[15] or by Eder and Valenta [16] cannot be decided at present owing to the lack of a satisfactory description of them. The carbon and sulfur lines that appeared in the spectra owed their presence, no doubt, to the rubber and wax connections between the tube and vacuum line; and the bromine was introduced through contamination with KBr. The only lines of sodium that appeared were the doublets of the principal series of Na I.

[15] G. D. Liveing and J. Dewar, Phil. Trans. Roy. Soc. (London), [A] **179**, 27 (1888).
[16] J. M. Eder and E. Valenta, Beiträge zur Photochemie and Spectralanalyse, p. 1-28 (K. und K. Hof- und Universitäts Buchhandlung. Vienna, 1904).

The lines in table 2 have been obtained from different sources. As stated above, we have had at our disposal unpublished lists of observations in the extreme ultraviolet by Bowen, by Weinberg, and by Boyce. In addition to these, there is a list extending to 1300 A published by Vaudet.[17] The wave lengths in the first column are adjusted mean values for all lines given by more than one author. The intensities in the second column are the maximum estimates given by any one of the authors. The numbers in parentheses after the intensities refer to the sources from which the data have been drawn, as follows: (1) for Bowen, (2) for Boyce, (3) for Vaudet, and (4) for Weinberg.

Except for lines indicated above as doubtful, we believe that the wave lengths recorded in tables 1 and 2 give a thorough description of the spectrum emitted by singly ionized chlorine atoms. Qualitatively there is good agreement between our list and the corrected list published by L. and E. Bloch.[18] All lines common to the two lists appear in table 1, but each list contains faint lines not to be found in the other. Such lines that cannot be satisfactorily accounted for by term combinations are probably due to impurities not yet recognized.

2. TERM STRUCTURE

The classified lines of Cl II may be fully accounted for as combinations of the terms given in table 4. The neutral atom has 17 extranuclear electrons, of which 10 fill all the available places within the K and L shells, leaving 7 to be assigned to the M and outer shells. In the unexcited state of the neutral atom, two of the seven valence electrons occupy s orbits and five occupy p orbits of the M shell, the configuration being designated symbolically as $3s^2\,3p^5$. In the process of excitation and ionization, one of the p or one of the s electrons may be raised to successively higher orbits until it is removed from control of the atom, leaving it ionized.

The terms that are descriptive of the energy states of the singly ionized atom when the electrons are in either of the configurations $3s^2\,3p^4$ or $3s\,3p^5$, are the limits approached by the series of Cl I as the excitation of the neutral atom proceeds towards ionization. Similarly, excitation of the ion will lead to sequences of terms which approach the basic terms of Cl III as limits. There will, therefore, be several families of terms of Cl II, each arising from adding the energy of the migrating valence electron, by the quantum methods, to that of either a basic or a higher term of Cl III, which are known from the work of

[17] G. Vaudet, Compt. rend. **185**, 1271 (1927).
[18] L. and E. Bloch, Ann. phys. [10] **8**, 397 (1927); [10] **9**, 554 (1928).

Bowen.[19] The terms thus expected, theoretically, are arrayed in table 3. The terms that have actually been found are listed in table 4, of which figure 1 is a graphical representation. The terms of Cl II

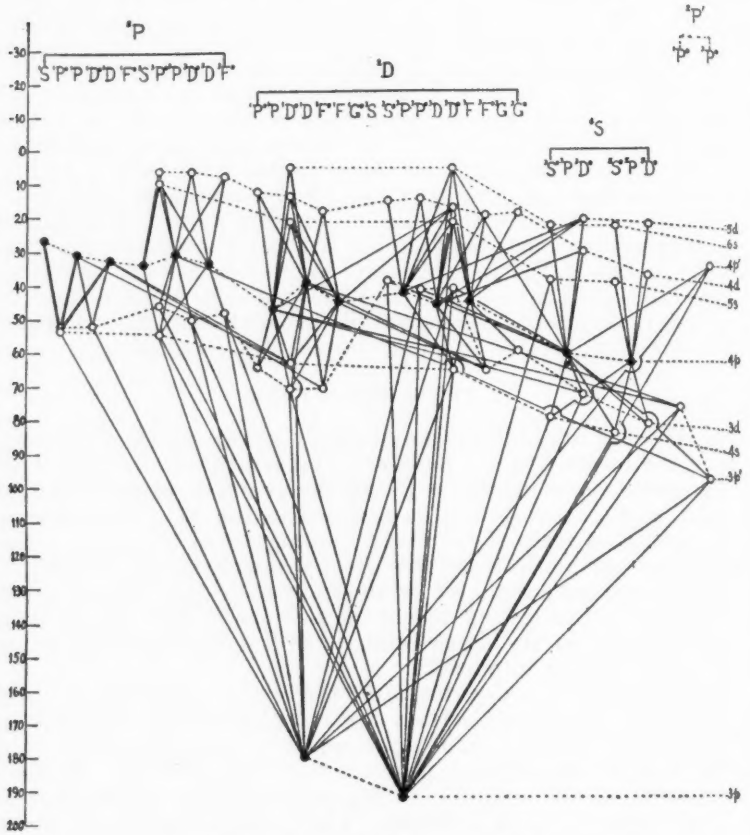

FIGURE 1.—*Term diagram for* Cl II.

● indicates even terms; ○ odd terms

are thus seen to belong to four, possibly to five, families. Of these, the terms arising from ^4S, ^2D, and ^2P of Cl III are the most conspicuous. They account for nearly all the lines of high intensity.

[19] I. S. Bowen, Phys. Rev. **45**, 403 (1934).

TABLE 3.—*Theoretical terms of* Cl II

TABLE 3.—*Theoretical terms of* Cl III

Electron configuration	Terms			
$3s^2\,3p^4$ $ns\,3p^5 = np'$ $3s\,3p^4ns = ns'$	$^3P,\ ^1D,\ ^1S$ $^3P^o,\ ^1P^o$ $^5P,\ ^3D,\ ^3P,\ ^3P,\ ^3S,\ ^1D,\ ^1P,\ ^1S$			
Basic terms of Cl III	$^4S^o$	$^3D^o$		$^2P^o$
$3s^2\,3p^3$				
$3s^2\,3p^3\,ns$	$^5S^o,\ ^3S^o$	$^3D^o$	$^1D^o$	$^3P^o$
$3s^2\,3p^3\,np$	$^5P,\ ^3P$	$^3F,\ ^3D,\ ^3P$	$^1F,\ ^1D,\ ^1P$	$^3D,\ ^3P,\ ^3S,\ ^1D,\ ^1P,\ ^1S$
$3s^2\,3p^3\,nd$	$^5D^o,\ ^3D^o$	$^1G^o,\ ^3F^o,\ ^3D^o,\ ^3P^o,\ ^3S^o,\ ^1G^o,\ ^1F^o,\ ^1D^o,\ ^1P^o,\ ^1S^o$		$^3F^o,\ ^3D^o,\ ^3P^o,\ ^1F^o,\ ^1D^o,\ ^1P^o$

TABLE 4.—*Observed terms of* Cl II

	Limit: $^4S = 321936$	Limit $\begin{cases} ^2D_{2\frac{1}{2}} = 303816 \\ ^2D_{1\frac{1}{2}} = 303883 \end{cases}$	Limit $\begin{cases} ^2P_{1\frac{1}{2}} = 292029 \\ ^2P_{0\frac{1}{2}} = 292124 \end{cases}$
$3p$	$^3P_2$ 192000 −697 $^3P_1$ 191303 −299 $^3P_0$ 191004	$^1D_2$ 180348	$^1S_0$
$4p$	$^5P_3$ 63270.2 67.3 $^5P_2$ 63337.5 40.6 $^5P_1$ 63378.1 $^3P_2$ 60232.6 12.6 $^3P_1$ 60245.2 −13.2 $^3P_0$ 60232.0	$^3F_4$ 44801.6 72.7 $^3F_3$ 44874.3 72.0 $^3F_2$ 44946.3 $^3D_3$ 45531.0 135.2 $^3D_2$ 45666.2 3.8 $^3D_1$ 45670.0 $^3P_2$ 42201.7 −154.1 $^3P_1$ 42047.6 −66.6 $^3P_0$ 41981.0 $^1F_3$ 44394.3 5651.3 $^1D_2$ 38743.0 7788.5 $^1P_1$ 46531.5	$^3D_3$ 33213.6 17.8 $^3D_2$ 33231.4 44.9 $^3D_1$ 33276.3 $^3P_2$ 30365.1 −19.9 $^3P_1$ 30345.2 −16.2 $^3P_0$ 30329.0 $^3S_1$ 33822.9 $^1D_2$ 32425.8 1774.2 $^1P_1$ 30651.6 4013.7 $^1S_0$ 26637.9
$3d$	$^5D_4^1$ 81704.2 −1.0 $^5D_3^1$ 81703.2 −2.7 $^5D_2^1$ 81700.5 −2.5 $^5D_1^1$ 81698.0 −1.5 $^5D_0^1$ 81696.5 $^3D_3^1$ 72190.1 10.9 $^3D_2^1$ 72201.0 −43.1 $^3D_1^1$ 72157.9	$^3G_5^1$ 59808.7 17.9 $^3G_4^1$ 59826.6 11.3 $^3G_3^1$ 59837.9 $^3F_4^1$ 65543.4 237.5 $^3F_3^1$ 65780.9 187.3 $^3F_2^1$ 65968.2 $^3D_3^1$ 40907.3 74.1 $^3D_2^1$ 40981.4 −115.2 $^3D_1^1$ 40866.2	$^3F_4^1$ 48003.7 −178.2 $^3F_3^1$ 47825.5 −169.1 $^3F_2^1$ 47656.4 $^3D_3^1$ 50650.4 339.6 $^3D_2^1$ 50990.0 270.0 $^3D_1^1$ 51260.0 $^3P_2^1$ 45987.1 $^3P_1^1$ ------- $^3P_0^1$ -------

TABLE 4.—*Observed terms of* Cl II—Continued

	Limit: $^4S=321936$	Limit $\begin{cases}^2D_{2\frac{1}{2}}=303816\\ ^2D_{1\frac{1}{2}}=303883\end{cases}$	Limit $\begin{cases}^2P_{1\frac{1}{2}}=292029\\ ^2P_{0\frac{1}{2}}=292124\end{cases}$
3*d*		$^3P_2^\circ$ 41318. 6 −131. 3 $^3P_1^\circ$ 41187. 3 $^3P_0^\circ$ -------	$^1F_3^\circ$ ------- $^1D_2^\circ$ 51740. 9 $^1P_1^\circ$ 52650. 0
		$^3S_1^\circ$ 38428. 8	
		$^1G_4^\circ$ ------- $^1F_3^\circ$ 70364. 9 $^1D_2^\circ$ 70501. 4 $^1P_1^\circ$ 64273. 1 $^1S_0^\circ$ -------	
	$^5D_4^\circ$ 37376. 2 1. 2 $^5D_3^\circ$ 37377. 4 3. 0 $^5D_2^\circ$ 37380. 4 1. 8 $^5D_1^\circ$ 37382. 2 1. 1 $^5D_0^\circ$ 37383. 3	$^3G_5^\circ$ 18722. 5 33. 6 $^3G_4^\circ$ 18756. 1 21. 2 $^3G_3^\circ$ 18777. 3	$^3F_4^\circ$ 7371. 9 −27. 1 $^3F_3^\circ$ 7344. 8 −3. 2 $^3F_2^\circ$ 7341. 6
		$^3F_4^\circ$ 19259. 1 90. 6 $^3F_3^\circ$ 19349. 7 77. 7 $^3F_2^\circ$ 19427. 4	$^3D_3^\circ$ 6134. 8 $^3D_2^\circ$ ------- $^3D_1^\circ$ -------
	$^3D_3^\circ$ 30203. 5 −111. 2 $^3D_2^\circ$ 30092. 3 −82. 1 $^3D_1^\circ$ 30010. 2	$^3D_3^\circ$ 17147. 4 32. 0 $^3D_2^\circ$ 17179. 4 34. 9 $^3D_1^\circ$ 17214. 3	$^3P_2^\circ$ 6235. 0 −140. 4 $^3P_1^\circ$ 6094. 6 $^3P_0^\circ$ ------
4*d*		$^3P_3^\circ$ 14183. 1 62. 7 $^3P_1^\circ$ 14245. 8 60. 6 $^3P_0^\circ$ 14306. 4	$^1F_3^\circ$ ------ $^1D_2^\circ$ ------ $^1P_1^\circ$ ------
		$^3S_1^\circ$ 14576. 9	
		$^1G_4^\circ$ ------- $^1F_3^\circ$ 17955. 0 $^1D_2^\circ$ 13460. 9 $^1P_1^\circ$ 12133. 0 $^1S_0^\circ$ -------	
	$^5D_4^\circ$ 22199. 8 0. 6 $^5D_3^\circ$ 22200. 4 . 5 $^5D_2^\circ$ 22200. 9 $^5D_1^\circ$ ------- $^5D_0^\circ$ -------		
5*d*	$^3D_3^\circ$ 21026. 4 −32. 2 $^3D_2^\circ$ 20994. 2 −45. 7 $^3D_1^\circ$ 20948. 5		

TABLE 4.—*Observed terms of* C III—Continued

	Limit: $^4S=321936$	Limit $\begin{cases}^3D_{3\frac{1}{2}}=303816\\ ^3D_{1\frac{1}{2}}=303883\end{cases}$	Limit $\begin{cases}^3P_{1\frac{1}{2}}=292029\\ ^3P_{0\frac{1}{2}}=292124\end{cases}$
$4s$	$^5S_2$ 84121.5 $^3S_1$ 79392.0	$^3D_3$ 65217.2 39.5 $^3D_2$ 65256.7 18.2 $^3D_1$ 65274.9 $^1D_2$ 62934.6	$^3P_2$ 54122.4 73.2 $^3P_1$ 54195.6 34.3 $^3P_0$ 54229.9 $^1P_1$ 53377.0
$5s$	$^5S_2$ 39766.9 $^3S_1$ 38366.9	$^3D_3$ 21424.5 40.4 $^3D_2$ 21464.9 20.4 $^3D_1$ 21485.3 $^1D_2$ 20790.8	$^3P_2$ 9551.3 76.4 $^3P_1$ 9627.7 34.4 $^3P_0$ 9662.1 $^1P_1$ -------
$6s$	$^5S_2$ 23326.4 $^3S_1$ 22753.4	$^3D_3$ 5101.7 37.3 $^3D_2$ 5139.0 16.7 $^3D_1$ 5155.7 $^1D_2$ 4858.6	
$3p'$	$^3P_2$ 98633.4 −632.1 $^3P_1$ 98001.3 −334.1 $^3P_0$ 97667.2 $^1P_1$ 76343.6	$4s'$ $^3P_2$ 31856.6 143.8 $^3P_1$ 32000.4 159.3 $^3P_0$ 32159.7 x' 27789.3 x'' 17743.7	
$4p'$	$^3P_2$ 34923.4 −590.2 $^3P_1$ 34333.2 −290.0 $^3P_0$ 34043.2 $^1P_1$ -------		

The terms of the ^4S family are quintets and triplets. The important multiplets of the quintet system are the groups described by Paschen. To these, our work and that of the Blochs have added a few more. The faint, diffuse lines at 6365 A probably represent a combination between $(^4S)4d\ ^5D°$ and the ^5F term to be expected from the configuration $(^4S)4f$; but at present there is no verification of this. The triplet terms of the ^4S family have been found by Murakawa and, independently, by us. For most of the term assignments, the two investigations are in agreement, but Murakawa adds to this system a term that he designates as $4f\ ^3F$. In table 4 this term is given the label x', indicat-

ing that, for the present, we prefer to leave it unassigned. The reasons for this are stated below. The intercombinations between the two systems of the ^4S family have now been found and Paschen's quintet multiplets, which have stood apart, are here tied up with the extensive triplet systems.

The terms of the ^2D family consist of singlets and triplets and constitute the largest group of Cl II. Some of the strongest lines of the spectrum are accounted for by the combinations of the $3d$ and $4s$ terms with the $4p$ terms. Less intense, but equally numerous, groups of lines come from the combinations of the $4d$, $5s$, and $6s$ with the $4p$ terms. Murakawa has reported all the triplet terms in this family from the $4s$, $4p$, $4d$, and $5s$ electron configurations, some from the $3d$ configuration, and a few singlet terms. In addition to these terms, we give in table 4 nearly all the singlets required for these configurations and the rest of the triplets of the $3d$ group.

The terms of the ^2P family are given here for the first time, except $3d\,^3D^\circ$, which is due to Bowen. The prominent lines of this family, as with the ^2D family, arise from the combination of the $4s$ terms, $^1P^\circ$ and $^3P^\circ$, with the $4p$ terms. The $3d$ terms, although approaching the $4s$ terms in stability, do not combine as readily with the $4p$ terms. This is revealed by the nonappearance of the multiplets $3d\,^3D^\circ$—$4p\,^3F$, $3d\,^3P^\circ$—$4p\,^3D$, $3d\,^3P^\circ$—$4p\,^3S$, and only the partial appearance of $3d\,^3P^\circ$—$4p\,^3P$, $3d\,^3P^\circ$—$4s'\,^3P$.

The singlets of both the ^2D and ^2P families presented some difficulty. After most of the triplet terms described above had been found, the remaining outstanding lines were searched for recurring, constant wave-number differences. Among these lines the differences 7,788.5, 5,651.2, and 1,774.2 cm^{-1} were recognized as significant. In particular, two pairs of lines with the difference 7,788 also exhibited the difference 13,409 cm^{-1} that separated two strong lines in the far ultraviolet. This clue led to the scheme of singlet terms as given in table 4, and further search revealed the intersystem combinations that tied them up with the triplets and quintets.

The terms of the ^4S, ^2D, and ^2P families described in the preceding paragraphs result from removal of a p electron from the configuration $3s^2\,3p^4$. The configuration $3s\,3p^5$ is also possible and the excitation of Cl^+ may proceed by removal of the s electron. This yields another family of $^3P^\circ$ and $^1P^\circ$ terms with $3p^5$ ($^2P'$) of Cl III as limit. The terms recognized as members of this family are distinguished by the configuration symbols $3p'$ and $4p'$ in table 4.

After the term assignments discussed above had been made, there remained undesignated three terms, $4s'\,^3P$ and two single terms x' and x'', for which no origin was obvious. These terms are of even parity and give some rather strong combinations. Murakawa has interpreted the term x' as $(^4S)4f\,^3F$. If this is correct, then x'' must be regarded as $(^4S)5f\,^3F$, because its behavior is closely similar to that of x'. In support of this view is the fact that if they result from addition of an f electron to ^4S then they are closely hydrogenic in character, their Rydberg denominators being 3.973 and 4.973, respectively. However, they do not exhibit the combinatory characteristics of ^3F terms. They combine strongly only with the $3d\,^3D$ terms of the ^4S, ^2D, and ^2P families. We have photographed the lines in question with high dispersion, in particular the three lines at 2250 A with the dispersion of 0.5 A/mm afforded by the large quartz-prism spectro-

graph, and find them to be sharp, without shading or satellites. The observational evidence indicates that the terms x' and x'' are single and with inner quantum number 2. If they belong to the ^4S family, they might be regarded as $^3P_2$ terms obtained by addition of np electrons to ^4S, but failure to observe close components of the multiple term argues against this view.

An alternative, though not satisfactory, view is to attribute the origin of the terms $4s'\ ^3P$, x', and x'' to the configuration $3s\,3p^4\,4s$ resulting from excitation of an s electron out of the ground state of Cl^+. Terms of this character are not known in other spectra related to Cl II, and a weighty objection to this interpretation is the non-appearance in the analysis of the other terms of the configuration, which might reasonably be expected to be present with some prominence.

3. SERIES AND IONIZATION POTENTIAL

The $^5S°$ and $^3S°$ terms of the ^4S family form excellent sequences from which to calculate absolute term values. For each series we have observed combinations with terms from the $4s$, $5s$, and $6s$ electrons. We may, therefore, rigorously solve the Ritz term formula

$$ms\ S=\frac{4R_{Cl}}{\{m+\alpha+\beta(msS)\}^2}$$

and evaluate the constants. For the quintet series, we find $4s\ ^5S_2=84{,}150\ cm^{-1}$; $\alpha=-1.6467$; and $\beta=0.8134\times10^{-6}$; and for the triplet series we find $4s\ ^3S_1=79{,}333\ cm^{-1}$; $\alpha=-1.5846$; and $\beta=-0.7917\times10^{-6}$.

Similar excellent sequences may be found in the terms of the $(^2D)\ ms$ groups. As an example, we may cite the series of $^3D_3$ terms that converge to $^2D_{2\frac{1}{2}}$ of Cl III. From three observed members we solve a Ritz formula similar to the above and find $4s\ ^3D_3=83{,}411\ cm^{-1}$; $\alpha=-1.6387$; and $\beta=8\times10^{-7}$. This value of $4s\ ^3D_3$, when reckoned from ^4S, must be diminished by $18{,}120\ cm^{-1}$, the distance between ^4S and $^2D_{2\frac{1}{2}}$. In the list of ultraviolet lines, table 2, may be found combinations between the lowest term of Cl II and the terms $4s\ ^5S_2^0$, $4s\ ^3S_1^0$, and $4s\ ^3D_3^0$. These give 192,032, 191,938, and 192,075 cm^{-1}, respectively, for the distance separating the ground states of Cl II and Cl III. Accordingly, we adopt $192{,}000\ cm^{-1}$ for the value of $3p\ ^3P_2$, corresponding to an ionization potential of 23.70 volts. This is in exact agreement with Murakawa's result.

It is well known that series from the d electron are not satisfactorily represented by the Ritz formula. For the ^5D terms of Cl II arising from ^4S, we can find only an approximate agreement with the formula. For the ^3D terms of the same family, the lack of agreement is quite pronounced, being aggravated by the perturbative influence of the term $3d\ ^3D$ of the ^2D family. The effect of this perturbation is to shift the term $4d\ ^3D$ from its normal position in the energy scale, and is further manifested in the shifted positions and the anomalous separations of the other terms of the series. This behavior is precisely that described by Shenstone and Russell [20] for the perturbed series of various elements.

[20] A. G. Shenstone and H. N. Russell, Phys. Rev. 39, 415 (1932).

4. COMPARISON WITH SIMILAR SPECTRA

The spectra Si, Cl II, A III, K IV, Ca V, etc., form an isoelectronic sequence, which it is instructive to examine in order to check term assignments and to discover the clues leading to new identifications. Partial term analyses have been made for each of these spectra: by Meissner, Bartelt, and Eckstein [21] and by Ruedy [22] for Si; by deBruin [23]

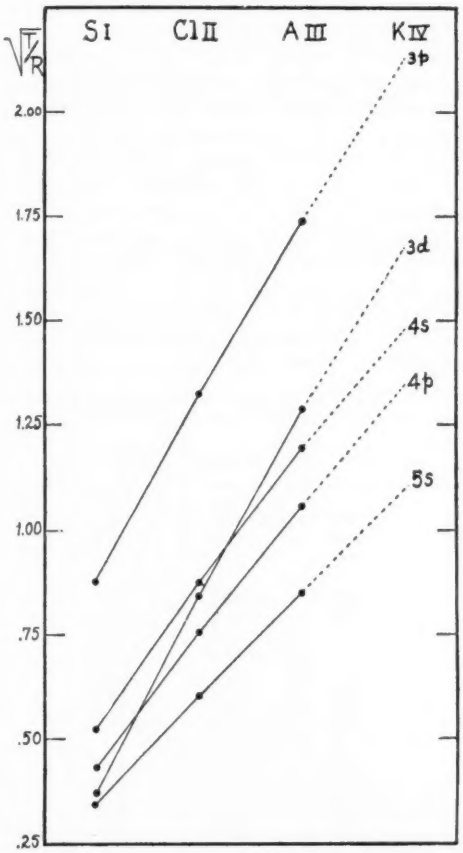

FIGURE 2.—*Moseley diagram for* Si *isoelectronic sequence.*

for A III; by Ram [24], and by Bowen [25] for K IV and Ca V. In only the first three spectra, however, have series been found from which absolute term values may be derived.

A striking feature of the term structure of these spectra is the increasing stability with atomic number of the 3*d* electron. In Si the 3*d* terms lie in the vicinity of the 4*p* group and combine with them to give lines, not yet observed, that fall far into the infrared. In Cl II, however, as shown in figure 1, the 3*d* terms approach the 4*s*

[21] K. W. Meissner, O. Bartelt, and L. Eckstein, Z. Physik **86**, 54 (1933).
[22] J. E. Ruedy, Phys. Rev. **44**, 757 (1933).
[23] T. L. deBruin, Proc. Acad. Sci. Amsterdam **40**, 340 (1937).
[24] M. Ram, Indian J. Phys. **8**, 151 and 163 (1933).
[25] I. S. Bowen, Phys. Rev. **46**, 791 (1934).

group in stability, while in A III and the succeeding spectra the $3d$ terms have dropped below the $4s$ groups. An exception to this statement is to be noted for some of the $3d$ terms of the ^2D family. We find that the $^3D°$, $^3P°$, and $^3S°$ terms of this group, if they have been correctly designated, lie above the $4p$ terms, and apparently are unrelated to the $^3G°$ and $^3F°$ terms. No simple explanation is apparent for this division of the terms of a configuration into two widely separated groups, but the behavior is quite analogous to that of the (^3P) $3d$ terms of Cl III as described by Bowen.

In table 5 are entered values of $\sqrt{T/R}$ for corresponding terms of S I, Cl II, and A III. Figure 2 is a Moseley diagram of these data and portrays the fidelity with which the prominent terms of the S I isoelectronic sequence obey the irregular doublet law. The dotted portions of the curves represent an extrapolation to the probable positions of the K IV terms for which absolute values are still lacking. The entries in the table for the (^2P) $4p$ terms of S I are out of harmony with the other values for the $4p$ group, which suggests that perhaps they have not been correctly identified. The $^1S_0$ term of the ground configuration has been given only for S I. If this has been correctly identified, we should expect the corresponding term of Cl II to have a value close to 164,500. A thorough search through the available wave length lists has failed to reveal the lines necessary to establish it.

TABLE 5.—*Values of* $\sqrt{T/R}$ *for the* S I, Cl II, A III *isoelectronic sequence*

Term	S I	Δ	Cl II	Δ	A III
$3p\ ^3P$	0. 873	0. 450	1. 323	0. 413	1. 734
$3p\ ^1D$	. 823	. 459	1. 282		----------
$3p\ ^1S$	. 767		----------		----------
(^4S)$3d\ ^5D°$	. 378	. 485	. 863	. 436	1. 299
(^4S)$3d\ ^3D°$	. 350	. 461	. 811	. 445	1. 256
(^4S)$4s\ ^5S°$	. 531	. 345	. 876	. 315	1. 191
(^2D)$4s\ ^3D°$	. 507	. 365	. 872	. 315	1. 187
(^2P)$4s\ ^3P°$	. 531	. 344	. 875	. 324	1. 199
(^4S)$4p\ ^5P$	. 428	. 331	. 759	. 309	1. 068
(^2D)$4p\ ^3F$	. 429	. 328	. 757	. 308	1. 065
(^2P)$4p\ ^3D$	. 497	. 261	. 758	. 308	1. 066
(^2P)$4p\ ^3P$	. 512	. 229	. 741	. 297	1. 038
(^4S)$5s\ ^5S°$	. 342	. 260	. 602	. 248	. 850
(^2D)$5s\ ^3D°$	----------		. 600	. 248	. 848
(^2P)$5s\ ^3P°$	----------		. 600	. 248	. 848

In conclusion we express our indebtedness to our colleagues at the National Bureau of Standards who have aided us during various phases of the work described in these pages. Particularly do we wish to express our appreciation to I. S. Bowen, J. C. Boyce, and F. Weinberg for making available to us their unpublished observations of chlorine spectra in the Schumann region.

WASHINGTON, May 10, 1939.